Departament de Geologia, Facultat de Ciències, Universitat Autònoma de Barcelona

Registre sedimentari i icnològic del fini-Carbonífer, Permià i Triàsic continentals dels Pirineus Catalans

Evolució i crisis paleoambientals a l'equador de Pangea

Memòria presentada per Eudald Mujal Grané per optar al títol de Doctor en Geologia

Juny de 2017

Tesi doctoral dirigida per:

Dr. Oriol Oms Llobet, Departament de Geologia, Universitat Autònoma de Barcelona

Dr. Josep Fortuny Terricabras, Institut Català de Paleontologia Miquel Crusafont

Dr. Oriol Oms Llobet **Dr. Josep Fortuny Terricabras**

Eudald Mujal Grané

Annexes

Annex 1. *First footprints occurrence from the Muschelkalk detritical unit of the Catalan Basin: 3D analyses and palaeoichnological implications*

L'Annex 1 correspon al treball publicat a la revista *Spanish Journal of Palaeontology* el juliol de 2015:

Mujal, E., Fortuny, J., Rodríguez-Salgado, P., Diviu, M., Oms, O., Galobart, À., 2015. First footprints occurrence from the Muschelkalk detritical unit of the Catalan Basin: 3D analyses and palaeoichnological implications. Spanish Journal of Palaeontology, 30(1): 97–108.

En aquest article l'autor E. M. ha contribuït en: elaboració dels models fotogramètrics 3D de les icnites; anàlisis de sedimentologia i icnologia; interpretació i discussió de tots els resultats; redacció del manuscrit; preparació i maquetació de les figures 3 i 4; autor per correspondència amb la revista.

SPANISH JOURNAL OF PALAEONTOLOGY

First footprints occurrence from the Muschelkalk detritical unit of the Catalan Basin: 3D analyses and palaeoichnological implications

Eudald MUJAL[1], Josep FORTUNY[2], Pablo RODRÍGUEZ-SALGADO[1], Marc DIVIU[1], Oriol OMS[1] & Àngel GALOBART[2]*

[1] Universitat Autònoma de Barcelona. Departament de Geologia. 08193 Bellaterra, Spain; eudald.mujal@uab.cat; pablorodriguezsalgado@gmail.com; mdiviu@gmail.com; joseporiol.oms@uab.cat
[2] Institut Català de Paleontologia Miquel Crusafont. Mòdul ICP - Facultat de Biociències. Universitat Autònoma de Barcelona. 08193 Bellaterra, Spain; josep.fortuny@icp.cat; angel.galobart@icp.cat

* Corresponding author

Mujal, E., Fortuny, J., Rodríguez-Salgado, P., Diviu, M., Oms, O. & Galobart, À. 2015. First footprints occurrence from the Muschelkalk detrital unit of the Catalan Basin: 3D analyses and palaeoichnological implications. [Primer registro de huellas en la unidad detrítica del Muschelkalk de la Cuenca Catalana: Análisis 3D e implicaciones paleoicnológicas]. *Spanish Journal of Palaeontology*, 30 (1), 97-108.

Manuscript received 07 November 2013
Manuscript accepted 20 June 2014

ABSTRACT

Fossil vertebrate footprints are known from several Triassic localities of the Iberian Peninsula. Geological setting and palaeoichnological analyses are presented from the first recovered tetrapod footprints from the Middle Muschelkalk facies of the Iberian Peninsula. The studied outcrop is 40 km NW from Barcelona, in the Catalan Coastal Ranges (Catalan Basin, NE Iberian Peninsula). The stratigraphic section is ascribed to Middle Muschelkalk facies from Late Anisian-Early Ladinian age (Middle Triassic), and comprises mainly red mudstones with interbedded sandstones. Tetrapod footprints are located at the upper part of decimetric medium-grain size sandstone intercalated in metric-submetric mudstone beds sequence. The general palaeoenvironment is a floodplain with episodic torrential events. Several 3D models from footprints were made by photogrammetry technique, being useful in the morphological description and depth analyses as indicator of the trackmaker's pressure-weight distribution and locomotion-substrate interaction.

RESUMEN

En la Península Ibérica se conocen varias localidades de huellas fósiles de vertebrados del Triásico. En este trabajo se presentan el contexto geológico y los análisis paleoicnológicos de las primeras huellas fósiles de tetrápodos encontradas en facies Muschelkalk Medio de la Península Ibérica. El área de estudio está a 40 km al NW de Barcelona, en las Cordilleras Costero Catalanas (Cuenca Catalana, NE Península Ibérica). La sección estratigráfica pertenece a las facies Muschelkalk Medio de edad Anisiense superior-Ladiniense inferior (Triásico Medio), y está formada principalmente por lutitas rojas con intercalaciones de areniscas. Las huellas de tetrápodo se encuentran en la parte alta de una secuencia de capas de areniscas de grano medio decimétricas intercaladas con capas lutíticas métricas o submétricas. En general, el paleoambiente es una llanura de inundación con eventos torrenciales episódicos. Se generaron mediante fotogrametría diversos modelos 3D de las huellas, que ayudan en la descripción morfológica y análisis de profundidad como indicadores

Tetrapod footprints are preserved in convex hyporelief in a sandstone bed with ripple laminations, mud-cracks and invertebrate traces. Substrate under the sand was muddy and soft, with progressive desiccation. There are eight footprints from different specimens and trackmakers. Seven of them are attributed to *Isochirotherium* isp. and *Chirotherium* isp. In special, three of them clearly resemble the pentadactyl morphology of chirotheriid pes. Potential trackmakers are crurotarsians. The last footprint is isolated and is referable to *Rhynchosauroides* isp. Potential trackmaker is a lacertoid-type reptile. The finding partially confirms the presence of homogeneous fauna diversity in the Middle Triassic of Europe, dominated by the same ichnofamilies reported here.

Keywords: Middle Triassic, *Isochirotherium*, *Chirotherium*, *Rhynchosauroides*, photogrammetry.

de distribución presión-peso del productor e interacción locomoción-sustrato. Las huellas de tetrápodo se preservan en hiporelieve convexo en una capa de arenisca con ripples, grietas de desecación y trazas de invertebrados. El sustrato bajo la arena era fangoso y blando, con progresiva desecación. Hay ocho huellas de diferentes especímenes y productores. Siete de ellas se atribuyen a *Isochirotherium* isp. y *Chirotherium* isp. En especial, tres de ellas preservan la típica morfología pentadáctil de los pies de chirotheridos. Los potenciales productores son crurotarsos. La otra huella está aislada y se atribuye a *Rhynchosauroides* isp. El potencial productor es un reptil tipo lacértido. El hallazgo confirma la presencia de diversidad faunística homogénea en el Triásico Medio de Europa, dominado por las mismas icnofamílias citadas.

Palabras clave: Triásico Medio, *Isochirotherium*, *Chirotherium*, *Rhynchosauroides*, fotogrametría.

1. INTRODUCTION

Tetrapod footprints are known from several Iberian Peninsula localities of Buntsandstein and Lower Muschelkalk facies, mainly corresponding to Middle Triassic. These sites are in the Catalan Coastal Ranges (Calzada, 1987; Fortuny *et al*., 2011 and references therein), Iberian Ranges (Demathieu *et al*., 1978; García-Bartual *et al*., 1996; Gand *et al*., 2010; Díaz-Martínez & Pérez-García, 2012), Betic Ranges (Pérez-López, 1993; Demathieu *et al*., 1999), and Cantabrian Mountains (Demathieu & Saiz de Omeñaca, 1990). In Serra de Tramuntana (Mallorca, Balearic Islands), tetrapod footprints from Buntsandstein facies were described by Calafat *et al*. (1987). Nevertheless, in Middle Muschelkalk facies unit (detritical in the Catalan Coastal Ranges) vertebrate fossils have never been reported until now. Here are described the first tetrapod footprints recovered in this facies on Collcardús area from the Catalan Coastal Ranges.

Firstly, these footprints were cited but not described by Fortuny *et al*. (2012), and no detailed ichnotaxonomic studies were made. Footprints shape is difficult to assess because of the original environmental conditions and the current weathering effects. Fortunately, 3D photogrammetric models are useful for taxonomical implications and are herein made in several footprints. Thus, this is the first ichnological study applying photogrammetry on non-dinosaur Triassic footprints (see also Petti *et al*., 2009 and Belvedere *et al*., 2013) and the resulting data enhances the use of this technique on trace fossils.

Fortuny *et al*. (2011) presented a comprehensive review of the palaeobiogeographic evolution during the Triassic period and remarked the importance of revising the Triassic Iberian fossil localities. The tetrapod footprints reported here enlarge the knowledge of the continental faunas and their geological setting (Middle Muschelkalk facies) gives additional interest in their study as palaeobiogeographic indicators, because in the Catalan Basin the Middle Muschelkalk unit is not carbonated, like in other Triassic localities.

Thus, the main objectives of this work are (1) description and identification applying the photogrammetrical technique and (2) geological contextualization of the tetrapod ichnites.

2. MATERIAL AND METHODS

Morphological description of ichnites is based on quantitative and qualitative parameters, following the ones applied by Haubold (1971a, b) and Demathieu (1985), which are: footprint length and width, digits length, digits divarication (angle between digits), cross axis angle (digit III with metapodial-digit line), and manus/pes area ratio. Tetrapod traces are named footprints, ichnites and/or tracks. Digits are numbered from medial (inner) to lateral (outer) side, i.e., I-II-III-IV-V. Biometric measurements are taken with ImageJ v.1.46r (available from http://rsbweb.nih.gov/ij/).

The ichnological analyses are developed by using the photogrammetry technique. It consists in taking photographs in all the perspectives of the object to obtain a 3D model. A comprehensive review of the technique is given in Falkingham (2012). The photographs were taken with a digital camera Sony DSC-H50 9.1 Megapixels and were processed in different open access softwares: 1) VisualSfM v0.5.22 (http://homes.cs.wadhingtin.edu/~ccwu/vsfm/) software matches all the photographs and creates the 3D model point cloud; 2) MeshLab v.1.3.2 (http://meshlab.sourceforge.net/) software is used to create the mesh, scale and orientate the 3D model; 3) With the ParaView v.3.98.1 (http://www.paraview.org) software the 3D model is coloured to generate the depth map and put the contour lines.

Institutional abbreviations: Slab, in three parts, stored at Institut Català de Paleontologia Miquel Crusafont (ICP) at Sabadell, Catalonia, with the code number IPS-81873a, IPS-81873b, IPS-81873c.

3. GEOLOGICAL SETTING

The Triassic of the Catalan Coastal Ranges (CCR) is composed by the classic Germanic facies, which comprises six lithostratigraphic units (Calvet & Marzo, 1994; Dinarès-Turell *et al*., 2005): Buntsandstein, Lower, Middle and Upper Muschelkalk, Keuper and Imón formation, and it presents thickness from 500 to 800 m (Dinarès-Turell *et al*., 2005). These facies were developed in different rift systems in Central and Eastern Europe and consequently, they cannot be considered as time intervals; therefore there is facies diachronism (López-Gómez *et al*., 2002).

The studied area is located in the Prelitoral Range of the CCR, in Collcardús range (UTM 31T 411848 X, 4603632 Y) from Viladecavalls town, 40 km NW from Barcelona (Figs 1A-B). In this area the Triassic sequence is composed by four of the six main lithostratigraphic units: Buntsandstein, Lower, Middle and Upper Muschelkalk facies. At the base of the Triassic sequence the Buntsandstein facies lies unconformably over the hercynian basement. At the top of the sequence the Tertiary succession lies unconformably over the Upper Muschelkalk. As a result of the Palaeogene compressive phase, in this area the Triassic sequence is inverted and thrusted by the hercynian basement through thin skin tectonics processes (Fig. 1C).

Within the Triassic sequence, the finding is located in the Middle Muschelkalk facies (M2) that in CCR are dated as Late Anisian-Early Ladinian age by palynological methods (Solé de Porta *et al*., 1987). The Middle Muschelkalk is constituted mainly by red mudstones with interbedded sandstones, which is interpreted as floodplain from fluvial sedimentary palaeoenvironment. The slab bearing tetrapod footprints is located at the upper part of decimetric medium-grain size sandstone intercalated in metric-submetric mudstone beds sequence (Fig. 2). The alternation of medium grained sandstones with mudstones in addition with the primary sedimentary structures, such as planar cross stratification, suggests the ephemeral alluvial currents within a terminal fan model of the Guanta Unit (Calvet & Marzo, 1994). A combination of low-energy transport with episodic floods triggered during overflow moments is recorded. These processes generated a floodplain environment, optimal for the ichnite record and preservation.

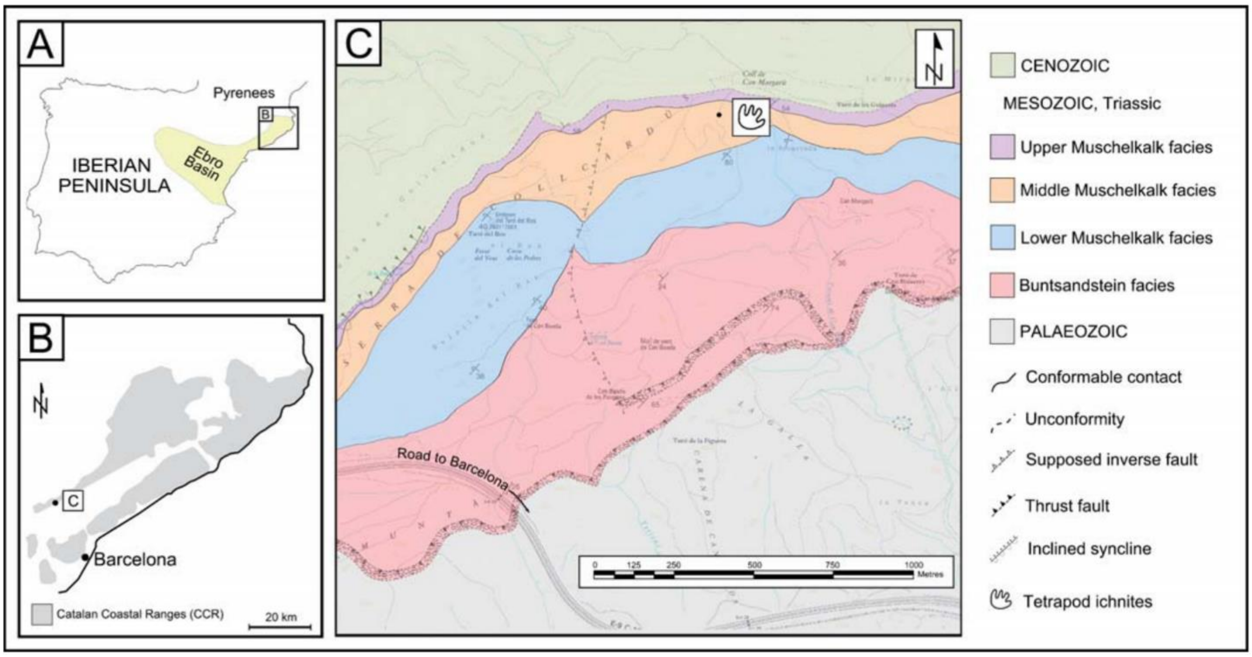

Figure 1. Geological setting. **(A)** Geographical situation. **(B)** Regional lithostratigraphy (modified from Durán, 1990). **(C)** Geological map from the studied area (topographic base modified from Institut Cartogràfic de Catalunya, http://www.icc.cat).

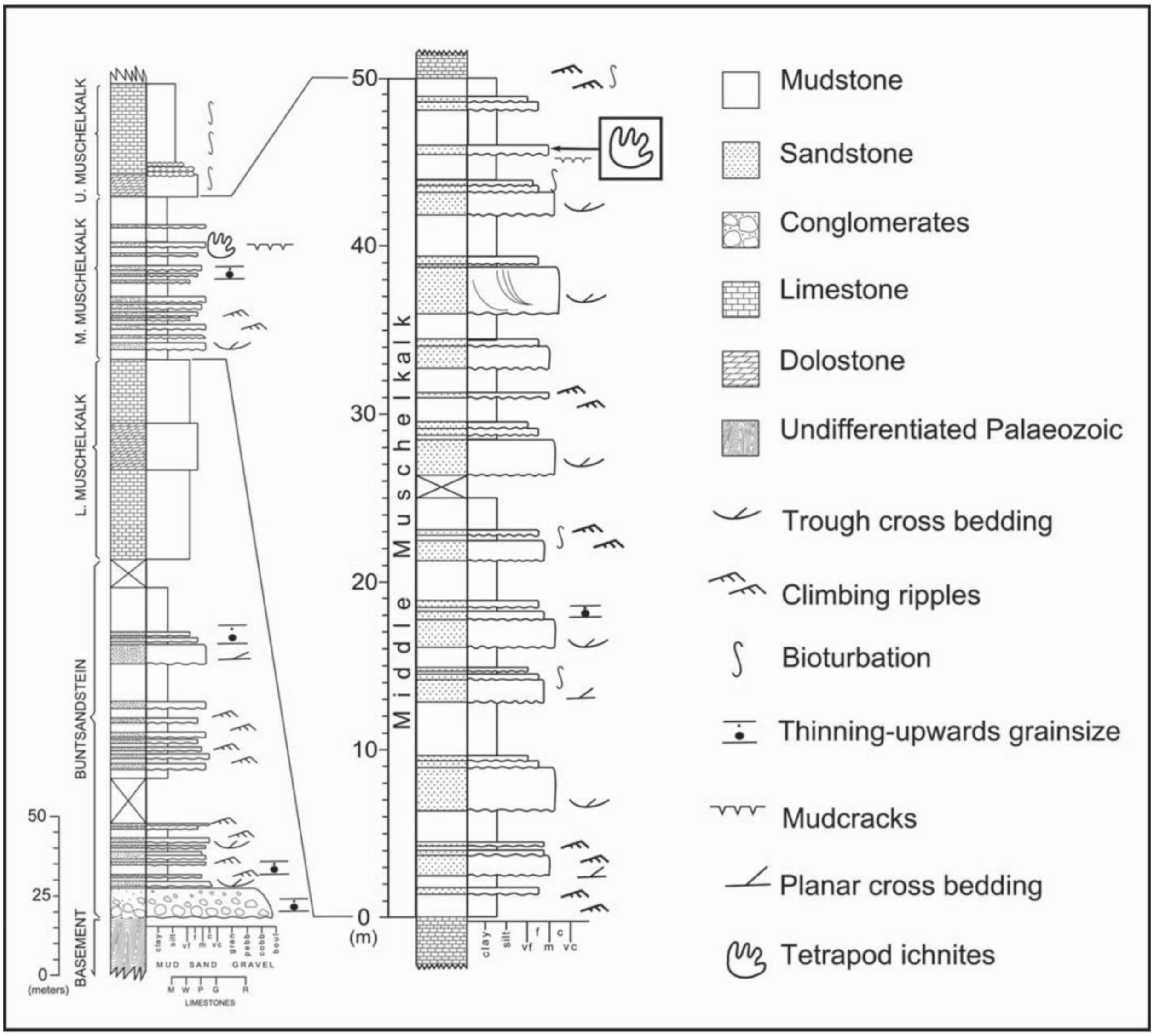

Figure 2. Collcardús Triassic stratigraphical sequence and detailed Middle Muschelkalk section, with ichnites stratigraphical situation.

4. SYSTEMATIC PALAEOICHNOLOGY

Ichnites are casts in convex hyporelief preserved in a fine to medium grain size sandstone. There are sedimentary structures corresponding to ripples and soft pebbles (observed in section), and mud-crack structures at the base surface, crossing the footprints. Vertical and sinuous invertebrate traces (burrows) are also present. There are eight tetrapod footprints on the slab base (Fig. 3). Seven ichnites are ascribed to chirotheriid ichnofamily while the other one to the rhynchosauroid ichnofamily.

Morpho-family **Chirotheriidae** Abel, 1935
Ichnogenus *Isochirotherium* Haubold, 1971b

Ichnospecies *Isochirotherium* isp. indet
(Figs 3, 4A-F; Table 1)

Referred specimens. Three pes and one manus footprints (IPS-81873a-c).

Description.

Pes. Within the three impressions, one of them is complete (*I*.3 in Figs 4A-C), one preserves digits II-V (Figs 4D-F) and the other one corresponds to the large expulsion rim close to the other chirotheriid ichnogenus footprint (*I*.4 in Fig. 3). Ichnites correspond to semiplantigrade pentadactyl impressions. They are longer than wider (174x136 mm for the complete one). Digits I-IV form a group, in which digit III is the longest, followed by the slightly shorter digit II.

Table 1. *Isochirotherium* isp., *Chirotherium* isp. and *Rhynchosauroides* isp. ichnites measures (in mm and degrees). Values in asterisk (*) are estimated.

	Chirotheriid pes footprints		
	***Isochirotherium* isp. (Fig. 4A-C)**	***Isochirotherium* isp. (Fig. 4D-F)**	***Chirotherium* isp. (Fig. 4G-I)**
Length	174.309	*166.064	164.915
Width	134.490	-	152.883
Digit I	71.446	-	48.442
Digit II	100.604	96.228	92.103
Digit III	104.831	100.489	121.689
Digit IV	74.223	76.438	107.905
Digit V	96.010	*95.569	95.078
Digits I-IV length	111.094	*135.306	145.074
Digits I-IV width	103.636	-	141.184
Divarication I-IV	36.441	-	52.595
Cross axis angle	86.949	*84.781	*84.485
Manus:Pes (area)	-	-	1:2.67

***Rhynchosauroides* isp. ichnite (Fig. 4J-L)**	
Length	38.678
Width	-
Digit I	-
Digit II	*12.931
Digit III	23.414
Digit IV	27.538
Digit V	-
Divarication II-IV	65.344

Digits II and III are closer than digits III and IV. Digits I and IV are similar in length. Digits I-IV divarication is 36.4º. Digits are straight, and pad impressions are wide and slightly convex. Large claw impressions are recognized in digits II, III and IV. The presence of claw impression in digit I remain uncertain due to the preservation. Digit V is rounded and clawless, and it is in a postero-lateral position and slightly outward rotated respect digits I-IV. Digit V pad is nearly as wide as long and is shallower impressed than digits I-IV group and situated at their base. A low ridge separates digit V from the group I-IV. Ichnites present a large expulsion rim, which is higher on the medial (inner, posterolaterally from digit I) part and shallower on the posterior and anterior parts.

Manus. Rounded ichnite, slightly wider than longer (62x67 mm), with a large expulsion rim, higher in the anterior part. This footprint is probably coupled with the partial pes impression (*I*.1 with *I*.2 in Fig. 3B).

Discussion. The longer than wider pes, the lengths and proportions of digits I-IV, the claw impressions, the situation and shape of digit V, and cross axis angles are diagnostic traits of *Isochirotherium* ichnogenus described by Haubold (1971b) and Demathieu (1985), being also the same reported in Demathieu & Demathieu (2004) and Klein *et al.* (2011). Otherwise, digit V is longer than I. This character differs from the description of Avanzini & Cavin (2009), but not from Fuglewicz *et al*. (1990), who described an *Isochirotherium* ichnospecies (*I. sanctacrucense*) with digit V even longer than digit III. These footprints are also similar to *Chirotherium* Kaup, 1835 ichnogenus, but it is discarded because digit IV is shorter than digit II, except for larger specimens (Klein & Haubold, 2003). Digit IV real length has been recognized after the detailed observation of the 3D photogrammetric model, as digit IV appears longer due to impression preservation. Pes footprints also resemble *Brachychirotherium* Beurlen, 1950, but the presence of large claws (despite bad preserved) and the width of digits I-IV (identified in the 3D model analyses) are characters that differ from this ichnogenus. Moreover, *Brachychirotherium* occurrences before Late Triassic are doubtful (Klein & Lucas, 2010; Coram & Radley, 2013; Hminna *et al.*, 2013). However, Gand *et al.* (2010) reported *Brachychirotherium* in Middle Triassic from the Iberian Ranges, thus this assignation may be take with caution. Ichnospecies remains uncertain as no trackway and manus morphologies are preserved.

Ichnogenus *Chirotherium* Kaup, 1835

Ichnospecies *Chirotherium* isp. indet.
(Figs 3, 4A-C, G-I; Table 1)

Referred specimens. One pes and two manus footprints (IPS-81873a).

Description.

Pes. Plantigrade pentadactyl pes impression, attributed to the right side. The footprint is slightly longer than wider (165x153 mm). Digit III is the longest, followed by

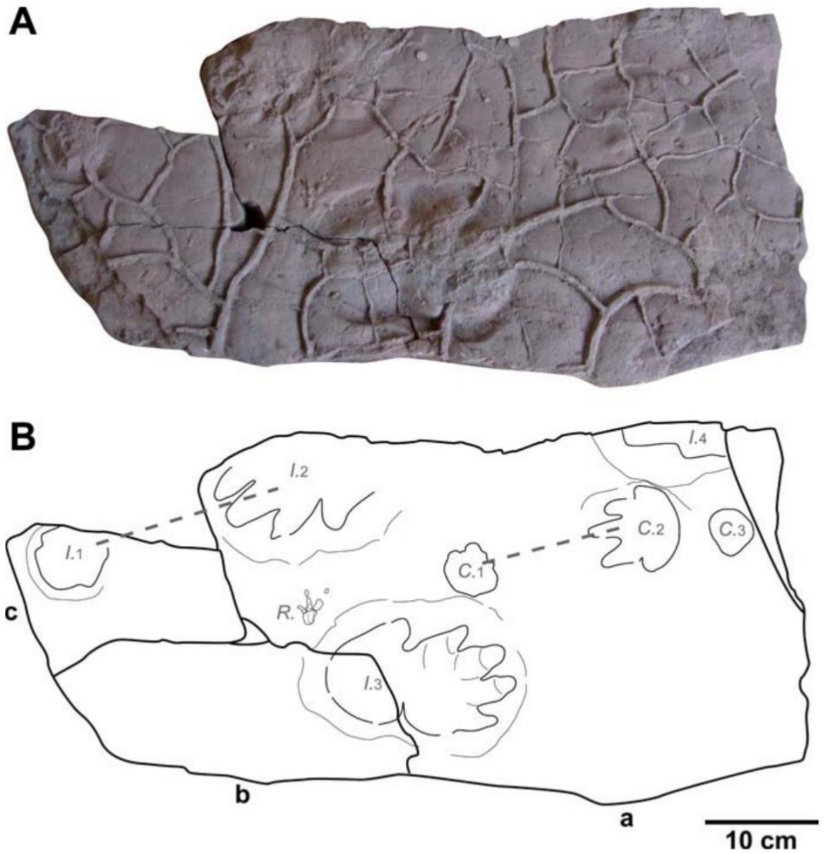

Figure 3. Sandstone slab IPS-81873a, b, c (each letter correspond to each part of the slab) with tetrapod footprints in convex hyporelief **(A)** and corresponding outline **(B)**. *C.*: *Chirotherium* isp. footprints. *I.*: *Isochirotherium* isp. footprints. *R.*: *Rhynchosauroides* isp. footprint. Dashed lines in *C.* and *I.* indicate manus-pes sets. Note the presence of abundant mud cracks.

digit IV. They are the deepest impressed digits. Digit II is shorter, and digit I is reduced, also being the shallowest impressed. Digits II to IV are nearly straight, with a slight curvature concave to the lateral (outer) part. Digit II is closer than digit IV to digit III. Digits I-IV divarication is 52.6º. Digit V is slightly posterior to the group I-IV, but the distal (anterior) part is close to the position of digit I anterior part. Digit V pad is posterior and deeper than digit I pad. There are no claw impressions preserved. Digit IV presents a shallow depression around the anterior part. Although footprint is not deeply impressed and has a smooth shape, an expulsion rim is observed on the medial (inner) part.

Manus. Two shallow rounded impressions (35-42x41-44 mm) with no expulsion rim are observed (*C.*1 and *C.*3 in Fig. 3B). One of them is beside the *Isochirotherium* isp. pes footprint (*C.*1 in Figs 4A-C), this manus is probably coupled with the previously *Chirotherium* described pes (*C.*1 with *C.*2 in Fig. 3B; see also manus/pes ratio in Table 1). None of the two ichnites preserve digits morphology.

Discussion. Pes footprint is attributed to *Chirotherium* as the general pes shape, digits morphology and relative length, digit V position, cross axis angle and manus/pes area ratio are diagnostic traits from this ichnogenus (e.g., Haubold, 1971a, b; Demathieu, 1985; Klein & Haubold, 2003; Demathieu & Demathieu, 2004). The impressions attributed to manus are tentatively assigned to *Chirotherium* because the association of one of them (*C.*1 in Figs 4A-C) with the pes ichnite, forming a manus-pes set. A similar specimen to pes footprint is described in Demathieu *et al.* (1978), which also presents a straight digit V, differing from the generally outward curved shape of the ichnogenus (e.g., Haubold, 1971a, b). Pes footprint presents characters from *Brachychirotherium*, like digit I-IV divarication and the relative large width. However, digits are much longer than wider, differing from *Brachychirotherium* (e.g., Haubold, 1971a, b; Demathieu & Demathieu, 2004). *Chirotherium* ichnospecies remains also uncertain due to the lack of manus characters and trackways, and also pes impression with more details preserved.

Morpho-family **Rhynchosauroidae** Haubold, 1966
Ichnogenus *Rhynchosauroides* Maidwell, 1911

Ichnospecies *Rhynchosauroides* isp. indet.
(Figs 3, 4J-L; Table 1)

Referred material. One partial ichnite (IPS-81873a).

Description. Small semiplantigrade left footprint of 39 mm long composed of three digits. Digits are relatively long, thin and inward curved. Digits are in increasing length from II to IV (from left to right; Figs 4J-L). Digit III (23.4 mm length) is the deepest impressed, two elongated and smooth phalangeal pads and a large claw cast are well-recognized. Digit II (12.9 mm length) is a shallow proximal elongated pad impression. Digit IV, the longest, (27.5 mm length) is distinguished by the proximal pad and a shallow claw impression. Digits divarication is 65.3º. Sole is partially impressed, outlined by an expulsion rim.

Discussion. Ichnite length, the slender and inward curved digits and their proportions and morphology are characters of *Rhynchosauroides* (e.g., Haubold, 1971a, b; Valdiserri & Avanzini, 2007). Digit impressions are attributed, from the shortest to the longest, to digits II, III and IV, as these are usually the deepest impressed digits in *Rhynchosauroides* ichnogenus (Demathieu & Demathieu, 2004). The footprint probably corresponds to a manus impression, because pes are commonly preserved just by the distal parts of the digits or even just by the claw impressions (Haubold, 1971a, b; Valdiserri & Avanzini, 2007; Diedrich, 2008), and herein described footprint preserves part of the sole. Ichnite distinction is rather difficult due to the presence of mud-cracks and invertebrate traces, the relative rough sediment in comparison with the small ichnite and the proximity of the *Isochirotherium* isp. pes footprint.

5. DISCUSSION

5.1. Ichnofaunal diversity and preservation

Three different ichnotaxa are present in the slab (*Isochirotherium* isp., *Chirotherium* isp. and *Rhynchosauroides* isp.), being the chirotheriid trackmakers (crurotarsians) the dominant group over rhynchosauroid trackmakers (lacertoid-type reptile) (*sensu* Gand *et al.*, 2010). The relative abundance of ichnites and the floodplain within alluvial system palaeoenvironment are indicative of proper conditions for life development and footprints preservation.

Substrate and environmental conditions influence on ichnites shape and preservation causing that footprints usually present extramorphological variations that can difficult the ichnotaxa assignation, overall at ichnospecies level (Klein *et al.*, 2011), as in the herein described footprints. Soft pebbles are observed within the basal part of the cross laminated sandstone, thus the original mudstone substrate surface was partially eroded during sand sedimentation. Mud cracks also influence in footprints preservation, because were formed after trackmakers impressions.

For a more precise ichnotaxonomic assignation, the sequence of structures and processes observed in the slab, in relation to ichnites, should be known, as in this way modifications on tetrapod traces are identified, therefore original footprint shape is recognized. Otherwise, the 3D photogrammetric models are useful in the identification of ichnites shape and sequence of structures formation, because depth maps generated establish the height from each part of the structures. Footprints were impressed at least in two episodes, represented by different ichnotaxa. Processes sequence (including footprints formation) and the inferred substrate conditions variations are as follow:

1) Muddy substrate water saturated. Impression of *Rhynchosauroides* isp. and *Isochirotherium* isp. footprints. Expulsion rims are observed in both ichnogenera, being in the chirotheriid footprint larger, in relation to footprint size. Although *Isochirotherium* isp. complete pes (*I.*3 in Figs 4A-C) is close to *Rhynchosauroides* isp. track (Figs 4J-L), there is no overprinting, and so the order of footprints impression remains uncertain. Preservation of relatively small details in *Rhynchosauroides* isp. ichnite such as claw impressions and digit pads indicates that substrate was soft and, despite trackmaker small weight and size, footprint is well-distinguished. Despite *Isochirotherium* isp. footprints are affected by desiccation structures, the resulting shape is not significantly modified. This is likely to the result of sediment compaction and water displacement due to trackmakers weight (trackmakers hardened substrate under pedes pressure). Therefore, displacements due to desiccation process are observed in footprints outer parts, where trackmakers pedes pressure was lower, and also in expulsion rims, which are clearly crossed by mud crack structures. It is clearly documented that footprints are cracked and not the other way round. Footprints are first impressed (substrate humid enough to develop an expulsion rim) and latter cracked (substrate on desiccation process). It is also important to remark that at the footprint centre, mud cracking is hardly noticeable.

2) Substrate desiccation process. Impression of *Chirotherium* isp. footprints. These footprints were impressed when substrate was decreasing in water content (i.e., it was hardening) and mud crack structures were forming. The smooth shape and the lack of morphological elements (e.g., claw marks and phalangeal pads) indicate that the footprint was impressed in a drying substrate. Despite mud cracks are crossing the footprints, they have no influence on the resulting shape, because there are no displacements in the impressions.

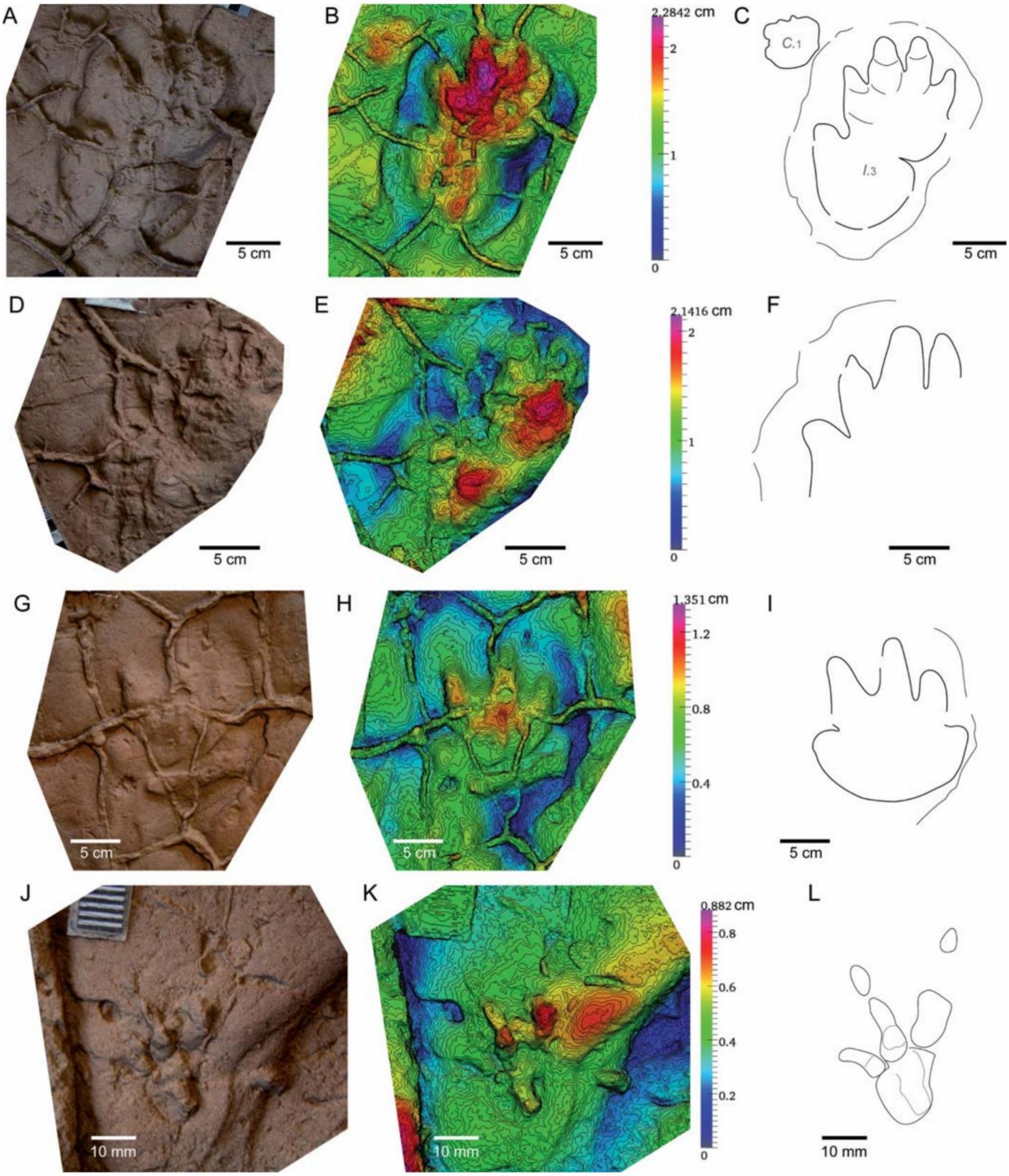

Figure 4. Tetrapod footprints **(A, D, G, J)** with their corresponding 3D photogrammetric models **(B, E, H, K)** and outlines **(C, F, I, L)**. *Isochirotherium* isp. right pes **(A-F)**, *Chirotherium* isp. right pes **(G-I)** and *Rhynchosauroides* isp. left ?manus **(J-L)**. In C, *C.*1 and *I.*3 reference *Chirotherium* and *Isochirotherium* respectively.

5.2. Age and palaeobiogeographic implications

A previous palynological study dated the Middle Muschelkalk facies from the Catalan Coastal Ranges as Late Anisian-Early Ladinian (Solé de Porta *et al*., 1987). The stratigraphic range from *Chirotherium* and *Rhynchosauroides* is larger (Klein & Lucas, 2010), so they are not useful in dating, but *Isochirotherium* isp. age interval is suspected as Anisian-Early Ladinian (Klein & Lucas, 2010), which is in agreement with the inferred age from palynology.

Marine facies on the Catalan Basin during Late Anisian are represented by the Lower Muschelkalk deposits (Calvet & Marzo, 1994; López-Gómez *et al*., 2002; Linol *et al*., 2009). According to Calvet & Ramón (1987), these deposits are indicative of a transgression (tidal to shoal bars deposits) followed by a punctual regression (sabkha deposits, Middle Muschelkalk facies) and the posterior transgression continuation. The studied footprints are in the clastic interval within Muschelkalk carbonates that, despite etymological unconsistency, this clastic unit has been referred as Middle Muschelkalk. Marine faunas are known from several Iberian localities from Ladinian age in Upper Muschelkalk facies (see Vía-Boada *et al*., 1977; Fortuny *et al*., 2011 for a review). The presence of ichnofauna in the continental deposits may represent palaeobiogeographic indicators: The marine transgression occurred in the Catalan Basin caused that continental fauna migrated while in other Iberian localities (e.g., Iberian Ranges, see Gand *et al*., 2010) the continental sedimentation persisted. We do not observe ichnotaxa dependence of the environment, i.e., ichnotaxa here reported in clastic sediments are also reported in carbonate settings. Connectivity between clastic and carbonate environments is does strongly suggested.

6. CONCLUSIONS

Tetrapod footprints from Middle Muschelkalk facies of the Catalan Basin are reported for the first time in the Iberian Peninsula. Footprints are preserved in convex hyporelief in a sandstone slab from floodplain and fluvial palaeoenvironments.

Three different ichnogenera (*Isochirotherium* isp., *Chirotherium* isp. and *Rhynchosauroides* isp.) have been identified within the eight tetrapod footprints analysed. The 3D models generated with photogrammetry technique permitted precise ichnotaxonomic identification. The application of this technique can be helpful in further analyses on Triassic tetrapod footprints.

During ichnites impression, environment was dry with seasonal humidity, while during the sand sedimentation there was a low to moderate energy aquatic environment.

The age interval provided by the ichnological data is Anisian-Early Ladinian, in agreement with the previous palynological analyses, denoting Late Anisian-Early Ladinian age.

Herein reported tetrapod footprints confirm homogeneous Middle Triassic ichnofauna. Despite facies differences due to transgression within Iberian and Catalan basins, ichnotaxa are similar, thus, connections with neighbouring basins probably persisted.

ACKNOWLEDGMENTS

Our thanks goes to the organizing committe of the XI EJIP "Encuentro de Jóvenes Investigadores en Paleontología" held in Atarfe (Granada) in 2013, and specially to Carlos Martínez-Perez and Pilar Navas-Parejo, as well as to Adán Pérez-García for abstract revision. We thank comments and suggestions from an anonymous reviewer and Alberto Pérez-López that improved a previous version of the manuscript, as well as to the Associated Editor Matías Reolid. Authors also want to thank Marina Bonet for her contribution in the finding of the ichnites. E.M. is supported by a PIF grant from the Universitat Autònoma de Barcelona and also by the SYNTHESYS Proyect (DE-TAF-2650 at Museum für Naturkunde; http://www.synthesys.info/).

REFERENCES

Abel, O. 1935. Vorzeitliche Lebensspuren. *Fischer*, Jena.

Avanzini, M. & Cavin, L. 2009. A new *Isochirotherium* trackway from the Triassic of Vieux Emosson, SW Switzerland: stratigraphic implications. *Swiss Journal of Geosciences*, 102, 353-361.

Belvedere, M., Jalil, N.-E., Breda, A., Gattolin, G., Bourget, H., Khaldoune, F. & Dyke, G.J. 2013. Vertebrate footprints from the Kem Kem beds (Morocco): A novel ichnological approach to faunal reconstruction. *Palaeogeography, Palaeoclimatology, Palaeoecology*, 383-384, 52-58.

Beurlen, K. 1950. Neue Fährtenfunde aus der fränkischen Trias. *Neues Jahrbuch für Geologie und Paläontologie, Monatshefte*, 1950, 308-320.

Calafat, F., Fornós, J., Marzo, M., Ramos-Guerrero, E. & Rodríguez-Perea, A. 1987. Icnología de vertebrados de la facies Buntsandstein de Mallorca. *Acta Geologica Hispanica*, 21-22, 515-520.

Calvet, F. & Marzo, M. 1994. *El Triásico de las Cordilleras Costero Catalanas: Estratigrafía, Sedimentología y Análisis Secuencial*. Cuaderno de Excursión. III Coloquio de Estratigrafía y Paleoestratigrafía del Pérmico y Triásico de España. Field Guide.

Calvet, F. & Ramón, X. 1987. Estratigrafía, sedimentología y diagénesis del Muschelkalk inferior de los Catalánides. *Cuadernos de Geología Ibérica*, 11, 141-169.

Calzada, S. 1987. Niveles fosilíferos de la facies Buntsandstein (Trias) en el sector norte de los Catalánides. *Cuadernos de Geología Ibérica*, 11, 256-271.

Coram, R.A. & Radley, J.D. 2013. A chirothere footprint from the Otter Sandstone Formation (Middle Triassic, late Anisian) of Devon, UK. *Proceedings of the Geologists' Association*, 124, 520-524

Demathieu, G. 1985. Trace fossil assemblages in middle Triassic marginal marine deposits, Eastern border of the Massif Central, France. In: *Biogenic structures* (ed. Curren H.A.). SEPM Special Publications, 35, 53-66.

Demathieu, G. & Demathieu, P. 2004. Chirotheria and other ichnotaxa of the European Triassic. *Ichnos*, 11, 79-88.

Demathieu, G. & Saiz de Omeñaca, J. 1990. Primeros resultados del estudio de un nuevo yacimiento de icnofauna triásica, en Peña Sagra (Cantabria, España). *Estudios Geológicos*, 46, 147-150.

Demathieu, G., Ramos, A. & Sopeña, A. 1978. Fauna icnológica del Triásico del extremo noroccidental de la Cordillera Ibérica (Prov. de Guadalajara). *Estudios Geológicos*, 34, 175-186.

Demathieu, G., Pérez-López, A. & Pérez-Lorente, F. 1999. Enigmatic ichnites in the Middle Triassic of Southern Spain. *Ichnos*, 6, 229-237.

Díaz-Martínez, I. & Pérez-García, A. 2012. Historical and comparative study of the first spanish vertebrate paleoichnological record and bibliographic review of the Spanish Chirotheriid footprints. *Ichnos*, 19, 141-149.

Diedrich, C. 2008. Millions of reptile tracks - Early to Middle Triassic carbonate tidal flat migration bridges of Central Europe. *Palaeogeography, Palaeoclimatology, Palaeoecology*, 259, 410-423.

Dinarès-Turell, J., Diez, J.B., Rey, D. & Arnal, I. 2005. “Buntsandstein” magnetostratigraphy and biostratigraphic reappraisal from eastern Iberia: Early and Middle Triassic stage boundary definitions through correlation to Tethyan sections. *Palaeogeography, Palaeoclimatology, Palaeoecology*, 229, 158-177.

Durán, H. 1990. El Paleozoico de les Guilleries. *Acta Geologica Hispanica*, 25, 83-103.

Falkingham, P.L. 2012. Acquisition of high resolution three-dimensional models using free, open-source, photogrammetric software. *Palaeontologia Electronica*, 15(1), 1-15.

Fortuny, J., Bolet, A., Sellés, A.G., Cartanyà, J. & Galobart, À. 2011. New insights on the Permian and Triassic vertebrates from the Iberian Peninsula with emphasis on the Pyrenean and Catalonian basins. *Journal of Iberian Geology*, 37, 65-86.

Fortuny, J., Bolet, A., Oms, O., Bonet, M., Diviu, M., Rodríguez, P. & Galobart, À. 2012. Permian and Triassic ichnites from the Catalonian and Pyrenean basins (Eastern Iberian Peninsula). 10th Annual Meeting of the EAVP, Abstract book, p. 73-75.

Fuglewicz, R., Ptaszyński, T. & Rdzanek, K. 1990. Lower Triassic footprints from the Swiqtokrzyskie (Holy Cross) Mountains, Poland. *Acta Palaeontologica Polonica*, 35, 109-164.

Gand, G., De La Horra, R., Galán-Abellán, B., López-Gómez, J., Fernández-Barrenechea, J., Arche, A. & Benito, M.I. 2010. New ichnites from the Middle Triassic of the Iberian Ranges (Spain): palaeoenvironmental and palaeogeographical implications. *Historical Biology*, 22, 1-17.

García-Bartual, M., Rincón, R. & Hernando, S. 1996. Propuesta de una nueva técnica de estudio mediante análisis digital de imagen en huellas quiroteroides encontradas en el Triásico de Nuévalos (Provincia de Zaragoza). *Cuadernos de Geología Ibérica*, 20, 301-312.

Haubold, H. 1966. Therapsiden- und Rhynchocephalen-Fährten aus dem Buntsandstein Südthüringens. *Hercynia, NF*, 3, 147-183.

Haubold, H. 1971a. Die Tetrapodenfährten des Buntsandsteins in der Deutschen Demokratischen Republik und in Westdeutschland und ihre Äquivalente in der gesamten Trias. *Paläntologische Abhandlungen, Abteilung a Paläozoologie*, 395-548.

Haubold, H. 1971b. *Ichnia Amphibiorum et Reptiliorum fossilium. Encyclopedia of Paleoherpetology 18*. Gustav Fischer Verlag, Stuttgart and Portland-USA.

Hminna, A., Voigt, S., Klein, H., Saber, H., Schneider, J.W. & Hmich, D. 2013. First occurrence of tetrapod footprints from the continental Triassic of the Sidi Said Maachou area (Western Meseta, Morocco). *Journal of African Earth Sciences*, 80, 1-7.

Kaup, J.J. 1835. Fährten von Beuteltieren. *Das Tierreich*, 246-248.

Klein, H. & Haubold, H. 2003. Differenzierung von ausgewählten Chirotherien der Trias mittels Landmarkanalyse. *Hallesches Jahrbuch für Geowissenschaften*, B25, 21-36.

Klein, H. & Lucas, S.G. 2010. Tetrapod footprints - their use in biostratigraphy and biochronology of the Triassic. *Geological Society London Special Publications*, 334, 419-446.

Klein, H., Voigt, S., Saber, H., Schneider, J.W., Fischer, J., Hminna, A. & Brosig, A. 2011. First occurrence of a Middle Triassic tetrapod ichnofauna from the Argana Basin (Western High Atlas, Morocco). *Palaeogeography, Palaeoclimatology, Palaeoecology*, 307, 218-231.

Linol, B., Bercovici, A., Bourquin, S., Diez, J.B., López-Gómez, J., Broutin, J., Durand, M. & Villanueva-Amadoz, U. 2009. Late Permian to Middle Triassic correlations and palaeogeographical reconstructions in south-western European basins: New sedimentological data from Minorca (Balearic Islands, Spain). *Sedimentary Geology*, 220, 77-94.

López-Gómez, J., Arche, A. & Pérez-López, A. 2002. Permian and Triassic. In: *The Geology of Spain* (eds. Gibbons, W. & Moreno, T.). Geological Society Publishing House, London, 185-212.

Maidwell, F.T. 1911. Notes on footprints from the Keuper of Runcorn Hill. *Proceedings of the Liverpool Geological Society*, 11, 140-152.

Pérez-López, A. 1993. Estudio de las huellas de reptil, del icnogénero *Brachychiroterium*, encontradas en el Trías Subbético de Cambil. *Estudios Geológicos*, 49, 77-86.

Petti, F.M., Avanzini, M., Nicosia, U., Girardi, S., Bernardi, M., Ferretti, P., Schirolli, P. & Sasso, C.D. 2009. Late Triassic (Early-Middle Carnian) chirotherian tracks from the Val Sabbia sandstone (Eastern lombardy, Brescian Prealps, Northern Italy). *Rivista Italiana di Paleontologia e Stratigrafia*, 115, 277-290.

Solé de Porta, N., Calvet, F. & Torrentó, L. 1987. Análisis palinológico del Triásico de los Catalánides (NE España). *Cuadernos de Geología Ibérica*, 11, 237-254.

Valdiserri, D. & Avanzini, M. 2007. A Tetrapod Ichnoassociation from the Middle Triassic (Anisian, Pelsonian) of Northern Italy. *Ichnos*, 14, 105-116.

Vía-Boada, L., Villalta, J.F. & Esteban-Cerdá, M. 1977. Paleontología y Paleoecología de los yacimientos fosilíferos del Muschelkalk superior entre Alcover y Mont-Ral (Montañas de Prades, provincia de Tarragona). *Cuadernos de Geología Ibérica*, 4, 247-256.

Annex 2. Rhynchosauroides *footprint variability in a Muschelkalk detrital interval (late Anisian–middle Ladinian) from the Catalan Basin (NE Iberian Peninsula)*

L'Annex 2 correspon al treball acceptat per publicació a la revista *Ichnos* el 28 de setembre de 2016:

Mujal, E., Iglesias, G., Oms, O., Fortuny, J., Bolet, A., Méndez, J.M., Accepted. *Rhynchosauroides* footprint variability in a Muschelkalk detrital interval (late Anisian–middle Ladinian) from the Catalan Basin (NE Iberian Peninsula). Ichnos (accepted 28/09/2016).

En aquest article l'autor E. M. ha contribuït en: plantejament del treball; tasques de camp, incloent prospecció i documentació de les traces fòssils; elaboració dels models fotogramètrics 3D de les icnites; anàlisis de sedimentologia i icnologia; interpretació i discussió de tots els resultats; redacció del manuscrit; preparació i maquetació de les figures 2–6; autor per correspondència amb la revista.

Rhynchosauroides footprint variability in a Muschelkalk detrital interval (late Anisian-middle Ladinian) from the Catalan Basin (NE Iberian Peninsula)

Eudald Mujal[1], Guillem Iglesias[1], Oriol Oms[1], Josep Fortuny[2,3], Arnau Bolet[3], Josep Manel Méndez[3]

[1]Departament de Geologia, Universitat Autònoma de Barcelona, E-08193 Bellaterra, Spain

[2] Centre de Recherches en Paléobiodiversité et Paléoenvironnements, UMR 7202 CNRS-MNHN-UPMC, Muséum national d'Histoire naturelle, Bâtiment de Paléontologie, 8 rue Buffon, CP38, F-75005 Paris, France

[3]Institut Català de Paleontologia Miquel Crusafont, ICTA-ICP building, c/ de les columnes, s/n, E-08193 Cerdanyola del Vallès, Spain

Corresponding author: Eudald Mujal, Departament de Geologia, Universitat Autònoma de Barcelona, E-08193 Bellaterra, Spain. E-mail: eudald.mujal@gmail.com

Abstract

The Middle Triassic successions of coastal and distal alluvial systems are often characterized by the presence of the tetrapod ichnotaxon *Rhynchosauroides*. Nevertheless, few studies paid attention on the paleoenvironmental implications of this widely distributed ichnogenus. The finding of a new *Rhynchosauroides*-dominated tracksite opens the window to the use of such footprints in paleoenvironmental studies. The tracksite is located in the active quarry of Pedrera de Can Sallent, at Castellar del Vallès (Catalan Basin, NE Iberian Peninsula). The footprints were recovered from the Middle Muschelkalk detrital unit, composed of a claystone-sandstone-gypsum succession from a sabkha setting of late Anisian-middle Ladinian age. This unit was deposited during a short regression interval within the main Middle Triassic transgression represented by the Muschelkalk facies. The ichnoassociation is composed of *Rhynchosauroides* isp., and a single, partially preserved, undetermined large footprint. Among *Rhynchosauroides* specimens, three different preservation states were recognized, corresponding to substrates in (1) subaqueous conditions (surfaces with scarce, deformed and deeply impressed ichnites), (2) occasionally flooded (mostly trampled surfaces, footprints commonly well preserved) and (3) subaerial exposition (surfaces with few footprints, sometimes corresponding to faint impressions or only preserved by claw marks). The footprint morphological variations of *Rhynchosauroides* are correlated to substrate rheology and further to the environmental conditions. *Rhynchosauroides* is a characteristic morphotype that often dominates in the Anisian-Ladinian coastal and distal alluvial settings of several European tracksites. Therefore, these ichnoassociations in such environments, awaiting further detailed analyses, may constitute a distinct ichnocoenosis.

Keywords

Vertebrate ichnology, Preservation, Ichnofacies, Sabkha, Middle Triassic

Introduction

Rhynchosauroides is a well-known and widely distributed ichnotaxon, with an age interval spanning from the Late Permian to the Late Jurassic (Valentini et al., 2007; Avanzini et al., 2010). This ichnogenus is especially abundant in the Middle Triassic (Anisian-Ladinian), with most of its record preserved in coastal (e.g., tidal and lagoon) and alluvial paleoenvironments (Demathieu, 1985; Avanzini and Renesto, 2002; Melchor and De Valais, 2006; Valdiserri and Avanzini, 2007; Avanzini and Mietto, 2008; Diedrich, 2008; Todesco et al., 2008; Gand et al., 2010; Klein and Lucas, 2010b; Klein et al., 2011; Mujal et al., 2015). Several ichnospecies have been erected (e.g., Haubold, 1971a, b; Hunt and Lucas, 2007c), but few of them remain valid (Klein and Niedźwiedzki, 2012), as the others were mostly derived from specimens with extramorphological features (substrate- and/or behavior-related). Hunt and Lucas (2007a, d) established the bases of vertebrate ichnofacies, and Lockley (2007) provided additional remarks. Nevertheless, *Rhynchosauroides* was only mentioned for its occurrence (together with *Synaptichnium* and *Rotodactylus*) in the Early-Middle Triassic *Chirotherium* ichnocoenosis of the *Batrachichnus* ichnofacies and the Late Triassic *Grallator-Brachychirotherium-Rhynchosauroides* ichnofacies (Hunt and Lucas, 2007a, d; Lockley, 2007).

At this point, a revision of the paleoenvironmental implications of *Rhynchosauroides* is needed. Our work deals with a new tracksite of the Catalan Coastal Ranges (CCR, NE Iberian Peninsula) bearing abundant *Rhynchosauroides* tracks and representing a well-documented example to contribute to the use of vertebrate trace fossils as indicators of substrate conditions (see Melchor and Sarjeant, 2004; Melchor, 2015).

Geological setting

The studied specimens were found in the outcrops of the Pedrera de Can Sallent quarry from Castellar del Vallès town (NNE of Barcelona, NE Iberian Peninsula). This region is located at the Prelitoral Range, corresponding to the Central Domain of the Catalan Coastal Ranges (CCR; Anadón et al., 1979; Fig. 1A, B). During the Triassic, the CCR corresponded to the so called Catalan Basin (Calvet and Marzo, 1994; Fortuny et al., 2011). The geological succession is constituted, from base to top, by the Cambro-Ordovician (Variscan) basement, the Triassic sequences and the Cenozoic cover. The Triassic sequences are composed of the classic Germanic facies, comprising six lithostratigraphic units, with a thickness ranging from 500 to 800 m (Calvet and Marzo, 1994). These facies are diachronic, as they were deposited in different rift systems in Central and Eastern Europe (López-Gómez et al., 2002).

At this quarry the Triassic sequence is lying unconformably over the Variscan basement, and is composed by four of the six main lithostratigraphic units, from base to top: Buntsandstein, Lower, Middle and Upper Muschelkalk. The Tertiary conglomerates unconformably cover the Triassic. Due to the compressive phase of the Paleogene (Alpine orogeny), the Cambro-Ordovician basement thrusts over the Triassic sequences, which are inverted (Fig. 1C). The Triassic sequences from the Pedrera de Can Sallent are generally defined by the following features, from base to top:

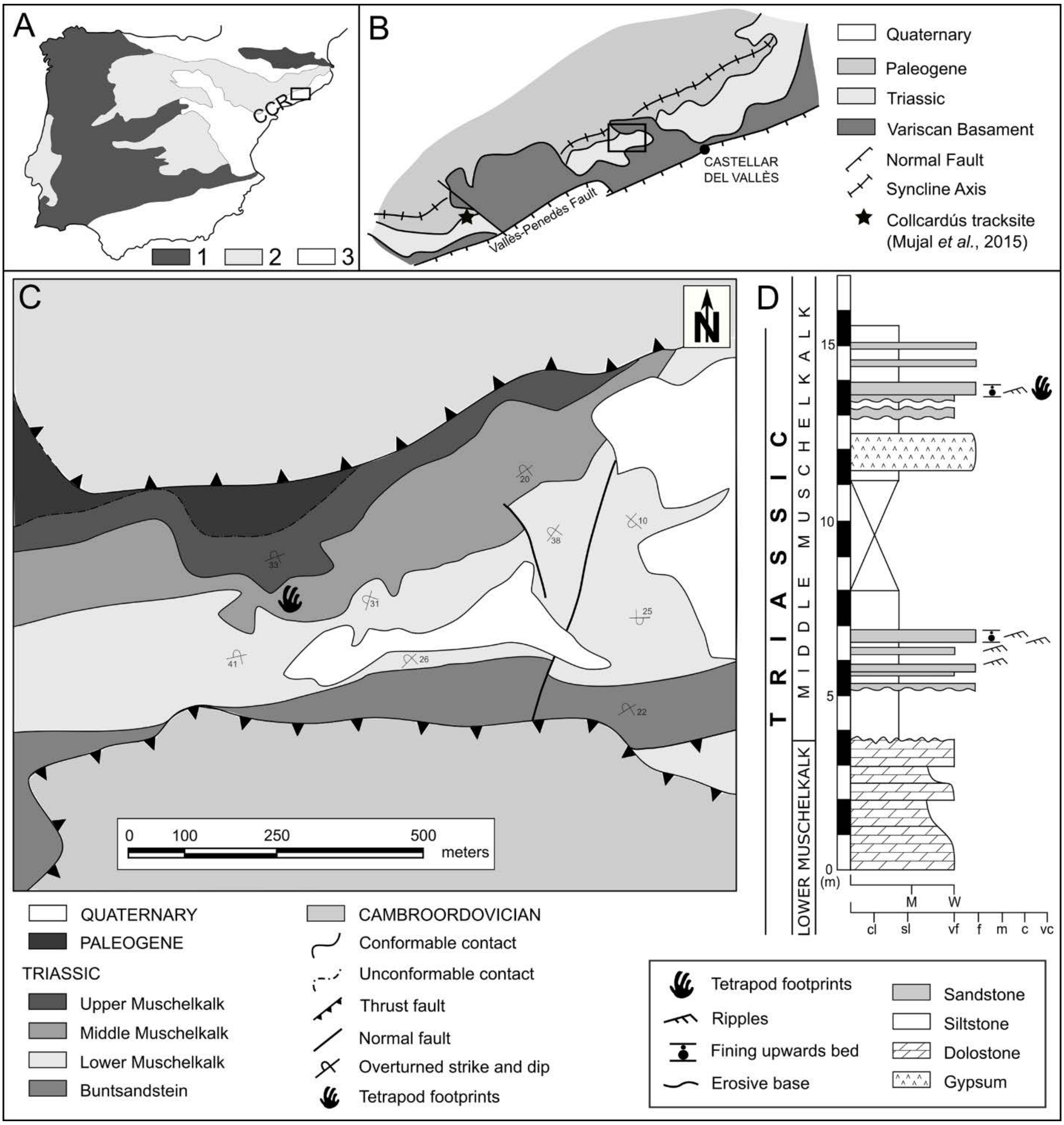

Figure 1. Geological setting. A. Geological and geographic situation (modified from Escudero-Mozo et al., 2015); 1. Variscan Massif; 2. Alpine Ranges; 3. Paleogene Basins. B. Regional structure and litostratigraphy of the Catalan Coastal Ranges (modified from Berástegui et al., 1996). C. Geological map of the studied area (squared in B) with the situation of the tracksite (WGS84 UTM 31T 420345E 4607521N). D. Detailed stratigraphic sequence of the Middle Muschelkalk outcrop in Pedrera de Can Sallent.

1. The Buntsandstein facies consist of a fining upwards sequence of reddish alluvial deposits generally ranging from braided fluvial systems (quartz conglomerates and coarse sandstones) to meandering and floodplain systems (channel-form sandstones with cross stratification and mudstones). At the top of the sequence versicolor mudstones are found, interbedded with limestone levels, and interpreted as paleosols (see Calvet and Marzo, 1994; Dinarès-Turell et al., 2005).

2. The Lower Muschelkalk facies correspond to a limestone sequence resulting from a marine transgression. Limestones are either laminated or massive, with some dolomitic intervals (of diagenetic origin); bioclasts, bioturbations and siliceous nodules occur (Calvet and Marzo, 1994).

3. The Middle Muschelkalk facies correspond to the unit containing the studied tracks, and are of detrital origin in the Catalan Basin (Calvet and Marzo, 1994; Pérez-López and Pérez-Valera, 2007). The succession is mainly composed of red mudstones and fine-grained sandstones with some gypsum layers interbedded. These facies broadly correspond to coastal and distal alluvial systems (i.e., environments with both continental and marine influence, see below for further details; Calvet and Marzo, 1994).

4. The Upper Muschelkalk facies consist of micritic limestones and dolostones with bioturbations, rough stratification, and occasionally with ooids. These deposits result from the second Triassic marine transgression (Escudero-Mozo et al., 2015).

The footprint-bearing unit

All herein reported footprints were recovered in the Middle Muschelkalk facies. This unit is dated as latest Anisian-middle Ladinian by palynology and conodonts (Solé de Porta et al., 1987; Márquez-Aliaga et al., 2000; Dinarès-Turell et al., 2005). Mujal et al. (2015) reported the first tetrapod footprints in the Middle Muschelkalk facies from the Iberian Peninsula, composed of an isolated track-bed from a distal alluvial setting at the nearby Collcardús region (Fig. 1B).

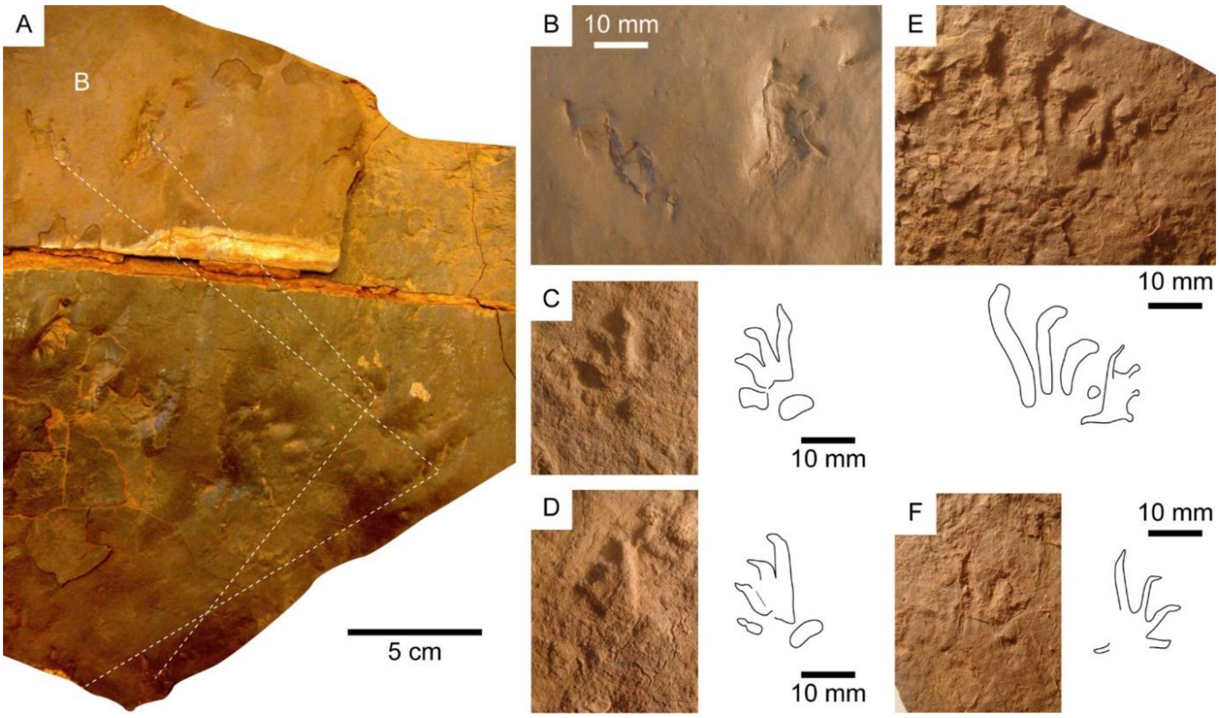

Figure 2. *Rhynchosauroides* isp. ichnites I. A-D. IPS-73695, with trackway (A) and detail of one manus-pes sets (B). C-F. Tracks of IPS-73688, with isolated manus in convex hyporelief (C, D), and a manus-pes set (E) and a manus (F) in concave epirelief.

Particularly, in the new tracksite herein reported, the basal part of the unit is constituted by reddish mudstones followed by an alternation of decimetric mudstones, very fine- and fine-grained sandstones, some of undulated geometry, fining upwards and with abundant ripples. After a covered interval, the basal portion continues with a decimetric level of gypsum followed by red mudstones interbedded with three fine- to very fine-grained centimetric sandstones (Fig. 1D). Several track-bearing beds, *in situ*, were found in this basal part.

The middle part of the sequence is constituted by an alternation of reddish mudstones with fine- to very fine-grained sandstone layers. These beds are of 4-5 cm thick in average. They are highly laminated, with abundant flow and wave ripples. Several *ex situ* slabs with the grain size of the described sandstone layers were found in this middle part of the unit. Due to tectonics, this succession is deformed, with several S-shape folds, thus precluding a correct measurement of the succession thickness.

The upper portion of the Middle Muschelkalk unit do not expose surfaces, and in some parts is not cropping out. When observed, it presents a similar pattern to the middle part of the sequence.

The thickness of the succession, despite highly deformed in some intervals, is estimated to be of approximately 100 m (López-Blanco, 1994). The alternation of mudstones and sandstones, and the evaporite (gypsum) levels, as well as sedimentary structures such as flow and wave ripples and raindrop impressions, indicate ephemeral floods after long desiccation periods. Wrinkle structures are also observed in surfaces preserving scarce and faint footprints. Nevertheless, the only structures denoting subaerial exposure are rain drop impressions in some slabs, but no other desiccation structures such as mud-cracks are observed. Calvet and Marzo (1994) interpreted these deposits as either playa-lake or sabkha systems. After our sedimentary and ichnological analyses and interpretations, we suggest that the most reliable setting is that of a sabkha system (see discussion for further details).

Material and methods

Fieldwork was performed in the active quarry of Pedrera de Can Sallent (PCS, Castellar del Vallès, Barcelona) during Summer of 2012 (paleontological prospections), Winter-Spring of 2014 and Winter of 2016 (stratigraphic and sedimentological analyses). The slabs bearing footprints were collected and placed in the logged stratigraphic sections and geological maps. The ichnological study was carried out following both classical and modern techniques. Nomenclature follows that of Haubold (1971a, b) and Leonardi (1987). Ichnites were outlined in transparency films and subsequently digitized with a vector-based drawing software. Several 3D photogrammetric models were performed in order to distinguish small features and extramorphological variations. Photographs were taken with a digital compact camera Sony T-200 of 8.1 Megapixel and were processed using three open access software: Visual SFM (v0.5.22, http://www.ccwu.me/vsfm/; to obtain the point cloud), MeshLab (v.1.3.2, http://meshlab.sourceforge.net/; to crate, scale and orientate the 3D mesh), and ParaView (v.4.1.0, http://www.paraview.org; to create the color depth maps and contour lines) (see further details in

Mujal et al., 2015, 2016a, b). The recovered slabs are stored at the Institut Català de Paleontologia (IPS, Sabadell, Catalonia, Spain).

Systematic paleoichnology

The reported specimens are found in very fine- to fine-grained sandstones and in different states of preservation, ranging from isolated faint impressions to trampled surfaces and deep and deformed ichnites, hence morphological or ichnotaxonomic affinities, as well as the recognition of trackways and even manus-pes sets, are difficult to discern in some cases.

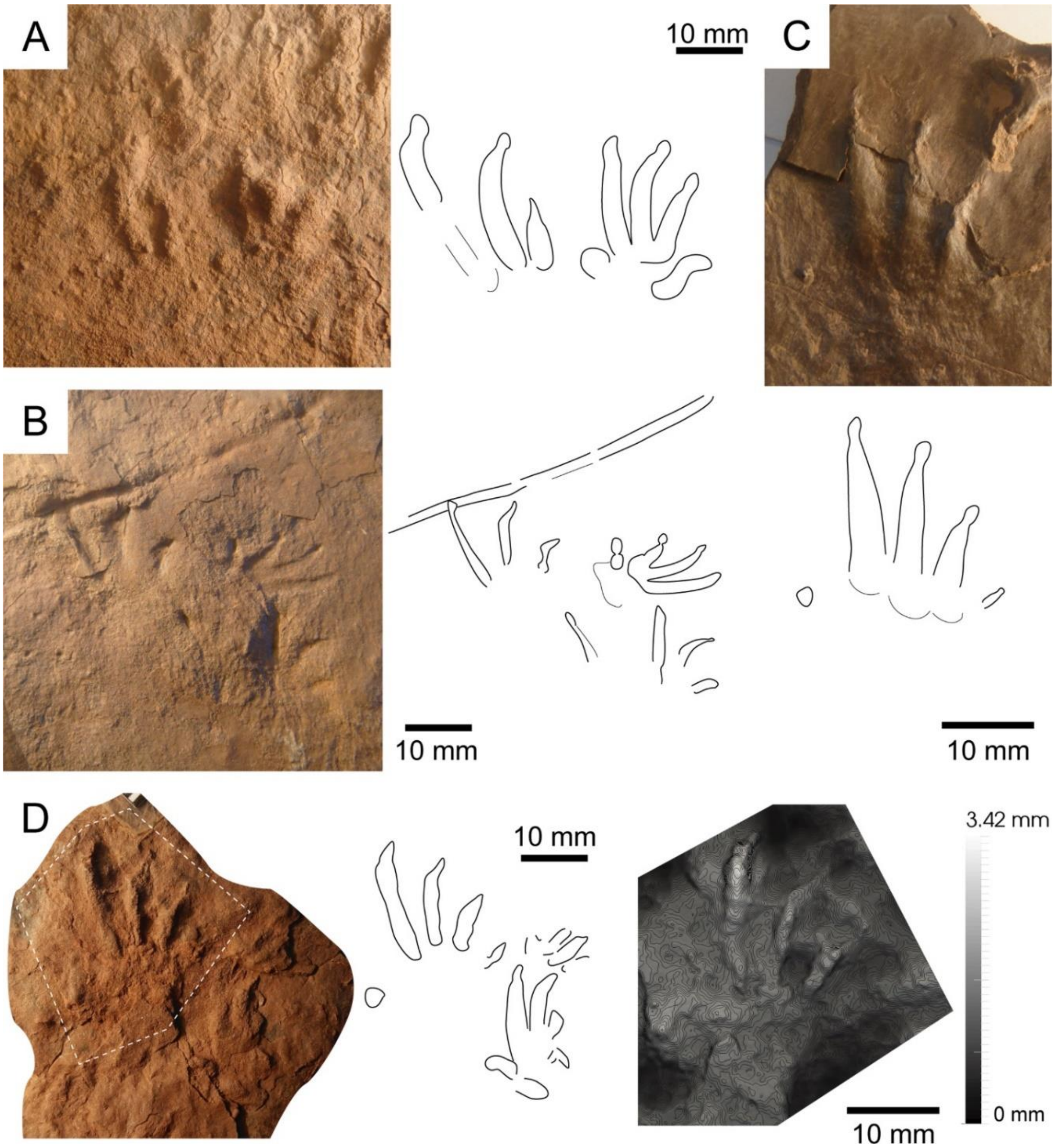

Figure 3. *Rhynchosauroides* isp. ichnites II. A. Manus-pes set of IPS-73688. B. Manus-pes set and isolated manus with tail mark of IPS-89574. C. Pes of IPS-73695. D. Pes with the 3D model (dashed white line) and possible manus track of IPS-89587 (G).

Morpho-family Rhynchosauroidae Haubold, 1966

Ichnogenus *Rhynchosauroides* Maidwell, 1911

***Rhynchosauroides* isp.**

Figs. 2, 3, 4

Material: Slabs bearing footprints in both convex and concave relief, including trampled surfaces and isolated tracks, as well as slabs with footprints in several layers. The track-bearing slabs are: IPS-73688, IPS-73689, IPS-73690, IPS-73692, IPS-73693, IPS-73694, IPS-73695, IPS-73696, IPS-73697, IPS-73698, IPS-73699, IPS-73700, IPS-73701, IPS-73702, IPS-73703, IPS-73704, IPS-73705, IPS-73706, IPS-73707, IPS-73708, IPS-73709, IPS-73710, IPS-73711, IPS-73712, IPS-73713, IPS-73714, IPS-73715, IPS-73716, IPS-73717, IPS-73718, IPS-73719, IPS-73720, IPS-73721, IPS-73722, IPS-89574, IPS-89575, IPS-89576, IPS-89577, IPS-89578, IPS-89579, IPS-89580, IPS-89581, IPS-89582, IPS-89583, IPS-89584, IPS-89585, IPS-89586, IPS-89587, IPS-89588, IPS-89589, IPS-89590.

Description: Pentadactyl footprints, with digitigrade to semiplantigrade pes and semiplantigrade to plantigrade manus. Both manus and pes tracks are highly asymmetric, with digits I to IV increasing in length, curved inwards and clawed. Manus digit I is occasionally oriented backwards. Manus digit V is the shortest, posteriorly positioned and rotated outwards, and occasionally rotated backwards. Some manus tracks preserve digit V with a wide and relatively deep pad (Fig. 2C, D). Pes tracks are much larger than manus tracks, mostly preserving digits I to IV, which are nearly parallel in some cases. Pes digits II, III and IV are nearly straight, with the tip being hook-like and strongly curved inwards (Figs. 2E, 3A, D). In some footprints, digits II, III and IV form a compact group with a straight base line perpendicular to digit III axis, and digit V is bent (hooked) outwards, with a wide and oval pad (Fig. 4). The base line of digit I is slightly posterior to that of digits II, III and IV. In some pes footprints, the distal phalangeal pads of digits I to IV are the widest and the most deeply impressed part of each digit (Fig. 3D). If preserved, digit V corresponds to a rounded tip impression and is posteriorly positioned and rotated outwards. In the trackway (IPS-73695), pes impressions are posterolaterally positioned to manus impressions (Fig. 2A, B). In other manus-pes sets, pes impressions partially or completely overstep the manus tracks laterally (Figs. 2E, 3A, B). With respect to the midline, pes tracks are rotated outwards and manus tracks are slightly rotated inwards. The stride length and pace angulation are of 187 mm and 103º in manus tracks, and of 179 mm and 70º, respectively, in pes tracks. A straight tail trace is observed in the specimen IPS-89574 (Fig. 3B).

Discussion: The characteristic relative length of the digits, the digitigrade pes and semiplantigrade-plantigrade manus, as well as the relative position of manus and pes and pace angulations are diagnostic features of *Rhynchosauroides* (e.g., Avanzini and Renesto, 2002). This ichnogenus is commonly found in Middle Triassic tracksites from transitional (continental to marine) paleoenvironments (e.g., Haubold, 1971a, b; Demathieu and Oosterink, 1983; Avanzini and Renesto, 2002; Melchor and De Valais, 2006; Valdiserri and Avanzini, 2007; Avanzini and Mietto, 2008; Diedrich, 2008), those being similar to that of the Middle Muschelkalk of the Catalan Basin. *Rhynchosauroides* footprints are often linked to extramorphologic variations (Hunt and Lucas, 2007c), therefore the ichnospecies assignation for the

Catalan footprints remains open, as a comprehensive revision of the ichnotaxon, out of the scope of the present work, is needed. Avanzini and Renesto (2002) attributed *Rhynchosauroides* to *Macrocnemus*, hence small tanystropheids (*sensu* Ezcurra, 2016) are probably the trackmakers of these Middle Triassic ichnites.

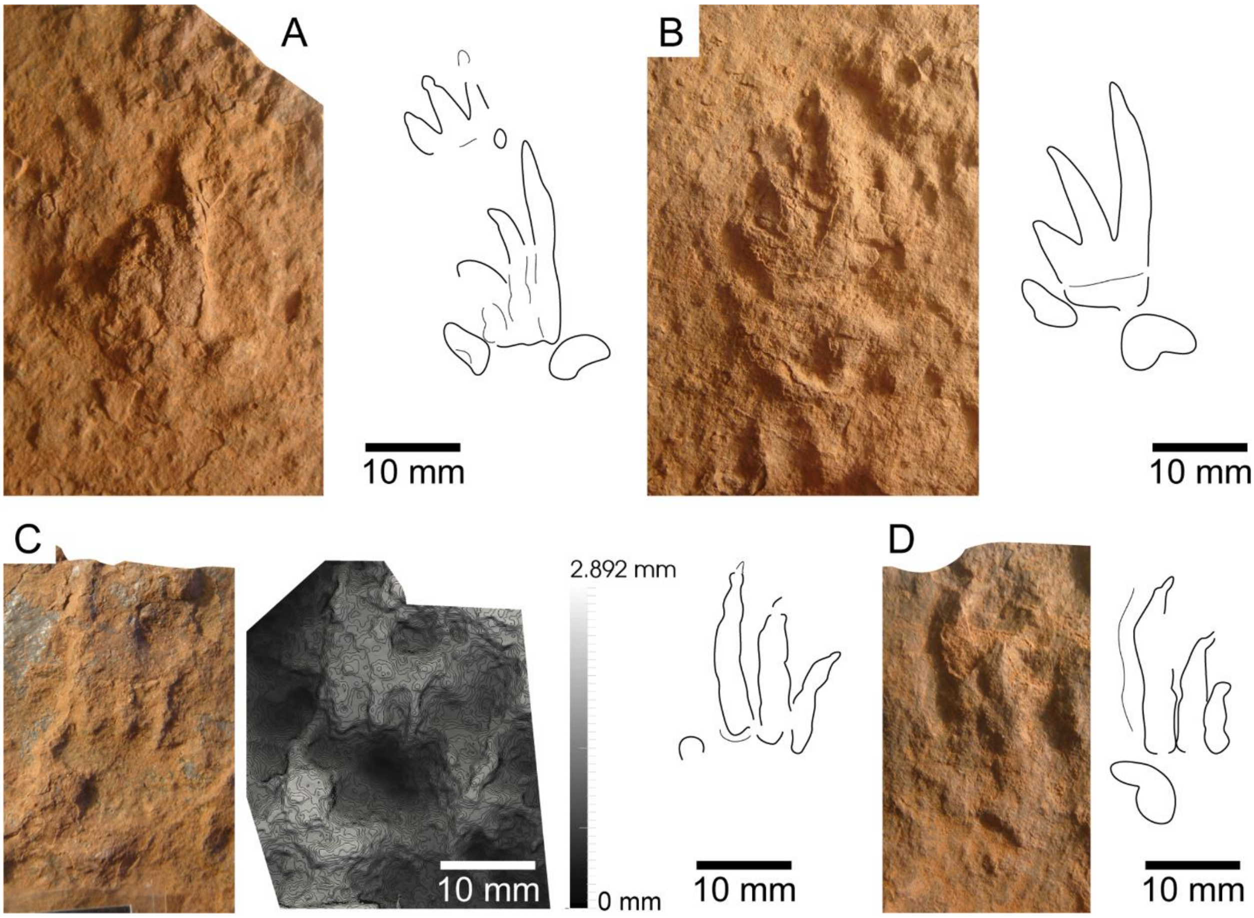

Figure 4. *Rhynchosauroides* ichnites III. A. IPS-73690. B. IPS-73690. C. IPS-89589. D. IPS-89582.

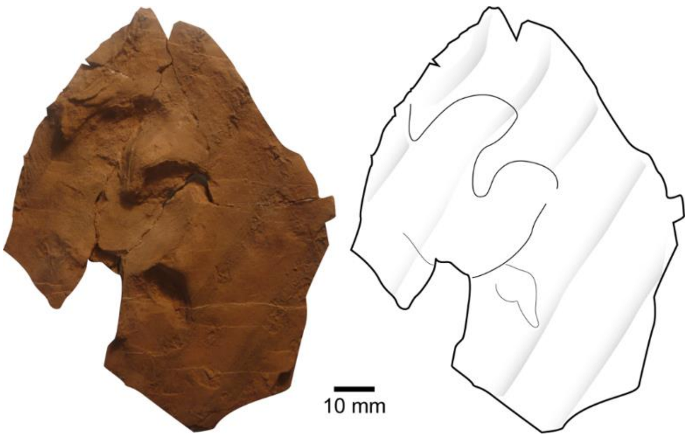

Figure 5. Partial track of IPS-73691 corresponding to an undetermined morphotype. Note the shallow ripples across the surface.

Undetermined morphotype

Fig. 5

Material: Track IPS-73691 preserved in concave epirelief.

Description: Partially preserved left track. The ichnite is composed by two complete rounded digits slightly curved inwards, a partial third digit and a possible pad impression below the first digit. Footprint appears to be wide, semiplantigrade and with a concave posterior margin.

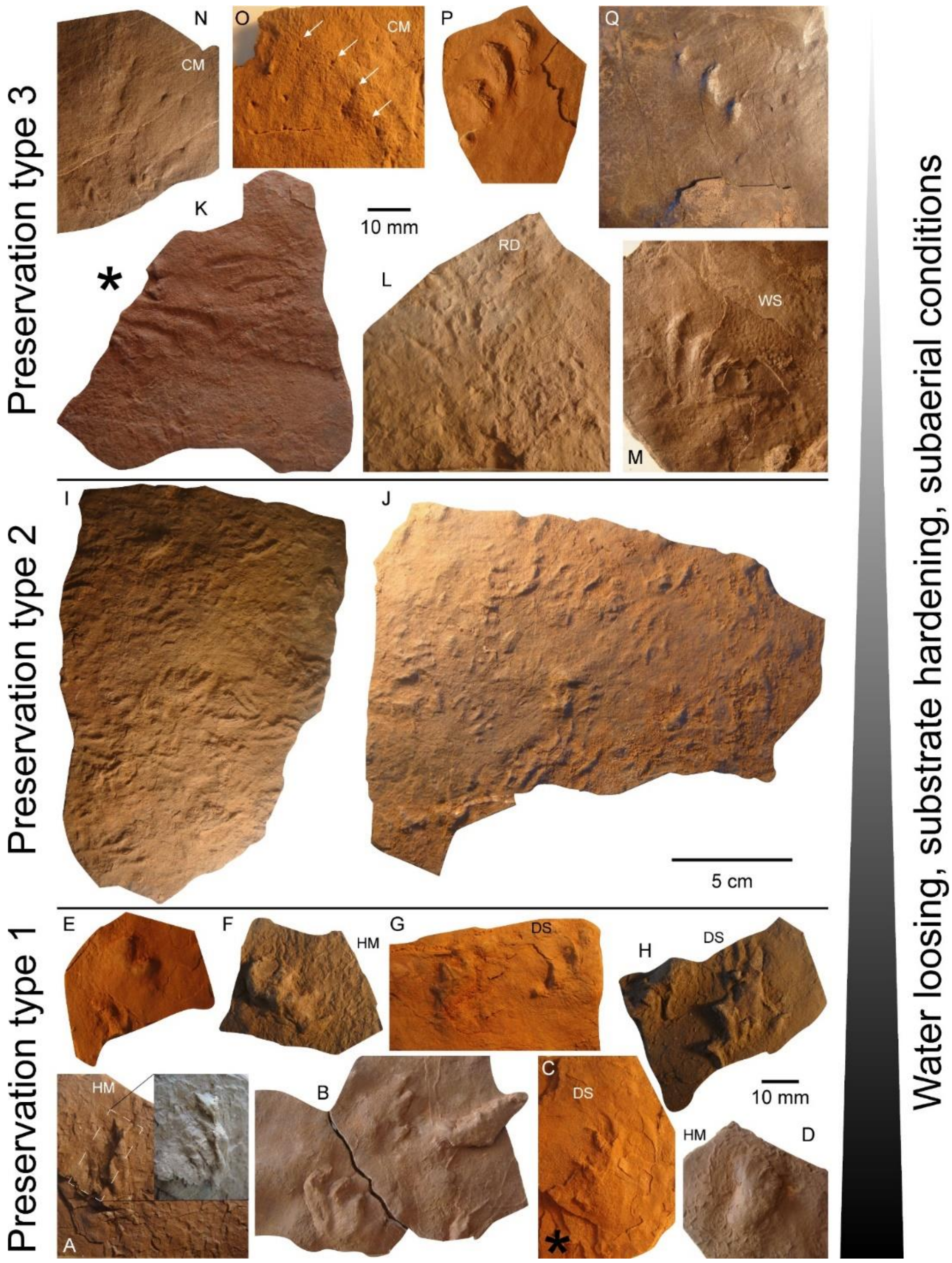

Figure 6. Preservation states of the Pedrera de Can Sallent footprints. From bottom to top and left to right: Type 1. IPS-73718 (A), IPS-73711 (B), IPS-73722 (C), IPS-73717 (D), IPS-73719 (E), IPS-73710 (F), IPS-73693 (G) and IPS-73707 (H). Type 2. IPS-73690 (I) and IPS-89574 (J). Type 3: IPS-73722 (K), IPS-73714 (L), IPS-73698 (M), IPS-89586 (N), IPS-73720 (O), IPS-73721 (P) and IPS-73695 (Q). CM: Claw marks. DS. Digit scratches. RD: Raindrops. HM: Halite molds. WS: Wrinkle structures. Asterisk (*) corresponds to specimens from the same slab in different surfaces.

Discussion: The track preservation precludes any ichnotaxonomic assignation. The shallow ripples observed (Fig. 5) indicate that a water flow may smoothed the original footprint soon after its impression. This ichnite is much larger than those of *Rhynchosauroides*, with a completely different shape of the digits. No other similar tracks (in dimensions and shape) have been recovered at the Pedrera de Can Sallent quarry, neither in the nearby Collcardús tracksite (Mujal et al., 2015), hence the affinity of this impression remains unknown.

Discussion

Preservation and paleoenvironmental implications

The preservation of the ichnites is controlled by the substrate conditions, as well as by the trackmakers locomotion (Melchor and Sarjeant, 2004; Falkingham, 2014; Melchor, 2015). Among a complex interaction of variables (Falkingham, 2014), the relative moisture of the substrate is one of the most relevant features (Brand, 1996; Melchor and Sarjeant, 2004; Melchor, 2015). Therefore, the resulting footprint morphologies provide information on water content and substrate rheology (Brand, 1996), factors closely related to the environment. Three main types of preservation are considered for the tracks herein reported (Fig. 6):

1) Deep and highly deformed impressions, often smoothed and with digit scratch traces. These ichnites are relatively scarce and mostly isolated; only manus-pes sets were identified (Preservation type 1 of Fig. 6A-H).

2) Moderately well preserved footprints, in some cases with recognizable claw marks and phalangeal pads, present in almost every finely laminated layer. This type of ichnites is abundant; surfaces are trampled, precluding the identification of trackways (Preservation type 2 of Fig. 6I-J).

3) Well preserved ichnites, often with recognizable claw marks and phalangeal pad impressions, although occasionally only faint impressions or claw traces are preserved. Footprints are hardly intersected, hence trackways can be identified (Preservation type 3 of Fig. 6K-Q).

The preservation variability is related to environmental changes in space and time. The first type of preservation indicates that ichnites were generated on a soft substrate with a relatively large amount of water, enhancing deep and deformed ichnites (e.g., Melchor and Sarjeant, 2004; Diedrich, 2008; Fig. 6A, B), and some of them with digit trailing traces (or scratches) in the anterior part (Fig. 6C, G, H). These features, together with the scarcity of footprints, indicate a decreased activity of the trackmakers. Small halite molds are commonly observed in these surfaces, denoting a high salinity of the environment (Fig. 6A, D, F). Micaceous minerals are also abundant in these beds. The second type of preservation represents substrate conditions prone to trackmaker activity, as indicated by the trampled surfaces (Melchor, 2015; Fig. 6I, J). The intermediate shallowness of the ichnites suggest an intermediate substrate moisture (Melchor and Sarjeant, 2004). The third type of preservation is recorded by several relatively shallow ichnites, ranging from footprints with well-defined shapes (Fig. 6K, L) to footprints just preserved by impressions of claws and faint phalangeal pads (Fig. 6M-Q). The low relief proves that the substrate was hard with a low relative moisture. Raindrop impressions preserved in some of these track beds (Figs. 2E, 6L), as well as wrinkle structures (Fig. 6M), possibly of microbial origin, indicate that surfaces underwent subaerial exposure during relatively long periods of desiccation.

In some cases, track-bearing surfaces (mostly of the third preservation type) are covered by fine-laminated layers with wave ripples corresponding to a shallow water table. In the surface containing the trackway, footprints present two main opposite orientations (Fig. 2A). Melchor (2015) related the trackway directions in such surfaces as paleocurrent indicators, hence in the case of the new Catalan footprints, the two main track directions would correspond to the bidirectional flow inferred by the wave ripples.

The lower surfaces of some beds of the studied succession, contain footprints indicating soft (wet) substrates, while the upper surfaces preserve footprints impressed in hard (dry) substrates (Figs. 2C-F, 6C, K). In addition, some surfaces contain footprints of both the second and third type of preservation, denoting moisture variability of the substrate. This variability of ichnites preservation in the same bed, or even in the same surface, indicates a recurrent alternation of the substrate rheology.

The abundance variability and wide morphologic range of *Rhynchosauroides* footprints is related to different substrate consistency influenced by water content, thus suggesting a wide tolerance of the trackmakers to different environments. No differences in footprint size are observed along the three main types of preservation. Similarly, in all types of preservation the same relative positions of manus and pes tracks along sets are documented (Figs. 2A, B, E, 3A, 6B, G). Therefore, *Rhynchosauroide*s trackmakers were able to accommodate easily to any changes in the walking substrate (see also Diedrich, 2008). As a result, morphologic variations of the Pedrera de Can Sallent *Rhynchosauroides* are mostly controlled by substrate conditions rather than other factors such as the trackmakers locomotion.

The fine laminated layers indicate low energy sedimentation conditions (mudstone levels), alternating with conditions of higher energy (fine- and very fine-grained sandstone layers). The remarkable absence of mud-cracking suggests that sediment did not undergo a general full desiccation. On the other hand, evidence of subaerial exposition (raindrop marks) and water evaporation and aridity (halite moulds and gypsum), together with additional regional geological inferences, seem to indicate a sabkha-like environment. The constant variations in substrate moisture, as evidenced by ichnite preservation, also seem to support this interpretation.

Paleobiogeography and age

The Middle Muschelkalk unit of the Catalan Basin, dated as late Anisian-middle Ladinian (Solé de Porta et al., 1987; Márquez-Aliaga et al., 2000; Dinarès-Turell et al., 2005), is of particular interest because it was deposited during a regression interval within the major transgression represented by the Lower and Upper Muschelkalk facies (Calvet and Marzo, 1994; Pérez-López and Pérez-Valera, 2007; Fortuny et al., 2011; Escudero-Mozo et al., 2015; Mujal et al., 2015). In the Iberian Basin (westwards of the Catalan Basin), Gand et al. (2010) reported Anisian-Early Ladinian tetrapod footprints, but corresponding to the Buntsandstein facies, denoting the diachronism of the Triassic units (López-Gómez et al., 2002). The Iberian footprint assemblage of Gand et al. (2010) is *Rhynchosauroides*-dominated as in the new tracksite herein reported, but chirotheriid footprints are also present, as they are in the nearby Middle Muschelkalk Collcardús tracksite (Mujal et al., 2015), developed in a distal alluvial setting. *Rhynchosauroides* footprints have also been reported from the Moroccan Argana Basin (Klein et al., 2011), dominated by chirotheriid tracks, from a more inland setting than that of the Pedrera de Can Sallent tracksite, but resembling the Collcardús tracksite of Mujal et al. (2015). In the European Middle Triassic localities of France (Demathieu, 1985; Demathieu and Demathieu, 2004), Italy (Avanzini and Renesto, 2002; Valdiserri and Avanzini, 2007; Avanzini and Mietto, 2008; Todesco et al., 2008), the Netherlands (Demathieu and Oosterink, 1983, 1988) and Germany (Diedrich, 2008), ichnoassociations and paleoenvironments are also similar to those of contemporaneous localities in the Catalan Basin. *Rhynchosauroides* specimens dominate in the coastal environments and in the continental settings with marine influence (Fig. 7).

Despite the marine transgression, connections among emerged lands and ephemeral flooded platforms persisted (Fig. 7). This allowed the migration of faunas, probably dominated by small tanystropheids in these paleoenvironments, as the wide distribution of *Rhynchosauroides* demonstrates. Herein reported specimens would represent the oldest evidence of this group of archosauromorphs in the Catalan Basin, recorded by body fossils in the southwestwards late Ladinian Upper Muschelkalk successions (Sanz and López-Martínez, 1984; Fortuny et al., 2011 and references therein). *Rhynchosauroides* can be stated as a characteristic ichnotaxon of such paleoenvironments of the Anisian-Ladinian interval.

Tetrapod ichnocoenosis and Rhynchosauroides

Usually, vertebrate ichnocoenosis are based on morphological criteria (independent from depositional or biological environments; Hunt and Lucas, 2007a), whereas continental invertebrate ichnofacies are defined mostly by the environment (water column and/or climatic control of the trace fossil distribution; Melchor, 2015). Notwithstanding, the herein reported specimens preserve diagnostic characters of *Rhynchosauroides*, hence the shape variations and preservation are controlled by the substrate conditions rather than by the anatomical traits of the trackmaker. In this way, the distribution of *Rhynchosauroides* is independent of the substrate moisture. Otherwise, the footprint distribution and different preservation, together with the sedimentological analyses, provide accurate information of paleoenvironmental conditions, being similar to the function of the invertebrate ichnofacies.

Hunt and Lucas (2007a) established the bases of the vertebrate ichnofacies, with further remarks by Lockley (2007). Along ichnofacies, *Rhynchosauroides* appears within the *Batrachichnus* ichnofacies (see Hunt and Lucas, 2007d), and also in the Late Triassic *Grallator*-*Brachychirotherium*-*Rhynchosauroides* ichnofacies (the Chinle Group of the western USA, see Lockley, 2007). Diedrich (2002, 2008) mentioned the *Rhynchosauroides* ichnofacies and ichnocoenosis, constituted by tidal flat deposits with abundant

Procolophonichnium and scarce chirotheriid footprints from Germany and the Netherlands (see also Demathieu and Oosterink, 1983; Hunt and Lucas, 2007d; Klein and Lucas, 2010b). Here we provide additional remarks on the *Rhynchosauroides* Triassic record.

As previously mentioned, several European localities ranging from the Anisian to the Ladinian (Middle Triassic), corresponding to tidal flat and carbonate platform settings with continental influence, yield abundant (and often dominant) *Rhynchosauroides* footprints, with scarce but present larger footprints (e.g., from the chirotheriid group) (Demathieu and Oosterink, 1983, 1988; Demathieu, 1985; Diedrich, 2002, 2008; Valdiserri and Avanzini, 2007; Todesco et al., 2008). These tracksites may be similar to the Pedrera de Can Sallent tracksite herein interpreted as a sabkha. Regarding other early Mesozoic records, *Rhynchosauroides* has been reported from the Early Triassic (Melchor and De Valais, 2006; Klein and Lucas, 2010a, b; Klein and Niedźwiedzki, 2012; Lovelace and Lovelace, 2012; Mujal et al., 2016b) and from the Late Triassic (Hunt and Lucas, 2007b; Silva et al., 2008; Klein and Lucas, 2010b; Lagnaoui et al., 2012), being the corresponding deposits mostly from fluviatile and lacustrine settings. All in all, the European Anisian-Ladinian tracksites with abundant *Rhynchosauroides* and corresponding to coastal (with both marine and continental influence) settings (Fig. 7) present features of ichnocoenosis, i.e., restricted temporal and geographical ranges (Melchor, 2015). Similarly, Klein and Lucas (2010b) stated that the dominance of *Rhynchosauroides* in some assemblages is facies-controlled. Therefore, as was distinguished the *Chirotherium* ichnocoenosis from the *Batrachichnus* ichnofacies (Hunt and Lucas, 2007a, d), we suggest the potential characterization of a *Rhynchosauroides* ichnocoenosis, as a starting point to further inferences on the use of this ichnotaxon in paleoenvironmental analyses.

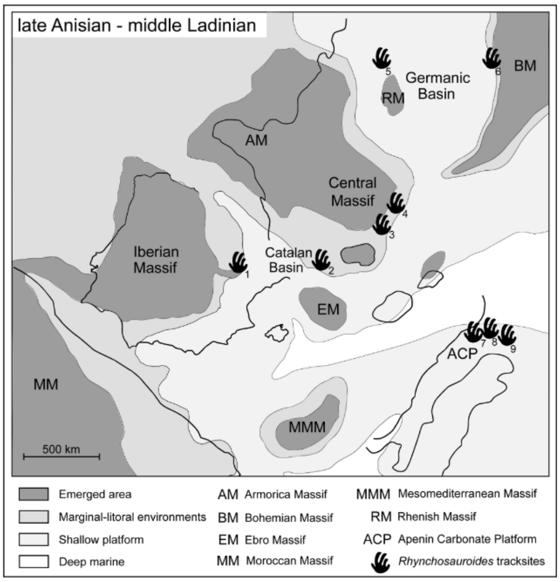

Figure 7. Paleobiogeography. Detailed distribution of *Rhynchosauroides* along the Middle Triassic basins (modified from Pérez-López and Pérez-Valera, 2007; Fortuny et al., 2011; Escudero-Mozo et al., 2015). 1. Spanish Iberian Basin (Gand et al., 2010); 2. Catalan Basin (this work); 3 and 4. French Central Massif outcrops (Demathieu, 1985; Demathieu and Demathieu, 2004); 5. Winterswijk (Demathieu and Oosterink, 1983, 1988); 6. Germanic outcrops (Diedrich, 2008); 7. Southern Italian Alps (Avanzini and Renesto, 2002; Avanzini and Mietto, 2008); 8. Val Duron, Italian Alps (Todesco et al., 2008); 9. Bad Gfrill, Italian Alps (Valdiserri and Avanzini, 2007).

Conclusions

In the last years, several works focused on the use of vertebrate footprints in paleoenvironmental analyses, but few of them payed attention to the widely known ichnogenus *Rhynchosauroides*. The identification of different preservation states for *Rhynchosauroides* footprints from Pedrera de Can Sallent (Catalan Basin, NE Iberian Peninsula) allows a better understanding of the environmental conditions and changes through space and time in coastal environments. The well documented gradation between the end-members of the studied tracks, indicate a direct correlation between ichnite morphology and substrate rheology.

The dominance of *Rhynchosauroides* combined with its wide adaptation to different substrate conditions make this ichnogenus a relatively precise paleoenvironmental analysis tool. Regarding the wide paleogeographic distribution and abundance of this ichnotaxon in similar paleoenvironments, the Anisian-Ladinian coastal settings with abundant *Rhynchosauroides* tracks would constitute an ichnocoenosis, although a comprehensive revision of this ichnogenus and tracksites is required to formally describe it.

Acknowledgments

We are deeply indebted to Fabio M. Dalla Vecchia, Judit Marigó and Francisco Guzman-Andrino for their fieldwork assistance and contribution in the finding of the tracksite, as well as to Pierre Demathieu for helpful discussion. E. Mujal obtained financial support from the PIF grant of the Geology Department at UAB, and from the Erasmus+ program of the UAB performed at the Paleontology Department from the Institut des Sciencies de l'Evolution (Université de Montpellier, France). J. Fortuny acknowledges the support of the postdoc grant "Beatriu de Pinós" 2014 – BP-A 00048 from the Generalitat de Catalunya. We acknowledge the comments and suggestions of an anonymous reviewer, Sebastian Voigt, the associate editor Hendrik Klein, as well as those of the guest editor Abdelouahed Lagnaoui, which largely improved a previous version of the manuscript. This work received support from CERCA program at Institut Català de Paleontologia (ICP) and from the projects "Vertebrats del Permià i el Triàsic de Catalunya i el seu context geològic" and "Evolució dels ecosistemes amb faunes de vertebrats del Permià i el Triàsic de Catalunya" (ref. 2014/100606), based at the Institut Català de Paleontologia and financially supported by the Departament de Cultura (Generalitat de Catalunya).

References

Anadón, P., Colombo, F., Esteban, M., Marzo, M., Robles, S., Santanach, P., and Solé Sugrañés, L. 1979. Evolución tectonoestratigráfica de los Catalánides. *Acta Geológica Hispánica. Homenatge a Lluís Solé i Sabaris*, 14: 242–270.

Avanzini, M., and Mietto, P. 2008. Lower and Middle Triassic footprints-based biochronology in the Italian Southern Alps. *Oryctos*, 8: 3–13.

Avanzini, M., Piñuela, L., and Garcia-Ramos, J.C. 2010. First report of a Late Jurassic lizard-like footprint (Asturias, Spain). *Journal of Iberian Geology*, 36 (2): 175–180.

Avanzini, M., and Renesto, S. 2002. A review of *Rhynchosauroides tirolicus* Abel, 1926 ichnospecies (Middle Triassic: Anisian–Ladinian) and some inference on *Rhynchosauroides* trackmaker. *Rivista Italiana di Paleontologia e Stratigrafia*, 108 (1): 51–66.

Berástegui, X., Losantos, M., Puig, C., and Casanova, J. 1996. Estructura de la Cadena Prelitoral Catalana entre el Llobregat y el Montseny. *Geogaceta*, 20 (4): 796–799.

Brand, L.R. 1996. Variations in salamander trackways resulting from substrate differences. *Journal of Paleontology*, 70 (6): 1004–1010.

Calvet, F., and Marzo, M. 1994. El Triásico de las Cordilleras Costero Catalanas: Estratigrafía, Sedimentología y Análisis Secuencial. *Cuaderno de Excursión. III Coloquio de Estratigrafía y Paleoestratigrafía del Pérmico y Triásico de España*, Cuenca, 27-29 de Junio de 1994, Field Guide. 53 p.

Demathieu, G. 1985. Trace fossil assemblages in middle Triassic marginal marine deposits, Eastern border of the Massif Central, France. *In* Curren, H.A. (ed.). Biogenic structures. SEPM Special Publications, 35: 53–66.

Demathieu, G., and Demathieu, P. 2004. Chirotheria and other ichnotaxa of the European Triassic. *Ichnos*, 11: 79–88.

Demathieu, G., and Oosterink, H.W. 1983. Die Wirbeltier-Ichnofauna aus dem Unteren Muschelkalk von Winterswijk (Die Reptilfährten aus der Mitteltrias der Niederlande). *Staringia*, 7: 1–51.

Demathieu, G., and Oosterink, H.W. 1988. New discoveries of ichnofossils from the Middle Triassic of Winterswijk (the Netherlands). *Geologie en Mijnbouw*, 67: 3–17.

Diedrich, C. 2002. Vertebrate track bed stratigraphy at new megatrack sites in the Upper Wellenkalk Member and *orbicularis* Member (Muschelkalk, Middle Triassic) in carbonate tidal flat environments of the western Germanic Basin. *Palaeogeography, Palaeoclimatology, Palaeoecology*, 183: 185–208.

Diedrich, C. 2008. Millions of reptile tracks—Early to Middle Triassic carbonate tidal flat migration bridges of Central Europe—reptile immigration into the Germanic Basin. *Palaeogeography, Palaeoclimatology, Palaeoecology,* 259: 410–423.

Dinarès-Turell, J., Diez, J.B., Rey, D., and Arnal, I. 2005. "Buntsandstein" magnetostratigraphy and biostratigraphic reappraisal from eastern Iberia: Early and Middle Triassic stage boundary definitions through correlation to Tethyan sections. *Palaeogeography, Palaeoclimatology, Palaeoecology*, 229: 158–177.

Escudero-Mozo, M.J., Márquez-Aliaga, A., Goy, A., Martín-Chivelet, J., López-Gómez, J., Márquez, L., Arche, A., Plasencia, P., Pla, C., Marzo, M., and Sánchez-Fernández, D. 2015. Middle Triassic carbonate platforms in Eastern Iberia: Evolution of their fauna and palaeogeographic significance in the western Tethys. *Palaeogeography, Palaeoclimatology, Palaeoecology*, 417: 236–260.

Ezcurra, M.D. 2016. The phylogenetic relationships of basal archosauromorphs, with an emphasis on the systematics of proterosuchian archosauriforms. *PeerJ*, e1778.

Falkingham, P.L. 2014. Interpreting ecology and behavior from the vertebrate fossil track record. *Journal of Zoology*, 292: 222–228.

Fortuny, J., Bolet, A., Sellés, A.G., Cartanyà, J., and Galobart, À. 2011. New insights on the Permian and Triassic vertebrates from the Iberian Peninsula with emphasis on the Pyrenean and Catalonian basins. *Journal of Iberian Geology*, 37 (1): 65–86.

Gand, G., De La Horra R., Galán-Abellán, B., López-Gomez, J., Barrenechea, J.F., Arche, A., and Benito, M.I. 2010. New ichnites from the Middle Triassic of the Iberian Ranges (Spain): paleoenvironmental and paleogeographical implications. *Historical Biology: An International Journal of Paleobiology*, 22 (1-3): 40–56.

Haubold, H. 1966. Therapsiden- und Rhynchocephalen-Fährten aus dem Buntsandstein Südthüringens. *Hercynia, NF*, 3 (2): 147–183.

Haubold, H. 1971a. Die Tetrapodenfährten des Buntsandsteins in der Deutschen Demokratischen Republik und in Westdeutschland und ihre Äquivalente in der gesamten Trias. *Paläntologische Abhandlungen, Abteilung a Paläozoologie*: 395–548.

Haubold, H. 1971b. Ichnia Amphibiorum et Reptiliorum fossilium. Encyclopedia of Paleoherpetology 18. Gustav Fischer Verlag, Stuttgart and Portland-USA, 124 p.

Hunt, A.P., and Lucas, S.G. 2007a. Tetrapod ichnofacies: a new paradigm. *Ichnos*, 14: 59–68.

Hunt, A.P., and Lucas, S.G. 2007b. Late Triassic tetrapod tracks of western North America. *New Mexico Museum of Natural History and Science Bulletin*, 40: 215–230.

Hunt, A.P., and Lucas, S.G. 2007c. A new tetrapod ichnogenus from the Upper Triassic of New Mexico, with notes on the ichnotaxonomy of *Rhynchosauroides*. *New Mexico Museum of Natural History and Science Bulletin*, 41: 71–77.

Hunt, A.P., and Lucas, S.G. 2007d. The Triassic tetrapod track record: Ichnofaunas, ichnofacies and biochronology. *New Mexico Museum of Natural History and Science Bulletin*, 41: 78–87.

Klein, H., and Lucas, S.G. 2010a. Review of the tetrapod ichnofauna of the Moenkopi formation/group (Early–Middle Triassic) of the American Southwest. *New Mexico Museum of Natural History and Science Bulletin*, 50: 1–167.

Klein, H., and Lucas, S.G. 2010b. Tetrapod footprints – their use in biostratigraphy and biochronology of the Triassic. *Geological Society London Special Publications*, 334: 419–446.

Klein, H., and Niedźwiedzki, G. 2012. Revision of the Lower Triassic tetrapod ichnofauna from Wióry, Holy Cross Mountains, Poland. *New Mexico Museum of Natural History and Science Bulletin*, 59: 1–62.

Klein, H., Voigt, S., Saber, H., Schneider, J.W., Fischer, J., Hminna, A., and Brosig, A. 2011. First occurrence of a Middle Triassic tetrapod ichnofauna from the Argana Basin (Western High Atlas, Morocco). *Palaeogeography, Palaeoclimatology, Palaeoecology*, 307: 218–231.

Lagnaoui, A., Klein, H., Voigt, S., Hminna, A., Saber, H., Schneider, J.W., and Wernerburg, R. 2012. Late Triassic tetrapod-dominated ichnoassemblages from the Argana Basin (Western High Atlas, Morocco). *Ichnos*, 19 (4): 238–253.

Leonardi, 1987. Glossary and Manual of Tetrapod Footprint Palaeoichnology. Departamento Nacional de Produção Mineral, Brasilia, 117 p.

Lockley, M.G. 2007. A tale of two ichnologies: the different goals and missions of invertebrate and vertebrate ichnotaxonomy and how they relate in ichnofacies analysis. *Ichnos*, 14: 59–68.

López-Blanco, M. 1994. Estructuras contractivas de la Cordillera Prelitoral Catalana entre la sierra de Les Pedritxes y el río Ripoll: evolución y relación con los depósitos del margen de la cuenca del Ebro. *Geogaceta*, 16: 43–46.

López-Gómez, J., Arche, A., and Pérez-López, A. 2002. Permian and Triassic. *In* Gibbons, W. and Moreno, T. (eds.). Geological Society Publishing House, London, 185–212.

Lovelace, D.M., and Lovelace, S.D. 2012. Paleoenvironments and paleoecology of a Lower Triassic invertebrate and vertebrate ichnoassemblage from the Red Peak Formation (Chugwater Group), Central Wyoming. *Palaios*, 27: 636–657.

Maidwell, F.T. 1911. Notes on footprints from the Keuper of Runcorn Hill. *Proceedings of the Liverpool Geological Society*, 11: 140–152.

Márquez-Aliaga, A., Valenzuela-Ríos, J.I., Calvet, F., and Budurov, K. 2000. Middle Triassic conodonts from northeastern Spain: biostratigraphic implications. *Terra Nova*, 12: 77–83.

Melchor, R.N. 2015. Application of vertebrate trace fossils to palaeoenvironmental analysis. *Palaeogeography, Palaeoclimatology, Palaeoecology*, 439: 79–96.

Melchor, R.N., and De Valais, S. 2006. A review of Triassic tetrapod track assemblages from Argentina. *Palaeontology*, 49 (2): 355–379.

Melchor, R.N., and Sarjeant, W.A.S. 2004. Small amphibian and reptile footprints from the Permian Carpacha Basin, Argentina. *Ichnos*, 11 (1-2): 57–78.

Mujal, E., Fortuny, J., Rodríguez-Salgado, P., Diviu, M., Oms, O., and Galobart, À. 2015. First footprints occurrence from the Muschelkalk detritical unit of the Catalan Basin: 3D analyses and palaeoichnological implications. *Spanish Journal of Palaeontology*, 30 (1): 97–108.

Mujal, E., Fortuny, J., Oms, O., Bolet, A., Galobart, À., and Anadón, P. 2016a. Palaeoenvironmental reconstruction and early Permian ichnoassemblage from the NE Iberian Peninsula (Pyrenean Basin). *Geological Magazine*, 153(4): 578–600.

Mujal, E., Gretter, N., Ronchi, A., López-Gómez, J., Falconnet, J., Diez, J.B., De la Horra, R., Bolet, A., Oms, O., Arche, A., Barrenechea, J.F., Steyer, J.-S., and Fortuny, J. 2016b. Constraining the Permian/Triassic transition in continental environments: Stratigraphic and paleontological record from the Catalan Pyrenees (NE Iberian Peninsula). *Palaeogeography, Palaeoclimatology, Palaeoecology*, 445: 18–37.

Pérez-López, A., and Pérez-Valera, F. 2007. Palaeogeography, facies and nomenclature of the Triassic units in the different domains of the Betic Cordillera (S Spain). *Palaeogeography, Palaeoclimatology, Palaeoecology*, 254: 606–626.

Sanz, J.L., and López-Martínez, N. 1984. The prolacertid Lepidosaurian *Cosesaurus aviceps* ELL. & VILL., a claimed "protoavian" from the Middle Triassic of Spain. *Geobios*, 17 (6): 747–756.

Silva, R.C., Ferigolo, J., Carvalho, I.S., and Fernandes, A.C.S. 2008. Lacertoid footprints from the Upper Triassic (Santa Maria Formation) of Southern Brazil. *Palaeogeography, Palaeoclimatology, Palaeoecology*, 262: 140–156.

Solé de Porta, N., Calvet, F., and Torrentó, L. 1987. Análisis palinológico del Triásico de los Catalánides (NE España). *Cuadernos de Geología Ibérica*, 11: 237–254.

Todesco, R., Watchtler, M., Dellantonio, E., and Avanzini, M. 2008. First reporto n a new late Anisian (Illyrian) vertebrate tracksite from the Dolomites (Northern Italy). *Studi Trentini di Scienze Naturali, Acta Geologica*, 83: 247–252.

Valdiserri, D., and Avanzini, M. 2007. A tetrapod ichnoassociation from the Middle Triassic (Anisian, Pelsonian) of Northern Italy. *Ichnos*, 14 (1): 105–116.

Valentini, M., Conti, M.A., and Mariotti, N. 2007. Lacertoid Footprints of the Upper Permian Arenaria di Val Gardena Formation (Northern Italy). *Ichnos*, 14 (3-4): 193–218.

Annex 3. Material suplementari del capítol 3

Data S1. Stratigraphic section of Coll de Sas NW

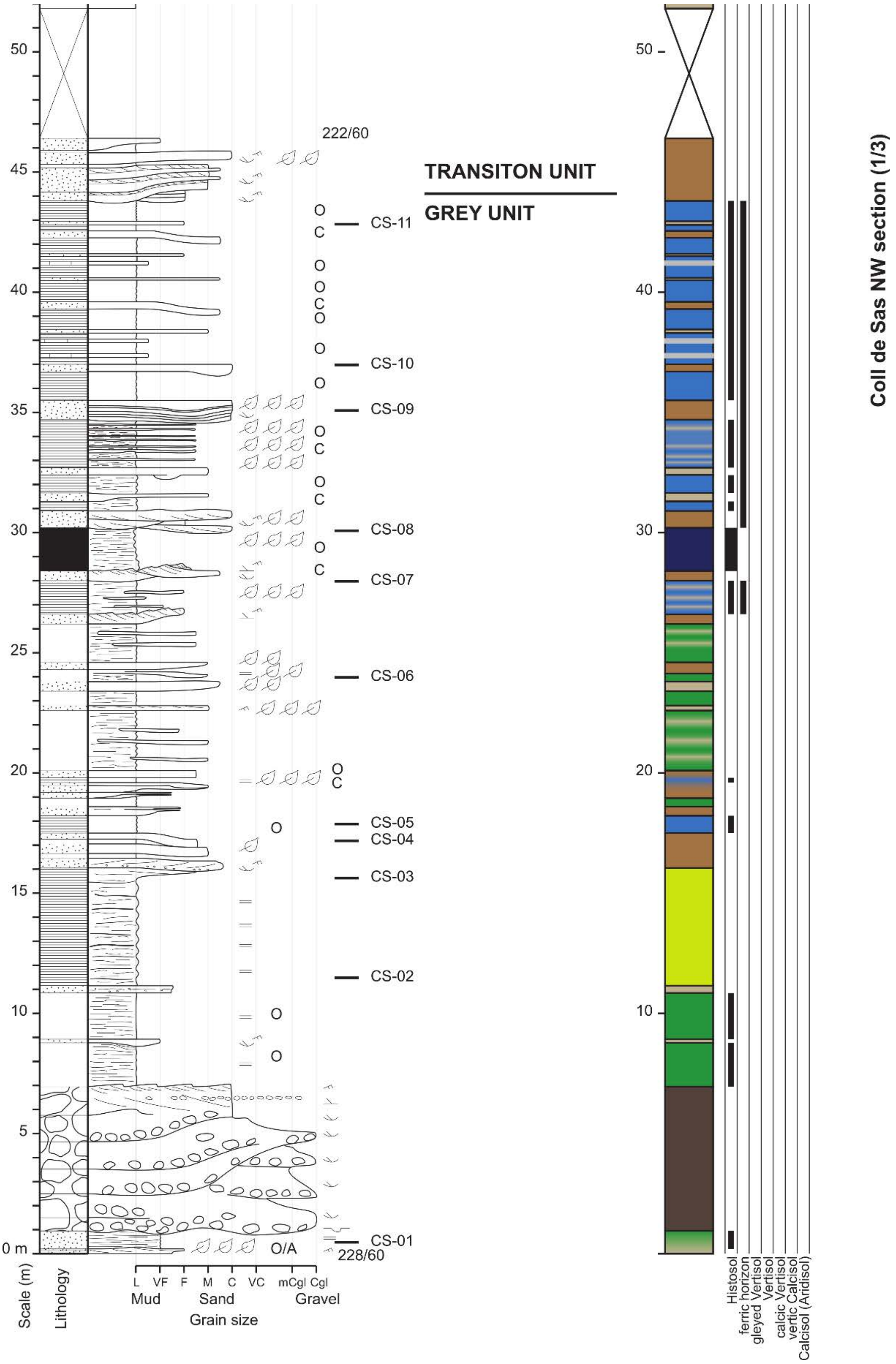

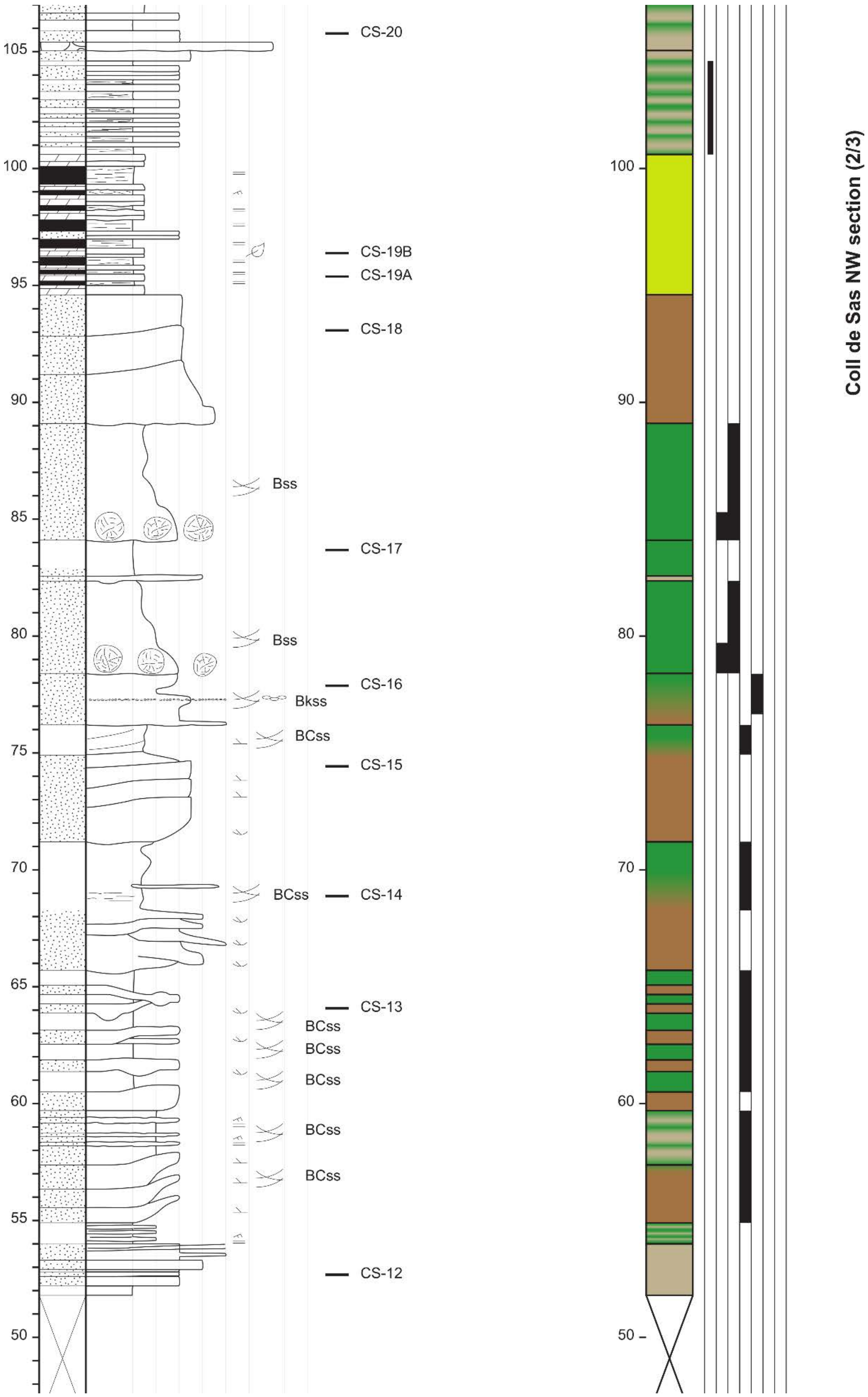
Coll de Sas NW section (2/3)
105
100
95
90
85
80
75
70
65
60
55
50
CS-20
CS-19B
CS-19A
CS-18
CS-17
CS-16
CS-15
CS-14
CS-13
CS-12
Bss
Bss
Bkss
BCss
BCss
BCss
BCss
BCss
BCss
BCss
100
90
80
70
60
50

COLL DE SAS

Base: 4697459N, 322643E (m) UTM WGS 84 31T
Top: 4697399N, 322555E (m)

- Dolostones
- Limestones
- Coal
- Carbonaceous mudstones
- Mudstones (claystone/siltstone)
- Sandstones
- Conglomerates
- Covered interval

- Parallel lamination
- Ripples
- Planar cross stratification
- Trough cross stratification
- Flow casts
- Plant remains (undifferenciated)
- Septarian nodules
- Carbonate nodules
- Slickensides
- O, B, etc. Paleosol horizons
- 228/60 Strike/Dip angles
- CS-(1-24) Paleomagnetism samples

- Lacustrine carbonates and mudstones (GU and TU)
- Floodplain coal (GU)
- Floodplain carbonaceous mudstones (GU)
- Floodplain mudstones (GU and TU)
- Overbank sandstones (GU and TU)
- Meandering sandstone channels (GU and TU)
- Braided conglomerate and sandstone channels (GU)
- Cinerites (volcanic ash)
- Pyroclastic deposits (LRU)

Grain size:

L: Lutites (Mudstones)	C: Coarse sandstone
VF: Very fine sandstone	VC: Very coarse sandstone
F: Fine sandstone	mCgl: micro-conglomerate/breccia
M: Medium sandstone	Cgl: Conglomerate/Breccia

Coll de Sas NW section

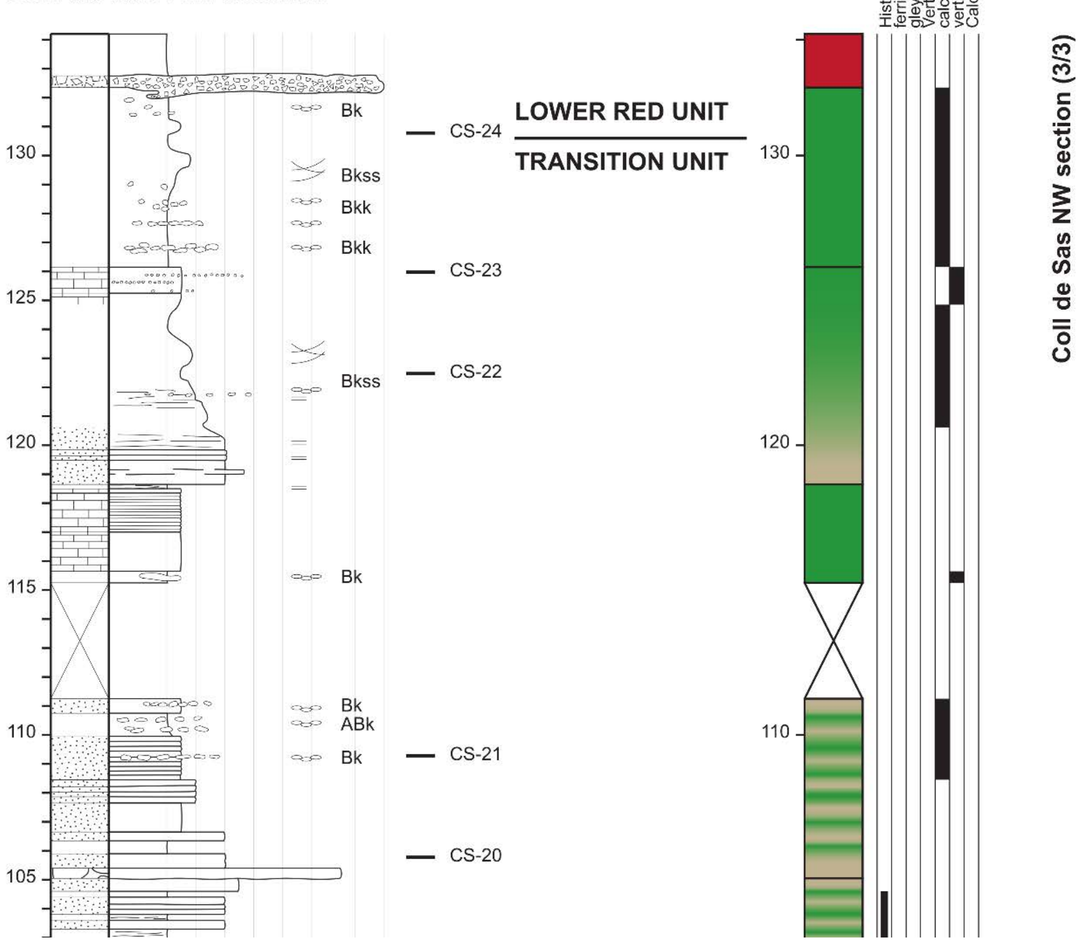

Data S2. Stratigraphic section of Les Esglésies.

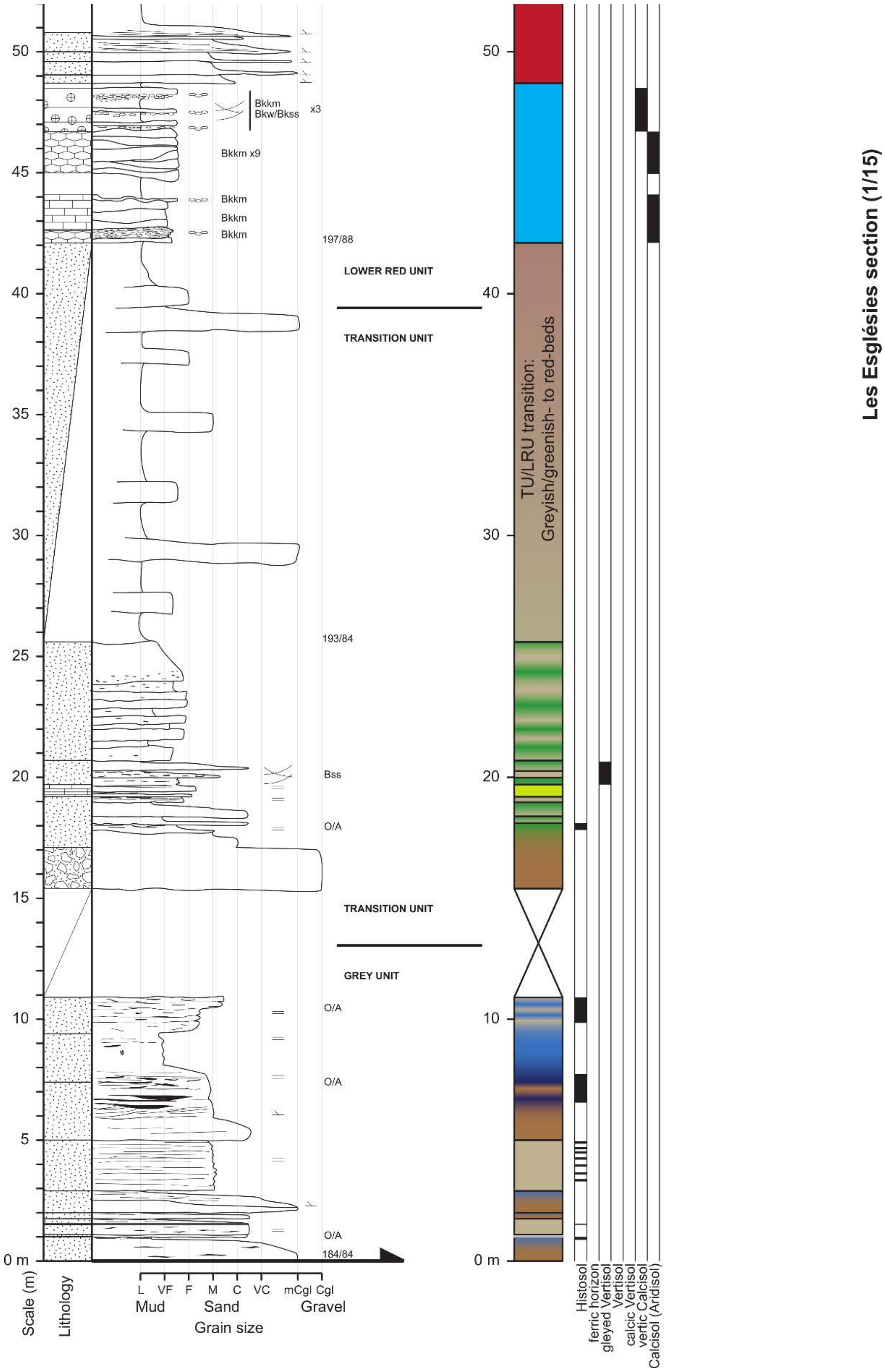

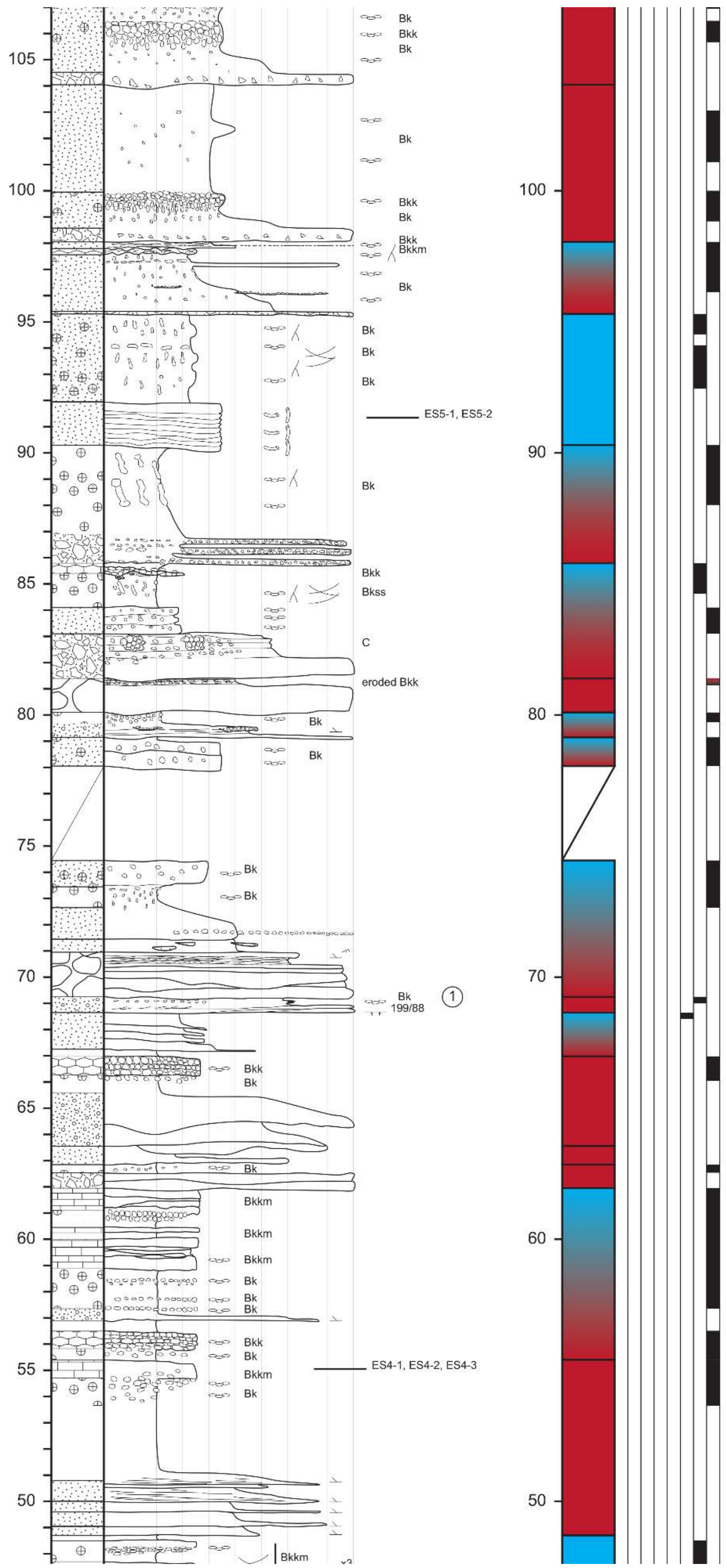

Les Esglésies section (2/15)

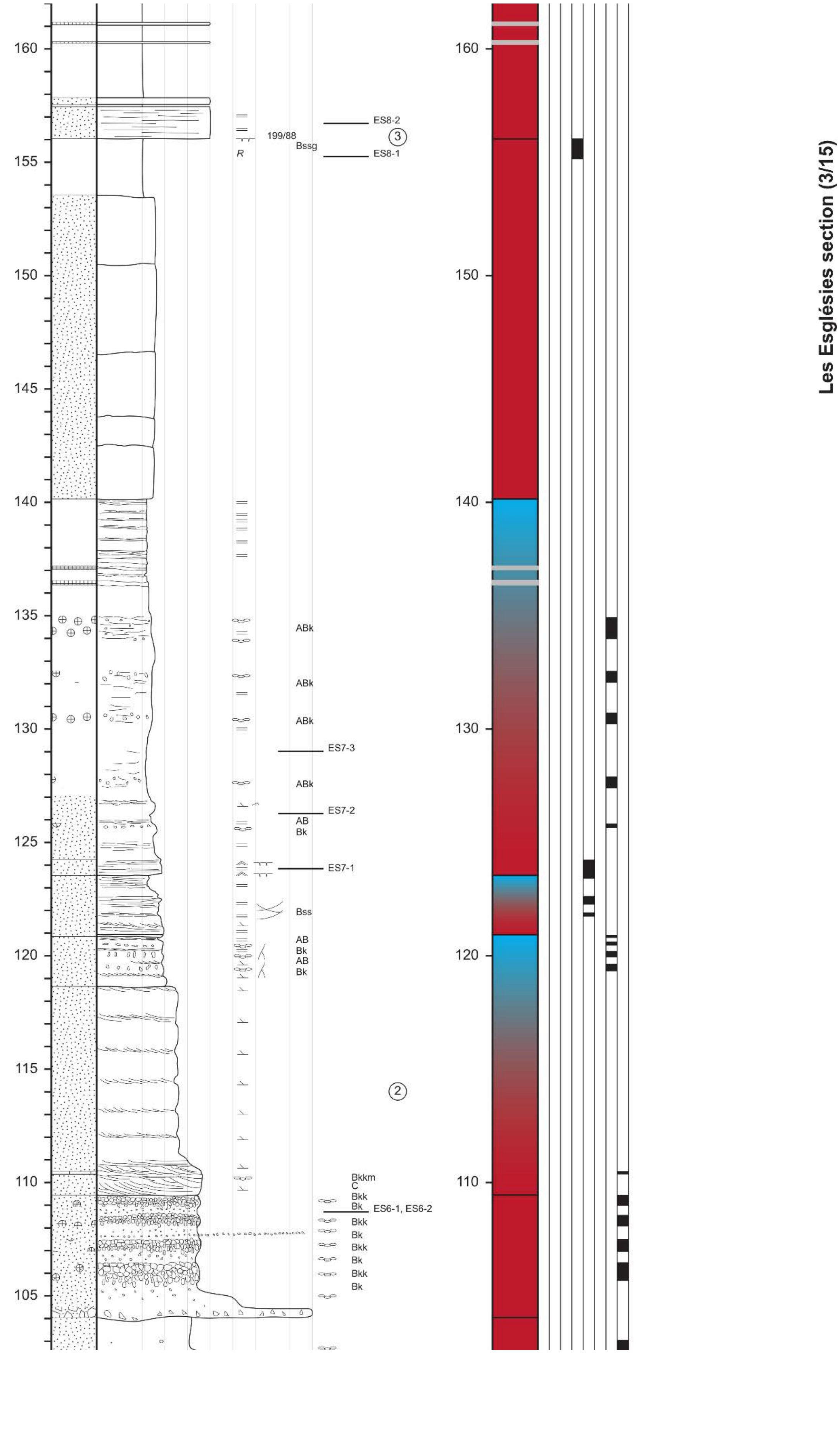
160
155
150
145
140
135
130
125
120
115
110
105
ES8-2
199/88
Bssg
ES8-1
R
3
ABk
ABk
ABk
ES7-3
ABk
ES7-2
AB
Bk
ES7-1
Bss
AB
Bk
AB
Bk
2
Bkkm
C
Bkk
Bk
ES6-1, ES6-2
Bkk
Bk
Bkk
Bk
Bkk
Bk
Les Esglésies section (3/15)

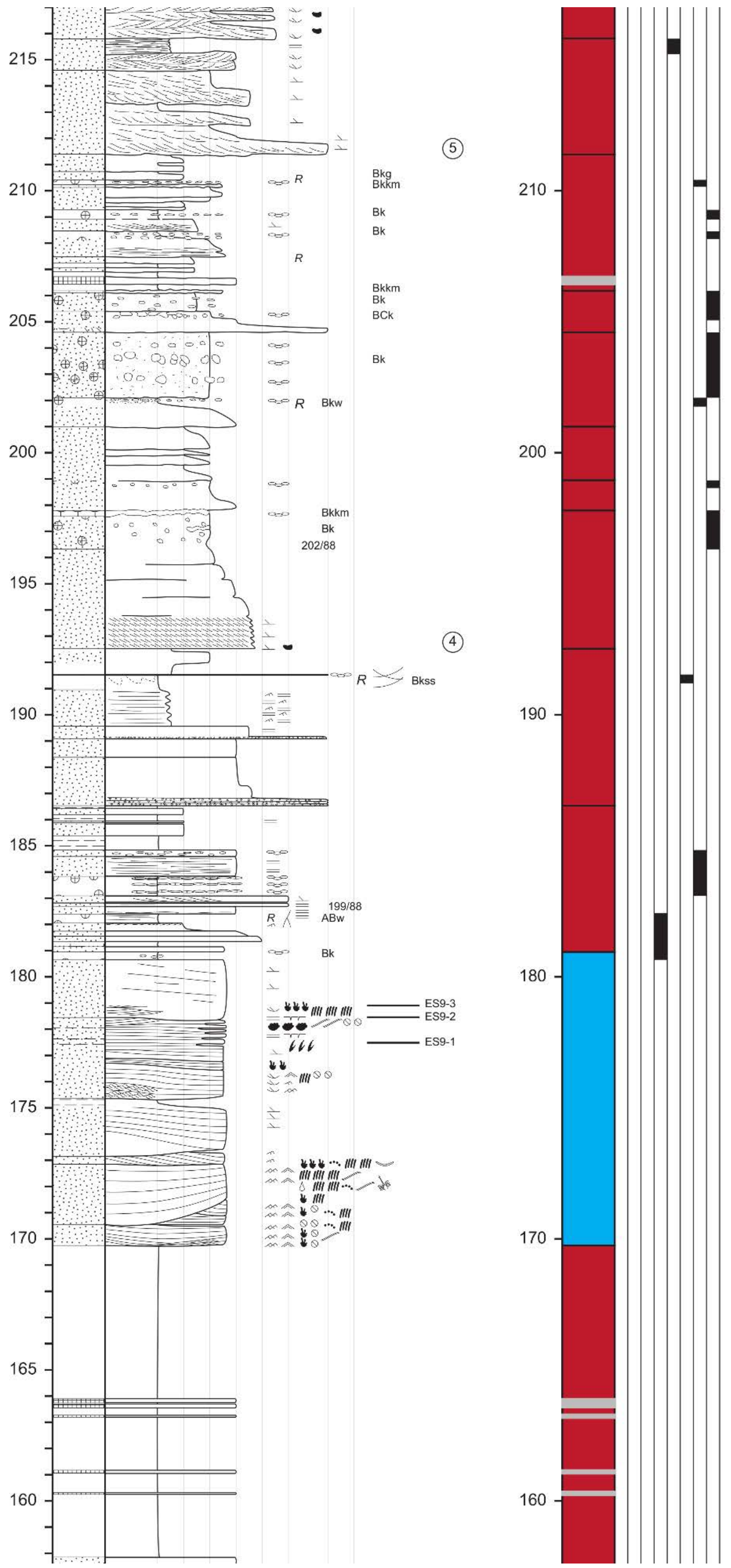

Les Esglésies section (4/15)

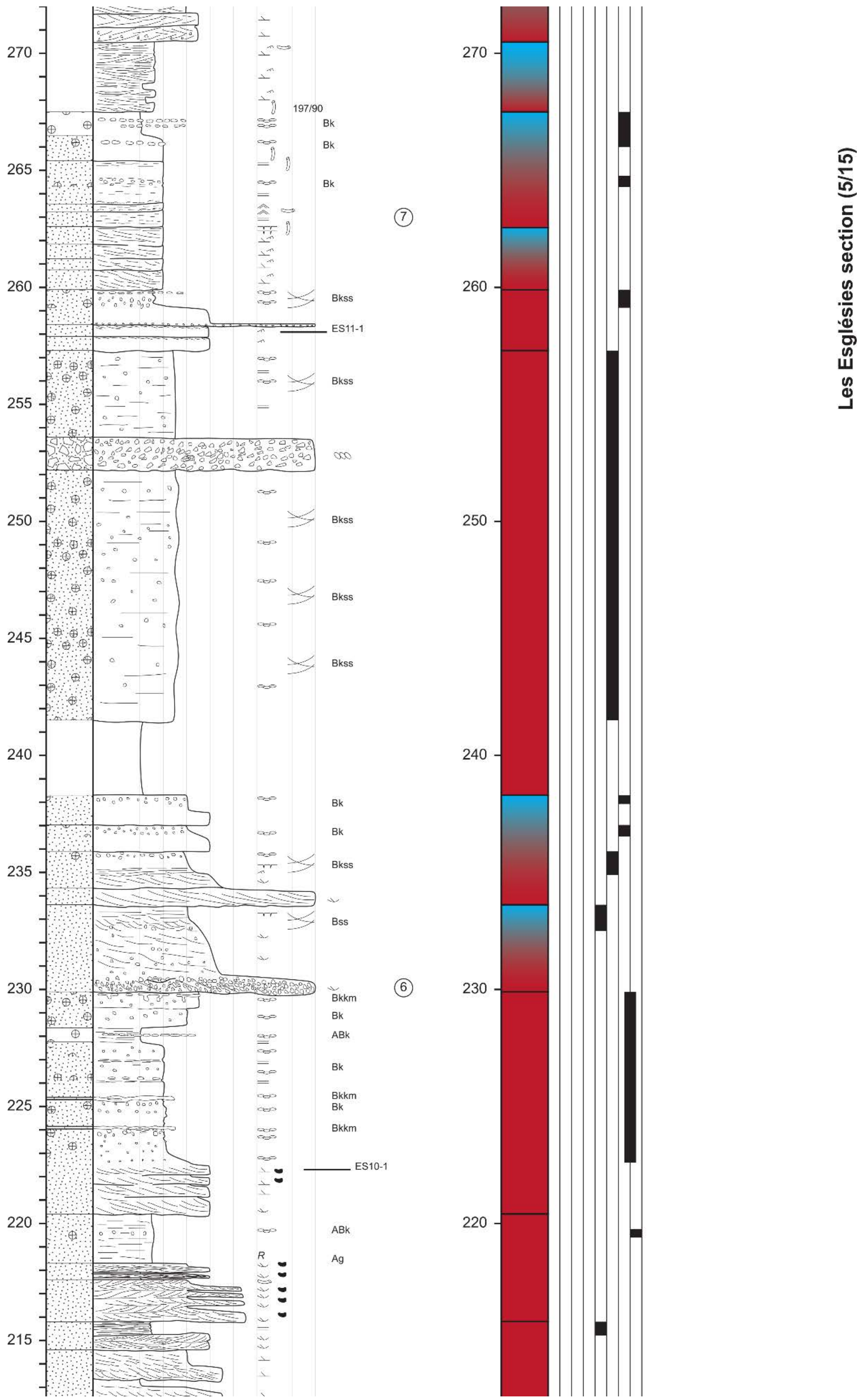
Les Esglésies section (5/15)
270
265
260
255
250
245
240
235
230
225
220
215
197/90
Bk
Bk
Bk
7
Bkss
ES11-1
Bkss
Bkss
Bkss
Bkss
Bk
Bk
Bkss
Bss
6
Bkkm
Bk
ABk
Bk
Bkkm
Bk
Bkkm
ES10-1
ABk
Ag
R

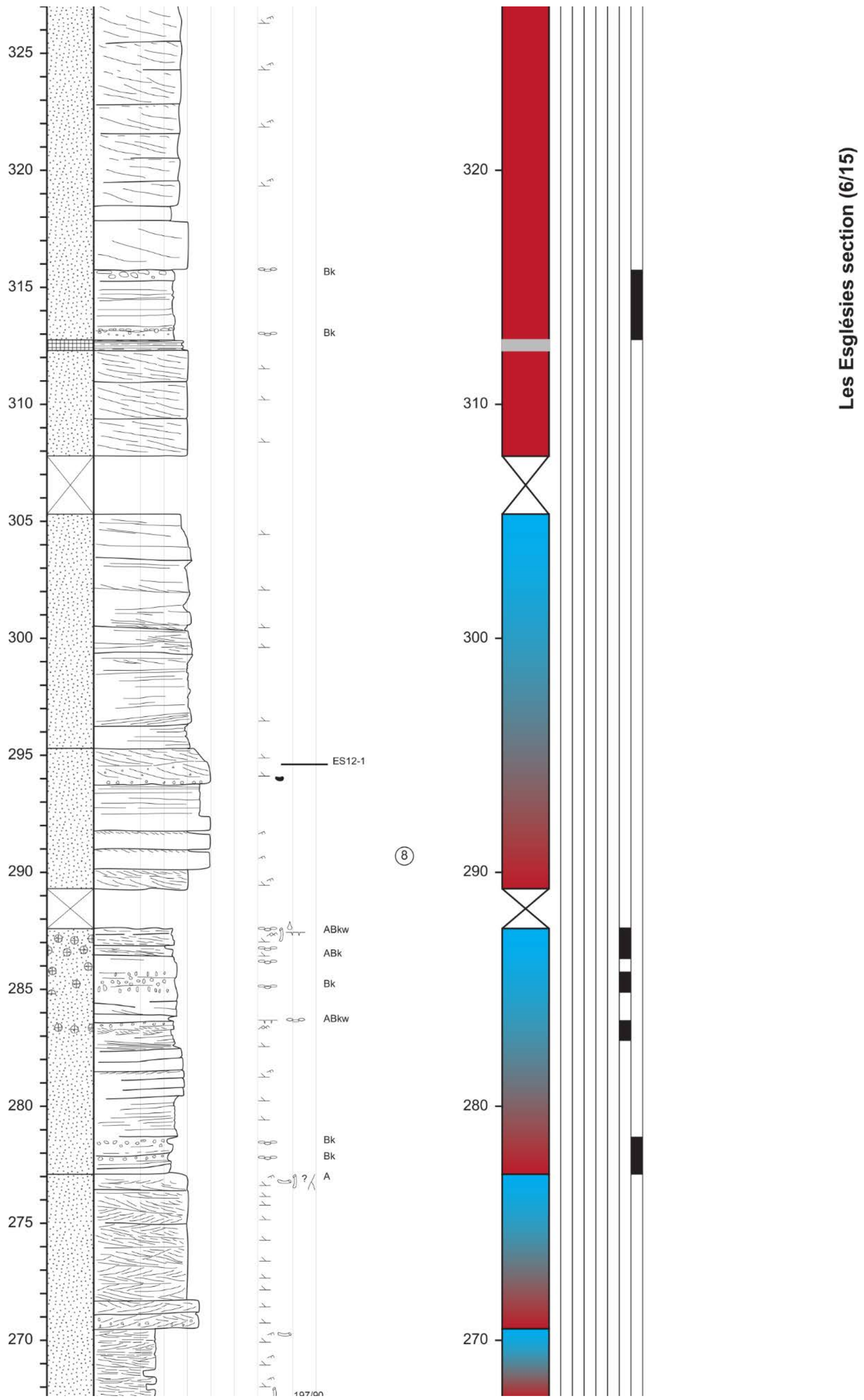
325
320
315
310
305
300
295
290
285
280
275
270
Bk
Bk
ES12-1
8
ABkw
ABk
Bk
ABkw
Bk
Bk
A
197/90
320
310
300
290
280
270
Les Esglésies section (6/15)

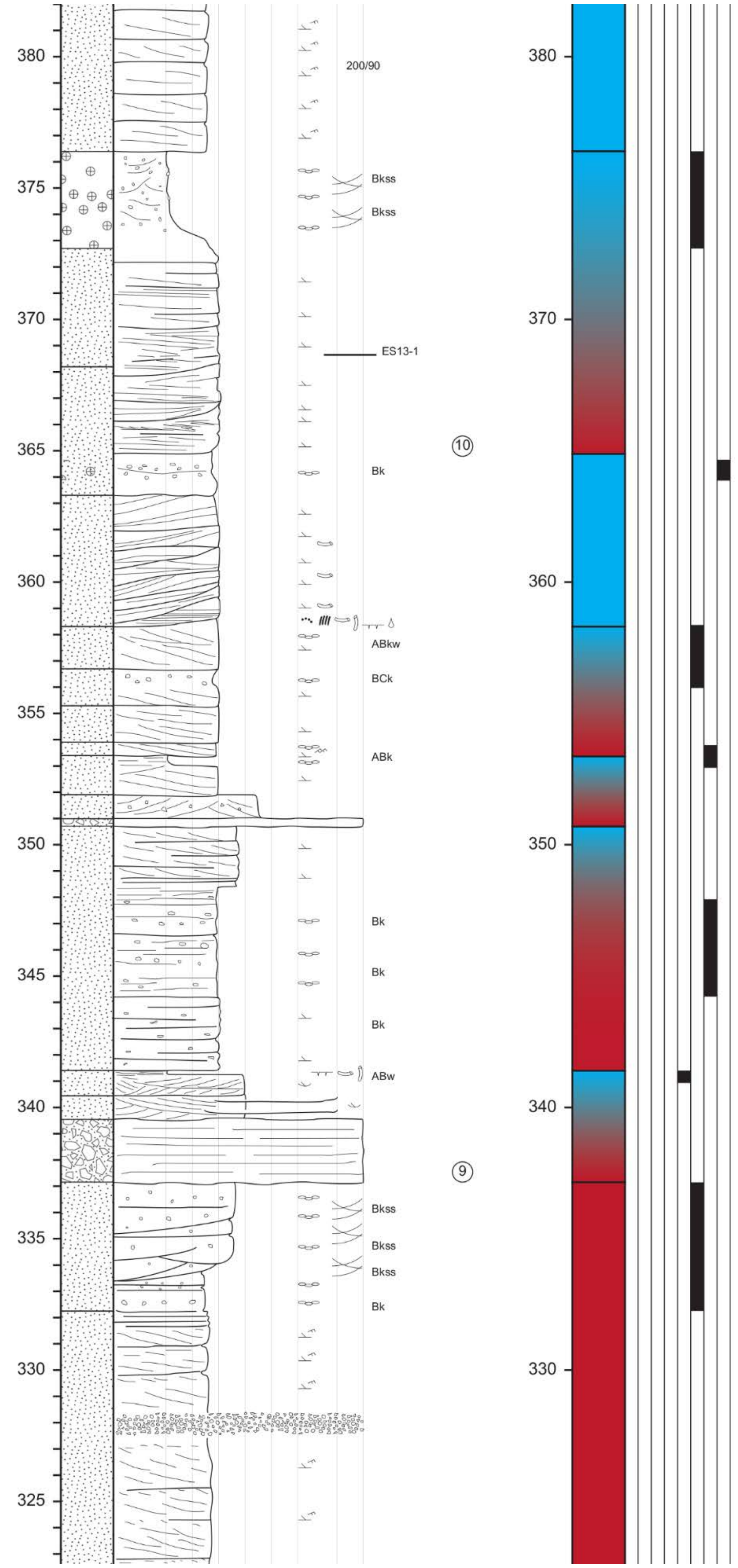

Les Esglésies section (7/15)

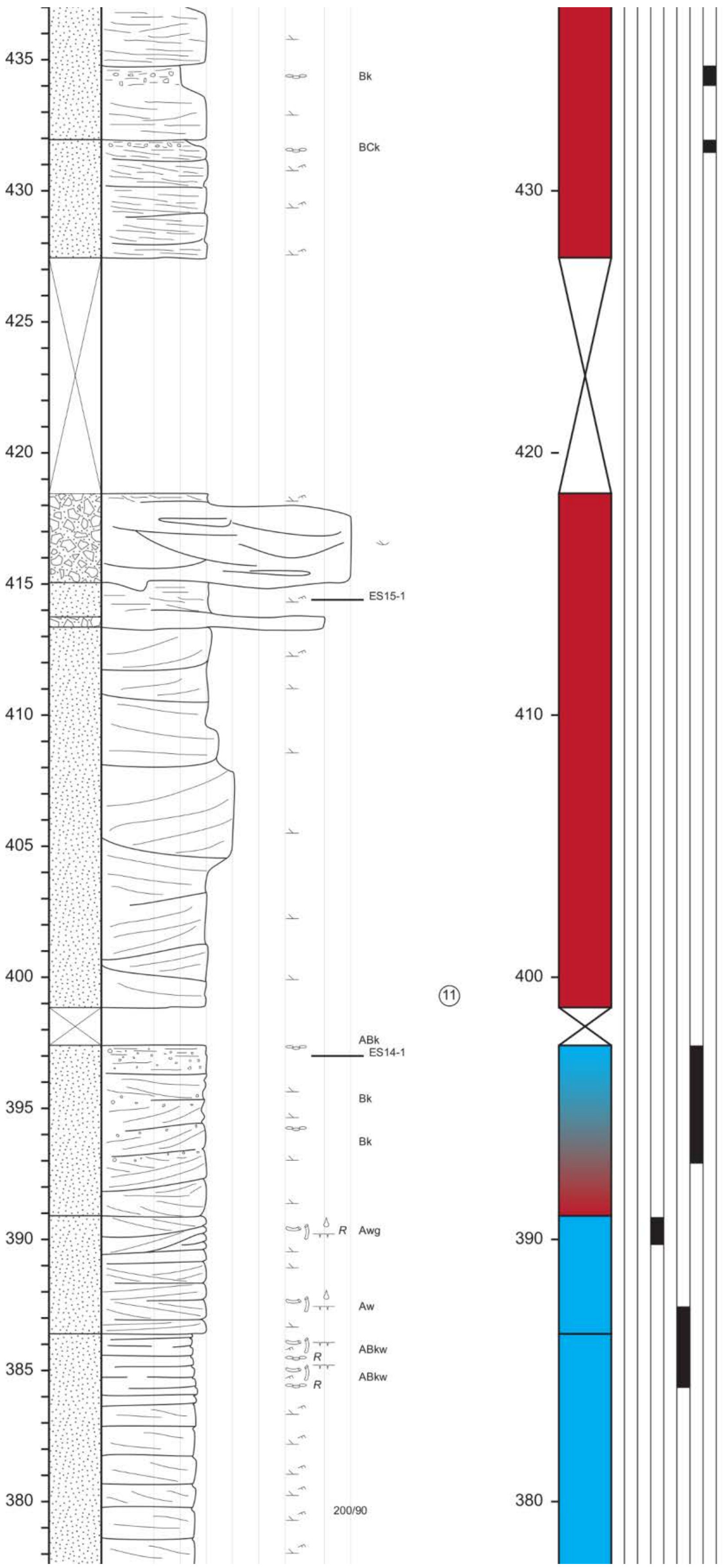

Les Esglésies section (8/15)

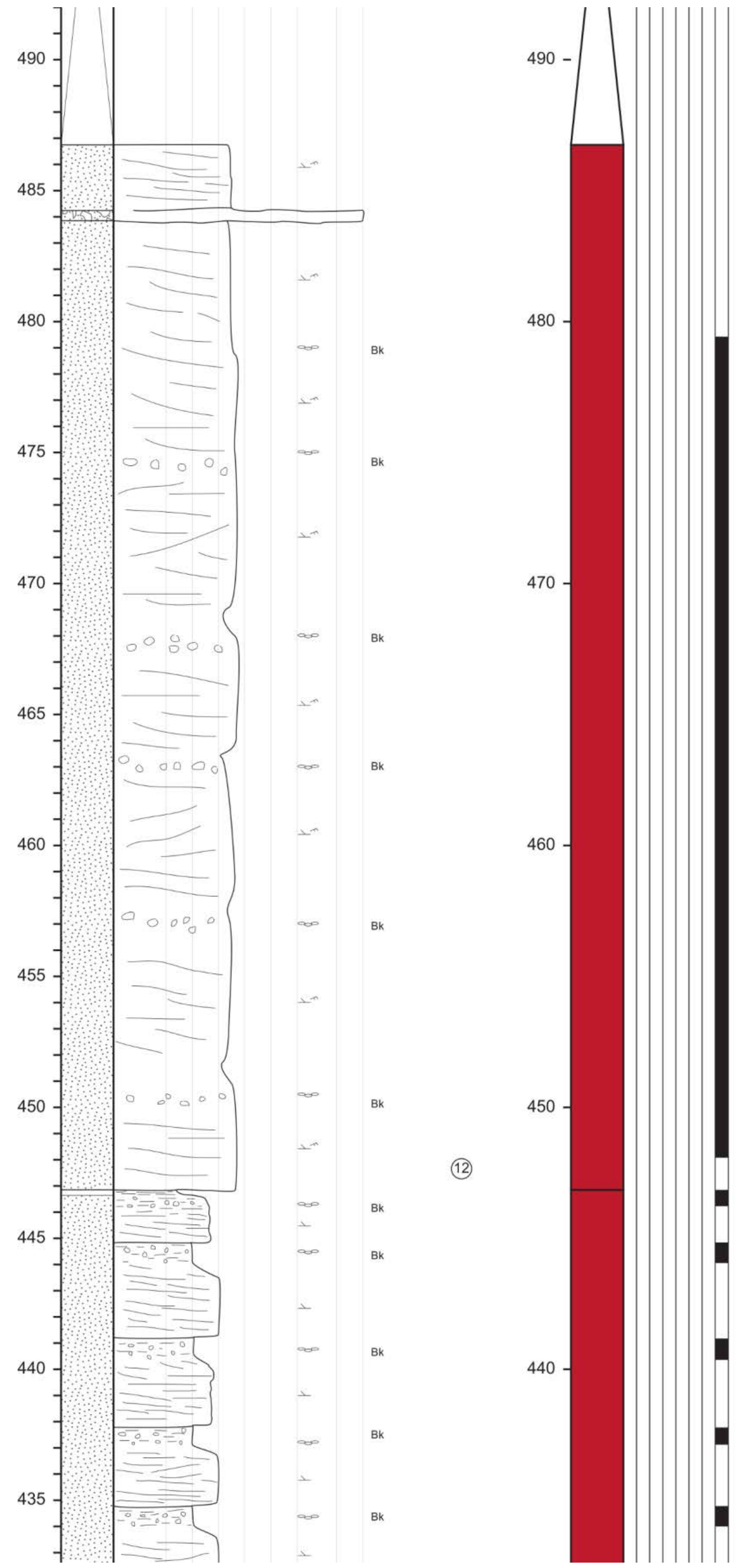

Les Esglésies section (9/15)

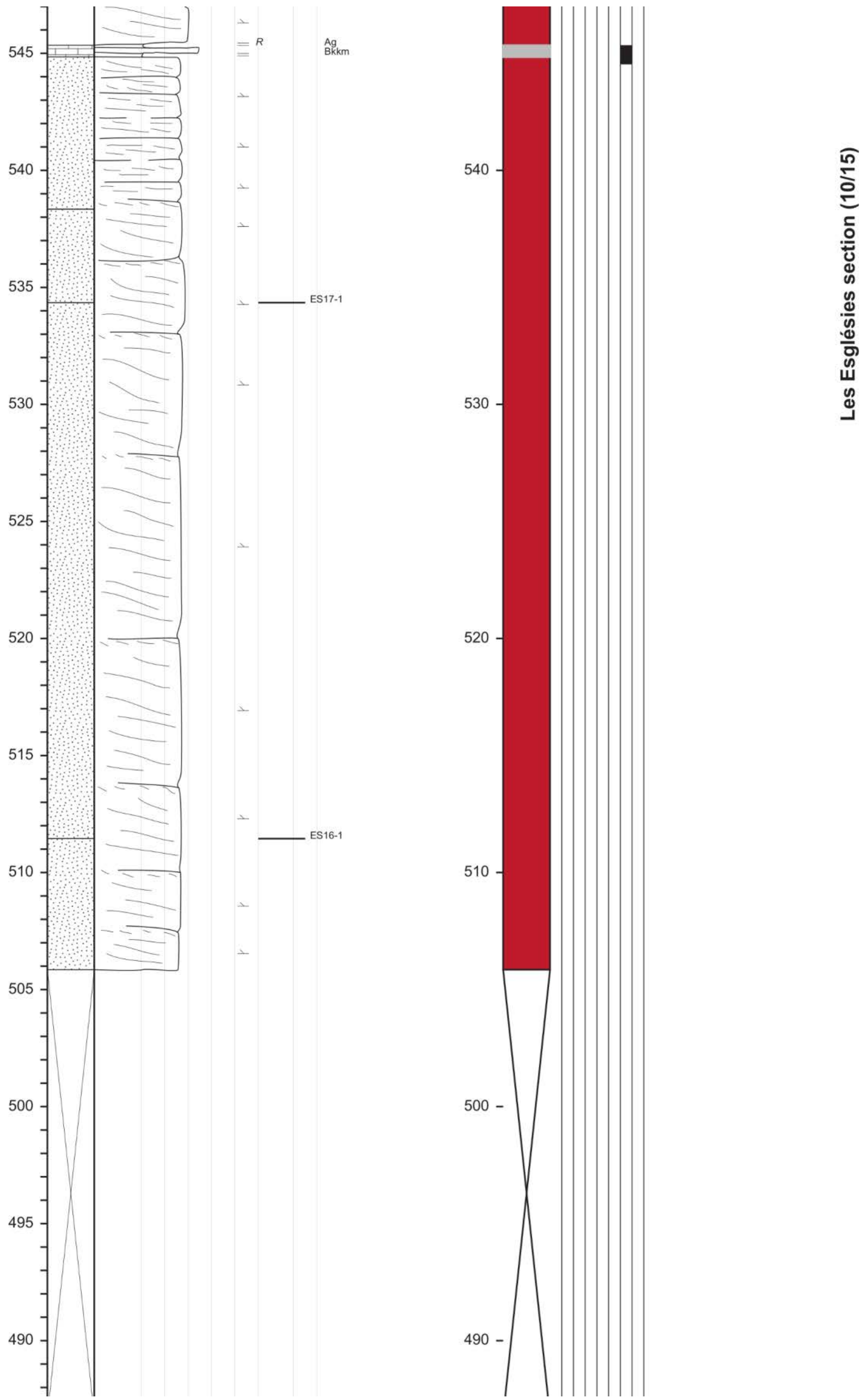
545
540
535
530
525
520
515
510
505
500
495
490
R
Ag
Bkkm
ES17-1
ES16-1
540
530
520
510
500
490
Les Esglésies section (10/15)

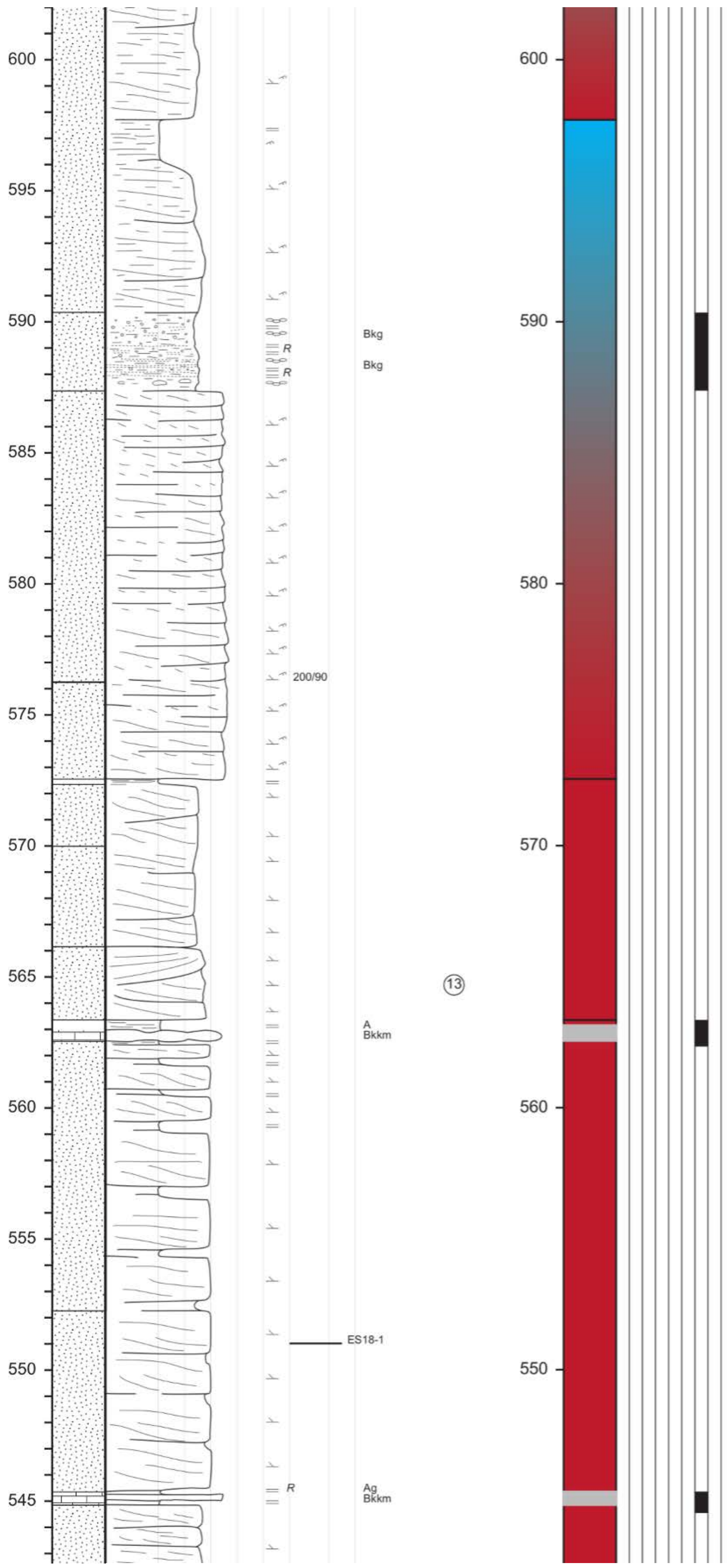

Les Esglésies section (11/15)

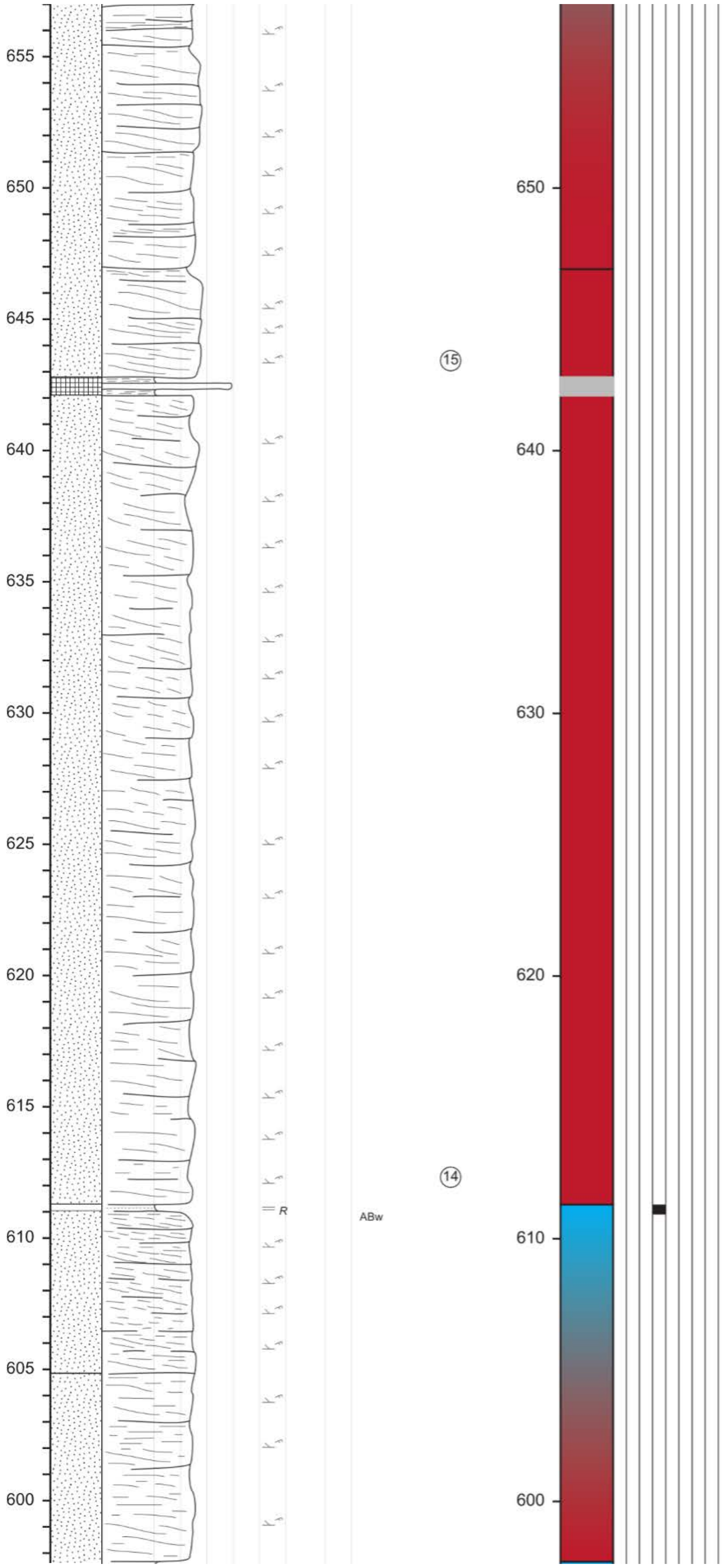

Les Esglésies section (12/15)

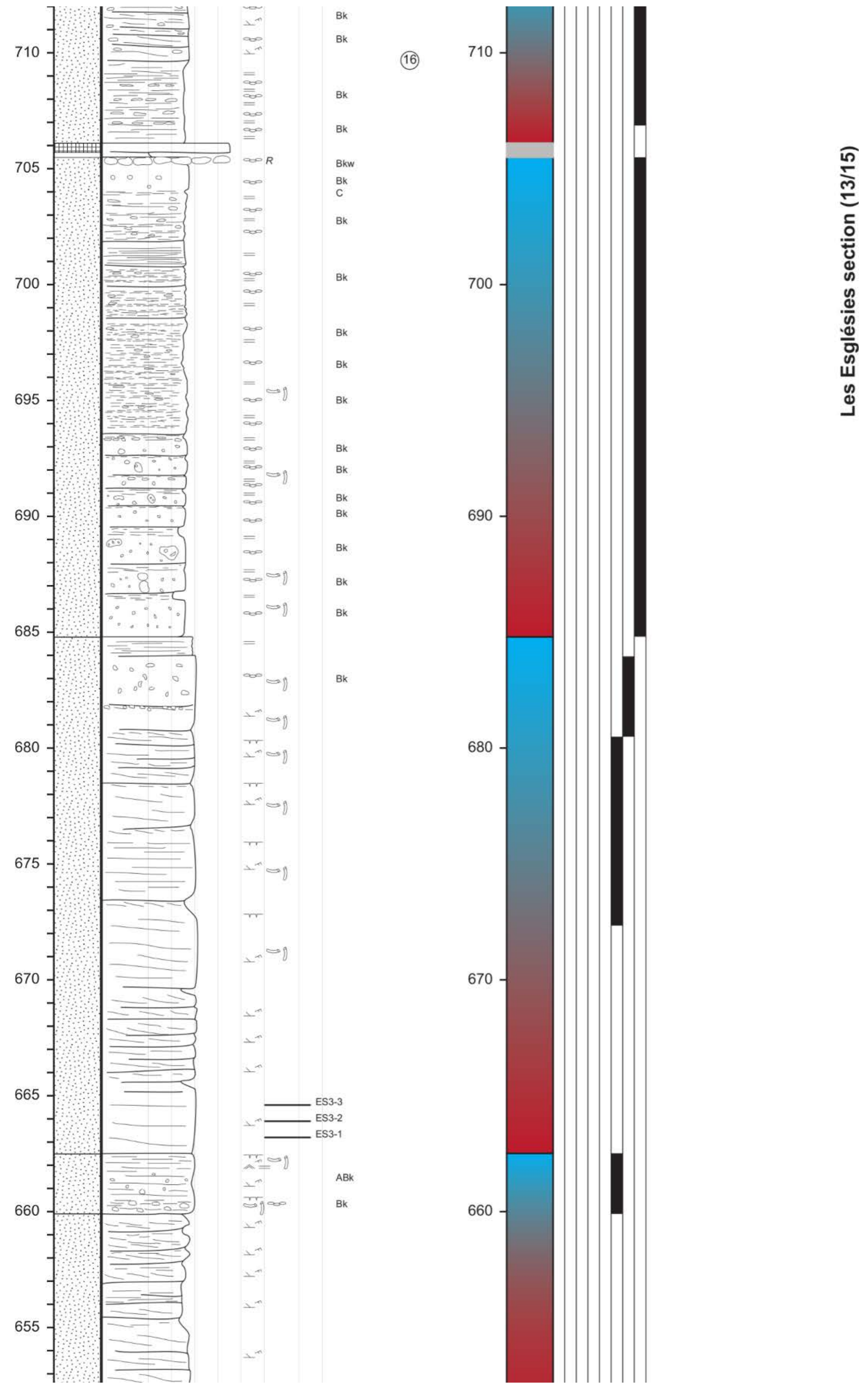
Les Esglésies section (13/15)
16
710
705
700
695
690
685
680
675
670
665
660
655
R
Bk
Bkw
C
ABk
ES3-3
ES3-2
ES3-1

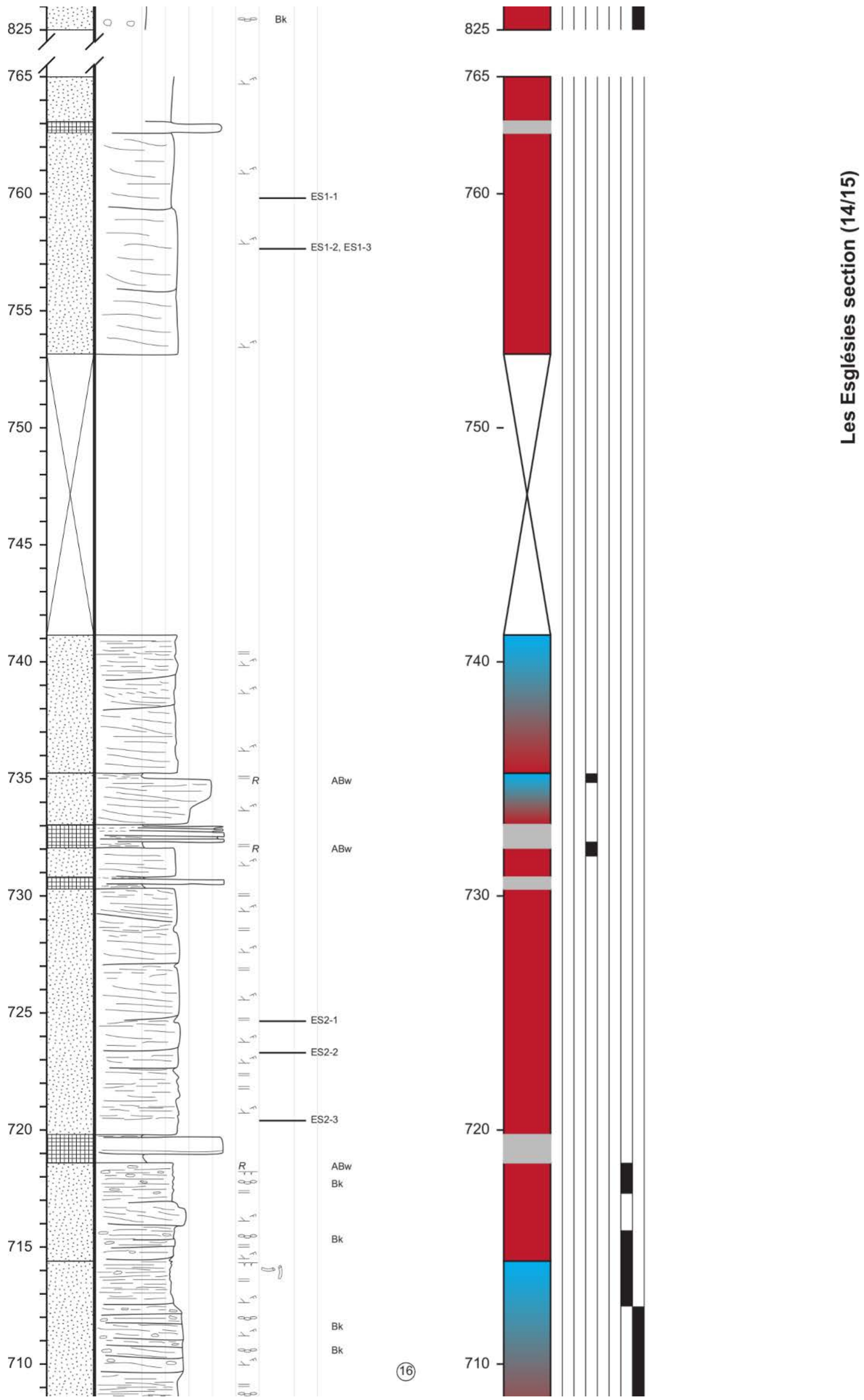
825
765
760
755
750
745
740
735
730
725
720
715
710
Bk
ES1-1
ES1-2, ES1-3
ABw
ABw
ES2-1
ES2-2
ES2-3
ABw
Bk
Bk
Bk
Bk
16
Les Esglésies section (14/15)

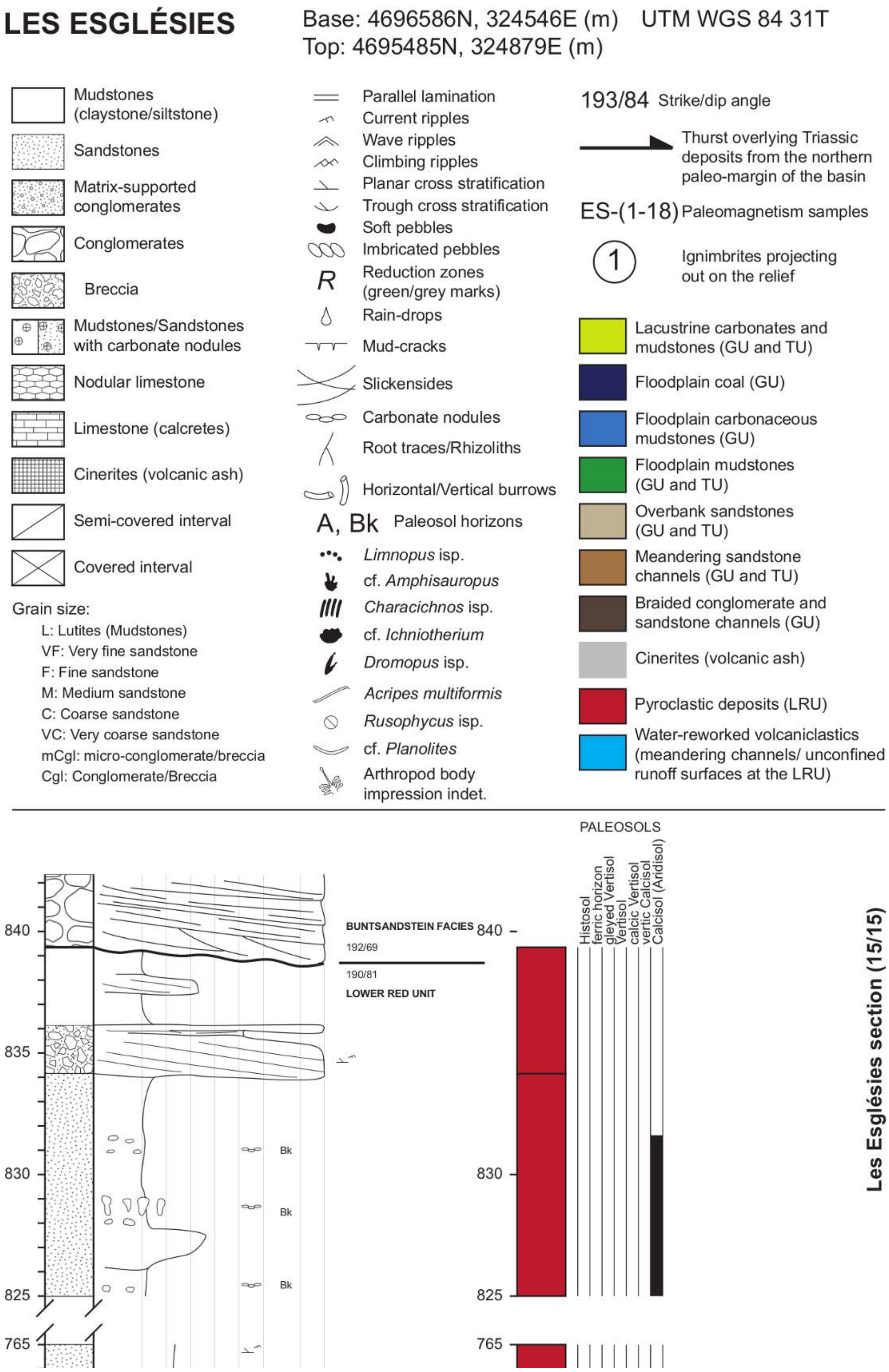
LES ESGLÉSIES
Base: 4696586N, 324546E (m) UTM WGS 84 31T
Top: 4695485N, 324879E (m)
Mudstones (claystone/siltstone)
Sandstones
Matrix-supported conglomerates
Conglomerates
Breccia
Mudstones/Sandstones with carbonate nodules
Nodular limestone
Limestone (calcretes)
Cinerites (volcanic ash)
Semi-covered interval
Covered interval
Grain size:
L: Lutites (Mudstones)
VF: Very fine sandstone
F: Fine sandstone
M: Medium sandstone
C: Coarse sandstone
VC: Very coarse sandstone
mCgl: micro-conglomerate/breccia
Cgl: Conglomerate/Breccia
Parallel lamination
Current ripples
Wave ripples
Climbing ripples
Planar cross stratification
Trough cross stratification
Soft pebbles
Imbricated pebbles
R Reduction zones (green/grey marks)
Rain-drops
Mud-cracks
Slickensides
Carbonate nodules
Root traces/Rhizoliths
Horizontal/Vertical burrows
A, Bk Paleosol horizons
Limnopus isp.
cf. Amphisauropus
Characichnos isp.
cf. Ichniotherium
Dromopus isp.
Acripes multiformis
Rusophycus isp.
cf. Planolites
Arthropod body impression indet.
193/84 Strike/dip angle
Thrust overlying Triassic deposits from the northern paleo-margin of the basin
ES-(1-18) Paleomagnetism samples
1 Ignimbrites projecting out on the relief
Lacustrine carbonates and mudstones (GU and TU)
Floodplain coal (GU)
Floodplain carbonaceous mudstones (GU)
Floodplain mudstones (GU and TU)
Overbank sandstones (GU and TU)
Meandering sandstone channels (GU and TU)
Braided conglomerate and sandstone channels (GU)
Cinerites (volcanic ash)
Pyroclastic deposits (LRU)
Water-reworked volcaniclastics (meandering channels/ unconfined runoff surfaces at the LRU)
840
835
830
825
765
Bk
BUNTSANDSTEIN FACIES
192/69
190/81
LOWER RED UNIT
PALEOSOLS
Histosol
ferric horizon
gleyed Vertisol
Vertisol
calcic Vertisol
vertic Calcisol
Calcisol (Andisol)
Les Esglésies section (15/15)

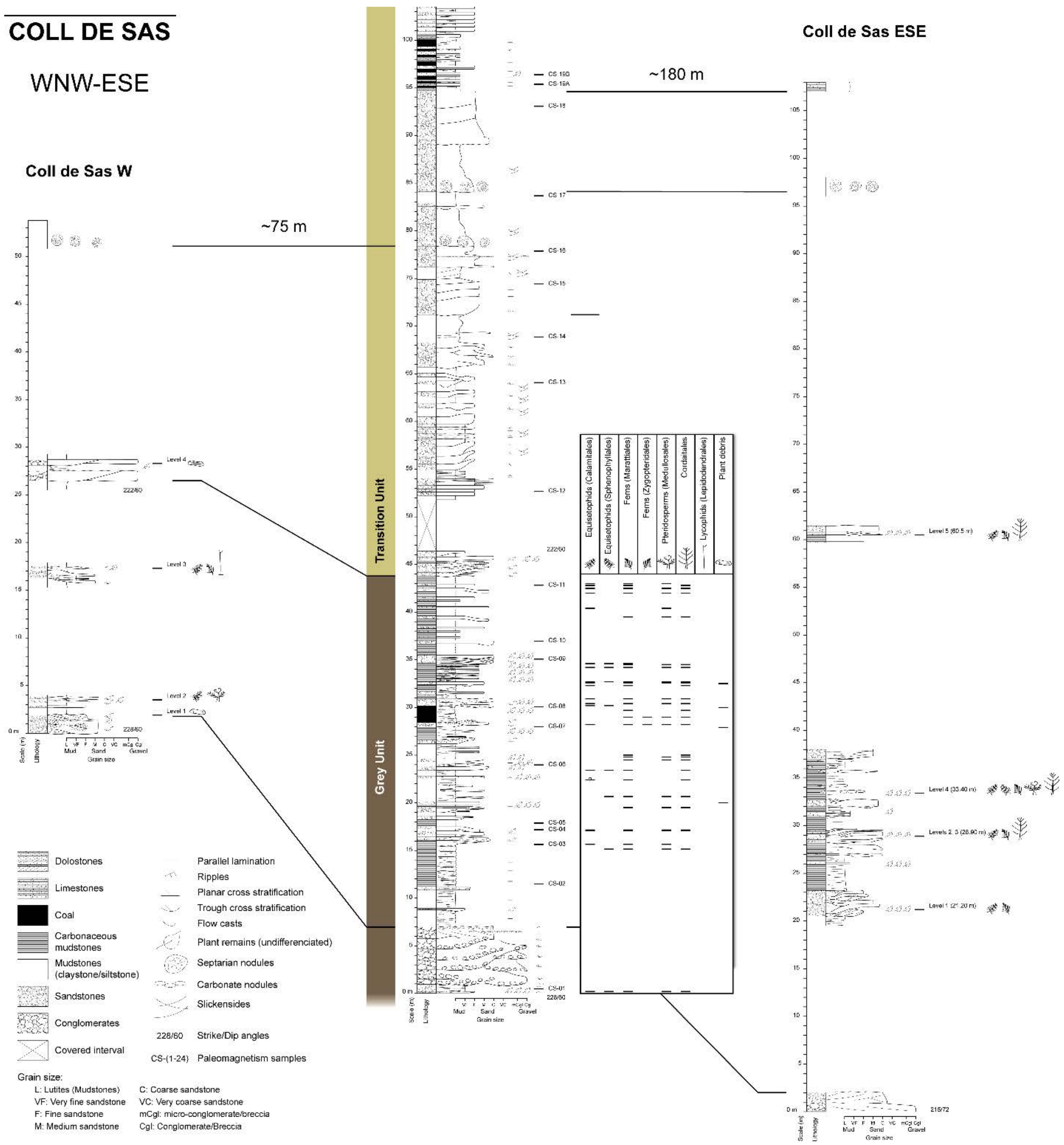

Figure S1. Stratigraphic sections from Coll de Sas with levels where plant fossils were collected.

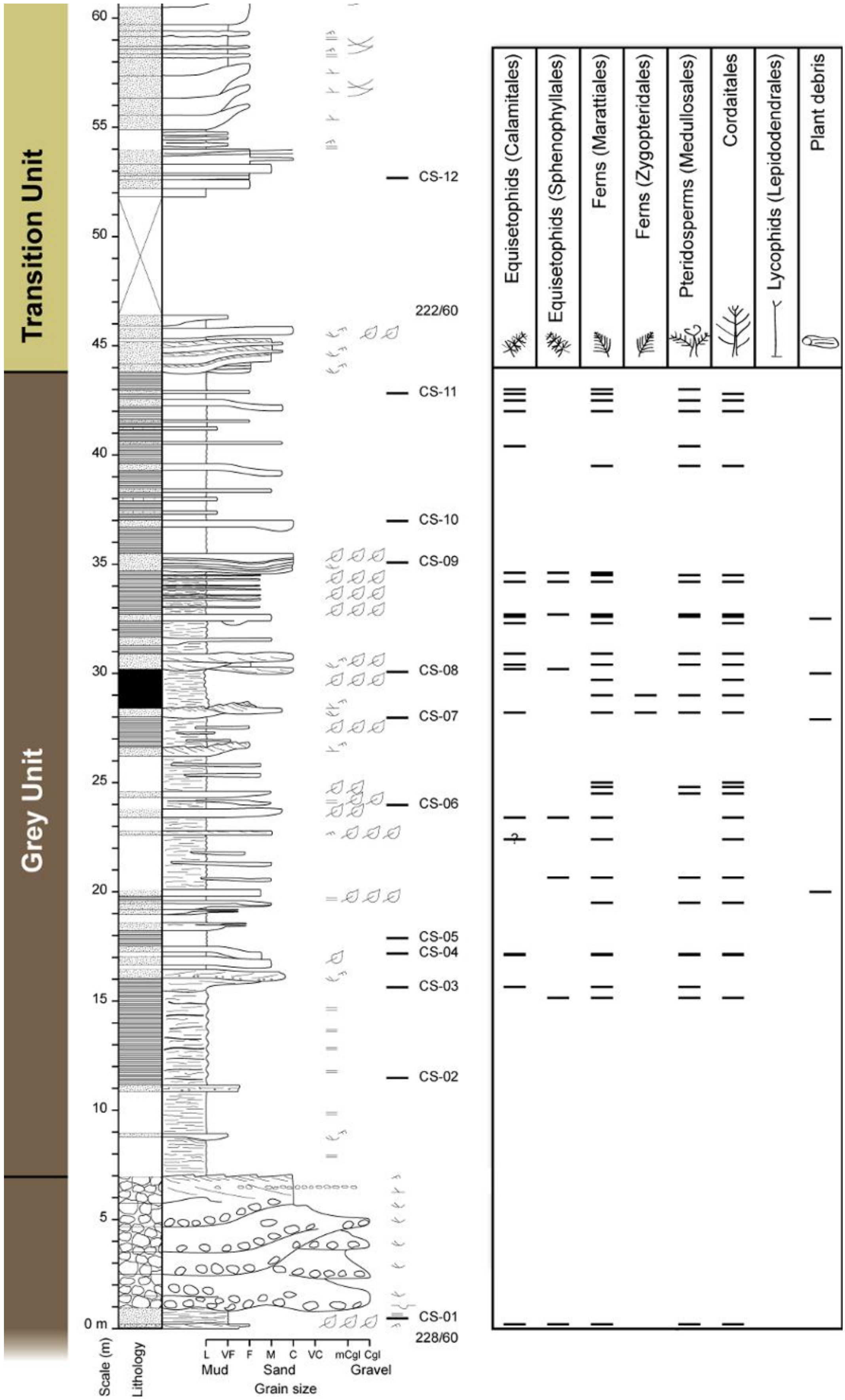

Figure S1. *(continued)* Detail of the main, middle section (Coll de Sas NW, see Data S1).

Supplementary Text S1. Paleobotanical content, lithology and taphonomy of the plant-bearing beds from Coll de Sas sections. See Figure S1 for the exact stratigraphic location of each bed. The plant fossil collection is stored at Institut Català de Paleontologia Miquel Crusafont (Sabadell, Spain; collection labelled IPS): each stratigraphic level has an associated IPS, thus all all taxa/specimens of each level share the same IPS label; taxa/specimens with specific IPS label are indicated.

COLL DE SAS NW (from base to top)

Level 1 (0.2 meters) – IPS-103100

Calamitales: *Annularia sphenophylloides*

Sphenophyllales: *Sphenophyllum oblongifolium*

Marattiales: *Pecopteris* sp.

Medullosales: *Alethopteris* sp., *Odontopteris brardii*

Cordaitales: *Cordaites* sp., cf. *Poacordaites*

<u>Lithology</u>: Siltstone/very fine-grained sandstone that grades to laminated fine-grained sandstone.

<u>Taphonomic observations</u>: Massive accumulation of plant remains mostly composed of partial leaves belonging to horsetails, ferns, pteridosperms and Cordaitales. Leaves of *Annularia* are preserved from a single isolated leafy whorl to several whorls attached to the central axis. Remains of *Pecopteris* and *Odontopteris* fronds consist of detached pinnae. Ribbon-shaped leaves of *Cordaites* are also fragmentary. Other plant remains consist of narrow (0.5 to 2 cm wide), partial stems of Calamitales.

From 0.2 m to 15.15 m

The above described interval is overlaid by conglomerates and coarse-grained sandstones corresponding to fluvial braided deposits and barren of fossils. These deposits are overlaid, until the subsequent plant fossil-bearing level, by a poorly exposed succession of mudstones and thin sandstone layers.

Level 2 (15.15 meters) – IPS-103101

Sphenophyllales: *Sphenophyllum* sp.

Marattiales: *Pecopteris* sp., *Diplazites* sp.

Medullosales: *Alethopteris* sp., *Callipteridium* sp., *Odontopteris* cf. *brardii*, *O.* cf. *cantabrica*

Cordaitales: *Cordaites* sp.

<u>Lithology</u>: Dark, carbonaceous lutite.

<u>Taphonomic observations</u>: Plant remains are less abundant compared to the bed below (0.2 meters). The fossil assemblage is mostly composed of leaf remains with some fragments of stems attributed to horsetails (*Sphenophyllum*). Leaf remains (mostly fragments of pinnae) were assigned to form-genera related to ferns and Medullosales. Fragments of ribbon-shaped leaves of *Cordaites* are also present in the sample.

Level 3 (15.65 meters) – IPS-103102

Calamitales: *Annularia* sp.

Marattiales: *Pecopteris* sp., *P.* cf. *arborescens*, *P. robustissima*

Medullosales: *Odontopteris* cf. *cantabrica*, *Callipteridium* sp.

Incertae sedis: Eusphenopteris sp.

<u>Lithology</u>: Dark lutite to fine-coarse grained sandstone bearing tiny coal fragments.

<u>Taphonomic observations</u>: Fragments of *Pecopteris* fronds are the most abundant plant remain. Detached pinnae of pteridosperm fronds were rather less numerous in the leaf litter. Equisetopsids are only represented by fragments of isolated

leafy whorls of *Annularia* as well as a few thin (0.4–0.6 cm wide) axes. The studied sample also included two fragments of stems (4 cm long) of uncertain botanical affinity.

Level 4 (17.10 meters) – IPS-103103

Calamitales: *Annularia sphenophylloides*, *Annularia* sp.

Marattiales: *Pecopteris* sp.

Medullosales: *Alethopteris* sp., *Callipteridium zeilleri*, *Odontopteris* cf. *brardii*, *O.* cf. *cantabrica*

Cordaitales: *Cordaites* sp.

Lithology: Dark lutite grading from a medium-grained sandstone.

Taphonomic observations: The sample is exclusively composed of leaves including horsetails (Calamitales), ferns (Marattiales), pteridosperms (Medullosales) and Cordaitales. *Annularia* is represented by isolated leafy whorls while fronds of ferns and pteridosperms only preserve fragments of detached pinnae. Leaves of Cordaitales are also fragmentary. Fragments are larger at the base of the bed and smaller but preserving more details at the top of the bed.

Level 5 (17.15 meters) – IPS-103104

Calamitales: *Annularia sphenophylloides*, cf. *Asterophyllites*

Marattiales: *Pecopteris* sp.

Medullosales: *Odontopteris* cf. *cantabrica*

Cordaitales: Cordaitales indet.

Lithology: Dark lutite with discontinuous layers bearing plant debris.

Taphonomic observations: Leaves dominate the assemblage. Horsetails consist of isolated leafy whorls of *Annularia* and possible branches of *Asterophyllites*. Ferns are represented by frond fragments of *Pecopteris*. The form-species *Odontopteris* cf. *cantabrica* gives evidence for the only remains of Medullosales. The leaf assemblage also includes fragments of ribbon-shaped leaves attributed to Cordaitales and stems of uncertain botanical affinity.

Level 6 (19.50 meters) – IPS-103105

Marattiales: *Pecopteris* sp.

Medullosales: *Odontopteris brardii*

Cordaitales: Cordaitales indet.

Lithology: Very fine sandstone laterally associated to a channel.

Taphonomic observations: Small fragments of pinnae bearing three to six pairs of pinnulae attached are common but it is difficult to assign them to a determinate form-genus because of their poor preservation. Among other remains, detached pinnae of *Pecopteris* sp. and *Odontopteris brardii* as well as partial leaves of Cordaitales were identified.

Level 7 (20.00 meters) – IPS-103106

Lithology: Mixed lutite and very fine sandstone bed underneath a medium-grained sandstone channel.

Taphonomic observations: This horizon contains fragments of pinnae of uncertain botanical affinity.

Level 8 (20.65 meters) – IPS-103107

Sphenophyllales: *Sphenophyllum* sp.

Marattiales: *Pecopteris* sp.

Medullosales: cf. *Alethopteris*, *Callipteridium* sp.

Cordaitales: Cordaitales indet.

Lithology: Medium-grained sandstone with incursions of coarser grains and millimetric coal debris, which is overlain by a laminated coal sandwiched between two sandstone bodies.

<u>Taphonomic observations</u>: The fossil assemblage is composed of fragments of pinnae assigned to the form-genera *Pecopteris* and *Callipteridium* as well as fragments of leaves of indeterminate Cordaitales. A few partial stems of *Sphenophyllum* are composed of several internodes.

Level 9 (22.40 meters) – IPS-103108

Calamitales: ?

Marattiales: *Pecopteris* sp.

Cordaitales: Cordaitales indet.

<u>Lithology</u>: Very fine to fine-grained sandstone.

<u>Taphonomic observations</u>: This bed has yielded partial stems of indeterminate sphenopsids as well as fragments of leaves assigned to *Pecopteris* sp. and indeterminate Cordaitales.

Level 10 (23.40 meters) – IPS-103109

Calamitales: *Annularia stellata*, *A. sphenophylloides*

Sphenophyllales: *Parasphenophyllum thonii*, *Sphenophyllum* sp.

Marattiales: *Pecopteris* sp., *Polymorphopteris polymorpha*

Cordaitales: *Cordaites* sp.

<u>Lithology</u>: Ochre siltstone to very fine sandstone.

<u>Taphonomic observations</u>: This sandstone bed shows heterogeneous granulometry, being the plant remains more abundant in the finest layers. The assemblage is composed of isolated leafy whorls of sphenopsids, detached pinnae of fern fronds and fragments of leaves of Cordaitales.

Level 11 (24.50−24.80 meters) – IPS-103110

Marattiales: *Pecopteris* sp., cf. *Diplazites*

Medullosales: *Alethopteris* sp., *Callipteridium* sp.

Cordaitales: Cordaitales indet.

<u>Lithology</u>: Sandy lutite and medium-grained sandstone with plant debris. Some sandstone layers are undulating. Most plant remains accumulate at the more carbonaceous base of the lutite.

<u>Taphonomic observations</u>: Fragments of detached pinnae of fern and pteridosperm fronds as well as ribbon-shaped leaves of Cordaitales.

Level 12 (25.00 meters) – IPS-103111

Marattiales: *Pecopteris* sp.

Cordaitales: *Cordaites* sp.

<u>Lithology</u>: Very fine to fine-grained sandstone sometimes showing lamination.

<u>Taphonomic observations</u>: Plant fossils mostly consist of fragment of fronds or detached pinnae assigned to *Pecopteris* sp. A single fragment of ribbon shaped leaf with parallelodromous venation was classified as *Cordaites*.

Level 13 (28.10 meters) – IPS-103112

<u>Lithology</u>: Lutite with plant debris close to sandstone channels.

<u>Taphonomic observations</u>: This level yielded only indeterminate plant remains.

Level 14 (28.40 meters) – IPS-103113, IPS-103114*[1], IPS-103115*[2]

Calamitales: *Annularia sphenophylloides*, *A. stellata*, *Calamostachys* sp.*[1]

Incertae sedis: cf. *Sphenopteris*

Zygopteridales: *Nemejcopteris feminaeformis**[2]

Marattiales: *Pecopteris* sp., *Lobatopteris* sp., *Diplazites* sp.

Medullosales: *Odontopteris brardii*, *Callipteridium zeilleri*

Cordaitales: Cordaitales indet.

Lithology: Very fine to medium-grained sandstones showing different coloration (greyish-greenish to ochre). There are oxidation zones.

Taphonomic observations: A single cone of *Calamostachys* is well preserved. However, the fossil assemblage is dominated by leaf remains. Among them, other evidence for Calamitales comes from isolated leafy whorls or axes with several whorls attached of the form-genus *Annularia*. Fern foliage includes fragments of detached pinnae as well as partial fronds. Pteridosperm fronds are only preserved as isolated pinnae. Ribbon-shaped leaves of Cordaitales are also fragmentary. Thin stem fragments showing longitudinal striation and several internodes likely belonged to indeterminate sphenophytes.

Level 15 (29.00 meters) – IPS-103116

Zygopteridales: cf. *Nemejcopteris*

Marattiales: *Pecopteris* sp., *Diplazites* sp., *Polymorphopteris polymorpha*?

Medullosales: *Callipteridium* sp., cf. *Neuropteris*

Cordaitales: Cordaitales indet.

Lithology: Dark, carbonaceous lutite.

Taphonomic observations: The assemblage is mostly composed of partial fronds and detached pinnae of ferns and pteriosperms. A fragment of pinna resembles those of the form-genus *Nemejcopteris* and fragments of ribbon-shaped leaves were assigned to indeterminate Cordaitales.

Level 16 (29.70 meters) – IPS-103117, IPS-103118*

Marattiales: *Pecopteris* sp.*

Cordaitales: Cordaitales indet.

Lithology: Medium-grained sandstone channel with many plant remains at the top. It is overlain by a lutite horizon bearing an accumulation of *Pecopteris* fronds. This is covered by fine sandstone with plant debris. Laterally, it evolves to very coarser sandstones (point bars) containing stems and coal fragments.

Taphonomic observations: Partial fronds of *Pecopteris* were abundant and overlapped in this bed which also included fragments of ribbon-shaped leaves likely belonging to Cordaitales.

Level 17 (30.10 meters) – IPS-103119

Lithology: Coarse sandstone with carbonaceous fragments.

Taphonomic observations: Fragment of stem with longitudinal grooves likely belonging to a horsetail.

Level 18 (30.20 meters) – IPS-103120

Calamitales: *Annularia stellata*, *A. sphenophylloides*

Marattiales: *Pecopteris* sp., cf. *Diplazites*

Lithology: Greyish lutite laterally to a sandy channel.

Taphonomic observations: Calamitales are represented by leafy whorls isolated or attached to the central axis. Fragments of fronds and detached pinnae of Marattiales are also preserved.

Level 19 (30.40 meters) – IPS-103121

Calamitales: Calamitales indet.

Marattiales: *Pecopteris* sp.

Medullosales: *Callipteridium* sp.

Cordaitales: cf. *Poacordaites*

Lithology: Fine-grained sandstone with interbedded siltstones that change laterally to coarse-very coarse sandstone bearing plant debris.

Taphonomic observations: A partial stem showing internodes ornamented with parallel grooves was assigned to an indeterminate Calamitales. Fragments of detached pinnae and fronds are very abundant and accumulated in very thin layers. They belonged to ferns and pteridosperms. Some narrow ribbon-shaped leaves resemble those of *Poacordaites*.

Level 20 (30.90 meters) – IPS-103122

Calamitales: *Annularia sphenophylloides*, *A.* cf. *stellata*

Marattiales: *Pecopteris* cf. *robustissima*, *P.* cf. *arborescens*

Medullosales: *Alethopteris* sp.

Cordaitales: *Cordaites*, cf. *Poacordaites*

Lithology: Mudstones and medium-grained to coarse sandstones (point bars).

Taphonomic observations: Plant remains are more abundant in mudstones and overbank deposits. Several axes of Calamitales bear a few leafy whorls attached. In other cases, leafy whorls are isolated. Marattiales ferns are represented from partial fronds to detached pinnae. Leaves of pteridosperms are less abundant and also very fragmentary. Partial ribbon-shaped leaves belonged to Cordaitales. Small stem fragments of uncertain botanical affinity also occur in the fossil assemblage of this horizon. Other partial stems could be attributed to indeterminate sphenophytes.

Level 21 (32.30 meters) – IPS-103123

Calamitales: *Annularia stellata*

Marattiales: *Pecopteris robustissima*, *Pecopteris* sp.

Cordaitales: Cordaitales indet.

Lithology: Dark, laminated and carbonaceous mudstones.

Taphonomic observations: Only a single leafy whorl testifies the presence of Calamitales in the sample. Marattiales ferns are preserved as fragments of detached pinnae. Ribbon-shaped leaf fragments of Cordaitales are also present in the sample.

Level 22 (32.50 meters) – IPS-103124

Lithology: Coarse-grained sandstone (building up lateral accretions).

Taphonomic observations: Plant fossil remains are very scarce and bad preserved. They consist of a partial log and fragments of pinnate fronds.

Level 23 (32.60 meters) – IPS-103125

Calamitales: *Annularia sphenophylloides*

Marattiales: *Pecopteris* sp., *P. robustissima*

Medullosales: *Callipteridium* sp.

Cordaitales: *Cordaites* sp.

Lithology: Fine-grained, grey sandstone.

Taphonomic observations: Plant remains are sparse in relation to the rock matrix. Remains of Calamitales consist of isolated whorls of *Annularia* and fragments of stems including some internodes. Among detached fragments of pinnae from fern and seed fern fronds, those of *Pecopteris* are the more abundant. Ribbon-shaped leaves of Cordaitales are also fragmentary.

Level 24 (32.70 meters) – IPS-103126

Calamitales: *Annularia sphenophylloides*, *A.* cf. *stellata*

Sphenophyllales: *Sphenophyllum* sp.

Marattiales: *Pecopteris* sp., *P.* cf. *arborescens*, *P.* cf. *jongmansii*, *P.* cf. *robustissima*.

Medullosales: cf. *Neuropteris*, *Callipteridium zeilleri*

Cordaitales: Cordaitales indet.

Lithology: Plant bearing lutite below a medium-coarse sandstone channel.

Taphonomic observations: Most of plant debris consists of leaf fragments. Most of Calamitales remains are isolated whorls. Sphenophyte rests also include a fragment of stem and a detached sporangium. Detached fragments of *Pecopteris* pinnae are abundant while those of pteridosperm affinity (*Neuropteris*, *Callipteridium*) are less frequent. Cordaitales are only represented by a fragment of ribbon-shaped leaf with parallelodromous venation.

Level 25 (34.20 meters) – IPS-103127

Calamitales: *Annularia sphenophylloides*, *A. stellata*

Sphenophyllales: *Sphenophyllum* sp.

Marattiales: *Pecopteris* sp., *Diplazites* sp., *Polymorphopteris polymorpha*

Medullosales: cf. *Callipteridium*

Cordaitales: *Cordaites* sp., cf. *Poacordaites*

Lithology: Very fine to fine sandstone interbedded with coal layers bearing lots of plant debris. About four meters toward the east, the plant content strongly diminishes and the bed is cut by a medium-grained sandstone channel.

Taphonomic observations: Remains of sphenophytes are very scarce and fragmentary; one isolated leafy whorl of *Annularia* and a fragment of internode of a stem. Fronds of *Pecopteris* are preserved from abundant detached fragments of pinnae to a partial frond with three pinnae in connection. There are also a few partially preserved ribbon-shaped leaves of *Cordaites*. A fragment of horsetail stem (*Sphenophyllum*) shows several nodes articulated.

Level 26 (34.50 meters) – IPS-103128

Marattiales: *Diplazites* sp., *Pecopteris* sp., *P.* cf. *robustissima*

Medullosales: cf. *Callipteridium*

Cordaitales: Cordaitales indet.

Lithology: Very fine to fine laminated sandstone and carbonaceous lutite. Below a sandy channel, there is very fine-grained sandstone with coal and lots of plant remains.

Taphonomic observations: There is a progression from larger plant remains (stems and partial fronds) at the base of the bed to detached fragments of pinnae at the top. Fragments of fronds of *Pecopteris* are very abundant. Remains of other taxa are scarcer.

Level 27 (34.60 meters) – IPS-103129

Calamitales: *Annularia sphenophylloides*

Sphenophyllales: *Sphenophyllum* sp.

Marattiales: *Pecopteris* sp.

Lithology: Fine-grained sandstone interbedded with coal layers toward the east.

Taphonomic observations: *Sphenophyllum* stems composed of several internodes are abundant. Leaves are scarcer than stems and consist of isolated leafy whorls or branch fragments of *Annularia*. The only evidence for Marattiales ferns is a single fragment of detached pinna.

Level 28 (39.50 meters) – IPS-103130

Marattiales: *Pecopteris* sp.

Medullosales: *Calllipteridium* sp., *Odontopteris brardii*

Cordaitales: Cordaitales indet.

Lithology: Medium to coarse-grained sandstone with sigmoid shape grading to laminated mudstones.

Taphonomic observations: Detached partial pinnae of fern and pteridosperm fronds. Fragments of ribbon-shaped leaves of Cordaitales.

Level 29 (40.40 meters) – IPS-103131

Calamitales: *Annularia sphenophylloides*

Medullosales: *Callipteridium* sp., *Odontopteris* sp.

Lithology: Laminated carbonaceous mudstones with interbedded thin (<10 cm) medium- to coarse-grained sandstone layers.

Taphonomic observations: Plant remains only consist of detached pinnulae and isolated leafy whorls.

Level 30 (42.00 meters) – IPS-103132

Calamitales: *Annularia sphenophylloides*, *A. stellata*

Marattiales: *Pecopteris* sp.

Medullosales: cf. *Callipteridium*, *Odontopteris brardii*

Cordaitales: Cordaitales indet.

Lithology: Very fine sandstone with some lamination.

Taphonomic observations: Calamitales are preserved as isolated whorls, being those of *Annularia stellata* the more abundant. Remains of fern and pteridosperm foliage consist of detached pinnae. Leaves of Cordaitales are preserved as elongated fragments.

Level 31 (42.50 meters) – IPS-103133

Calamitales: *Annularia sphenophylloides*

Marattiales: *Diplazites emarginatus*, *Pecopteris* sp., *P.* cf. *arborescens*, *P.* cf. *robustissima*

Medullosales: *Odontopteris brardii*

Cordaitales: Cordaitales indet., cf. *Poacordaites*

Lithology: Laminated mudstones grading from medium- to coarse-grained sandstone with sigmoid shape.

Taphonomic observations: Most of the assemblage is composed of leaves although several small stem fragments are present. *Annularia* remains are preserved from isolated whorls to several whorls connected to a central axis. Most of remains of ferns and pteridosperms consist of detached fragments of pinnae and a few partial fronds bearing two to four pinnae attached. Leaves of Cordaitales are also fragmentary.

Level 32 (42.80 meters) – IPS-103134

Calamitales: *Annularia sphenophylloides*

Marattiales: *Pecopteris* sp., *P. robustissima*

Cordaitales: *Cordaites* sp.

Lithology: Carbonaceous rock matrix.

Taphonomic observations: Plant remains consist of isolated leafy whorls of *Annularia*, detached fragments of pinnae belonging to fern fronds and fragments of elongated leaves of Cordaitales.

Level 33 (43.00 meters) – IPS-103135

Calamitales: *Annularia sphenophylloides*, *A.* cf. *stellata*

Marattiales: *Pecopteris* sp.

Medullosales: *Odontopteris* sp.

Lithology: Laminated carbonaceous mudstones.

Taphonomic observations: Plant remains are preserved as isolated leafy whorls of Calamitales as well as detached pinnae of fern fronds.

* At the two following sections (Coll de Sas W and ESE) only specific levels were excavated. These sections are correlated to Coll de Sas NW section (the main one).

COLL DE SAS W (from base to top)

* Base of the section at the top of the fluvial braided deposits, equivalent to those from Coll de Sas NW section.

Level 1 (1.90 m) – IPS-103136

Lithology: Fine-grained sandstone with flow ripples grading from a medium- to coarse-grained trough cross-laminated sandstone with lag deposits (conglomerates and microconglomerates).

Taphonomic observations: fragment of pinna of uncertain botanical affinity.

Level 2 (3.50 m) – IPS-103137

Calamitales: *Annularia sphenophylloides*

Medullosales: *Callipteridium* sp.

Lithology: Mudstones and very fine-grained sandstone with flow ripples grading from medium- to fine-grained sandstone with trough cross stratification and erosive base.

Taphonomic observations: *Annularia* axis with several leafy whorls attached as well as several detached pinnae of pteridosperm fronds.

Level 3 (17.3 m) – IPS-103138, IPS-103139*

Lepidodendrales: *Sigillariostrobus* sp.*

Calamitales: cf. *Asterophyllites*

Marattiales: *Pecopteris* sp.

Lithology: Fine- to medium-grained sandstone in a discontinuous layer interbedded with mudstones.

Taphonomic observations: Sphenophyte axes with several whorls attached and fragments of detached pinnae from fronds. There is also a partial cone of a lycophyte.

COLL DE SAS ESE (from base to top)

* Base of the section at the top of the fluvial braided deposits, equivalent to those from Coll de Sas NW section.

Level 1 (21.20 m) – IPS-103140

Calamitales: *Annularia sphenophylloides*

Marattiales: *Pecopteris* sp.

Lithology: Fine-grained laminated sandstone with medium- and coarse-grained sandstone layers and lag deposits; lutitic and carbonaceous intervals with plant fragments occur. The top of the sequence is a laminated lutite bearing the described plants.

Taphonomic observations: *Annularia* axis bearing some leafy whorls attached and some detached pinnae of *Pecopteris*. A fragment of a likely sphenophyte stem shows some nodes articulated.

Level 2 (28.90) – IPS-103141

Calamitales: *Annularia* sp.

Marattiales: *Pecopteris* sp.

Cordaitales: Cordaitales indet.

Lithology: Alternation of coarse-grained sandstone bodies (bearing plants and pebbles at the basal part) with carbonaceous mudstones. A dolostone layer appears at the base of the sequence.

Taphonomical observations: Remains of Calamitales consist of isolated leafy whorls and partial stems showing striation on the surface of internodes. *Pecopteris* fronds are strongly fragmented. Leaves of Cordaitales are also scrapped.

Level 3 (28.90) – IPS-103142

Lithology: The same as Level 2 (laterally equivalent).

Taphonomic observations: Fragment of a large horsetail stem with vertical grooves separated 2 cm from each other.

Level 4 (33.40 m) – IPS-103143

Calamitales: Calamitales indet.

Sphenophyllales: *Sphenophyllum* sp.

Marattiales: *Pecopteris* sp., *P. robustissima*

Medullosales: *Odontopteris* sp., *O. brardii*, *Neuropteris* sp., *Callipteridium* sp.

Cordaitales: cf. *Cordaites*

Lithology: Carbonaceous mudstones with lenticular bodies of very fine- to fine-grained sandstone with limestone component.

Taphonomic observations: Sphenophyte remains are preserved as isolated leafy whorls and small stem fragments. Detached pinnae of *Pecopteris* dominate the assemblage. Similar features are observed in frond remains of pteridosperms. Ribbon-shaped leaves of Cordaitales are fragmentary.

Level 5 (60.50 m) – IPS-103144

Calamitales: *Annularia sphenophylloides*

Marattiales: *Pecopteris* sp.

Cordaitales: cf. *Cordaites*

Lithology: Coarse-grained grading to fine-grained sandstone.

Taphonomic observations: Remains of sphenophytes are preserved as isolated leafy whorls and partial stems. Detached pinnae of *Pecopteris* and fragments of ribbon-shaped leaves of Cordaitales also occur in the assemblage.

Annex 4. Material suplementari del capítol 4

Appendix 1. Figures

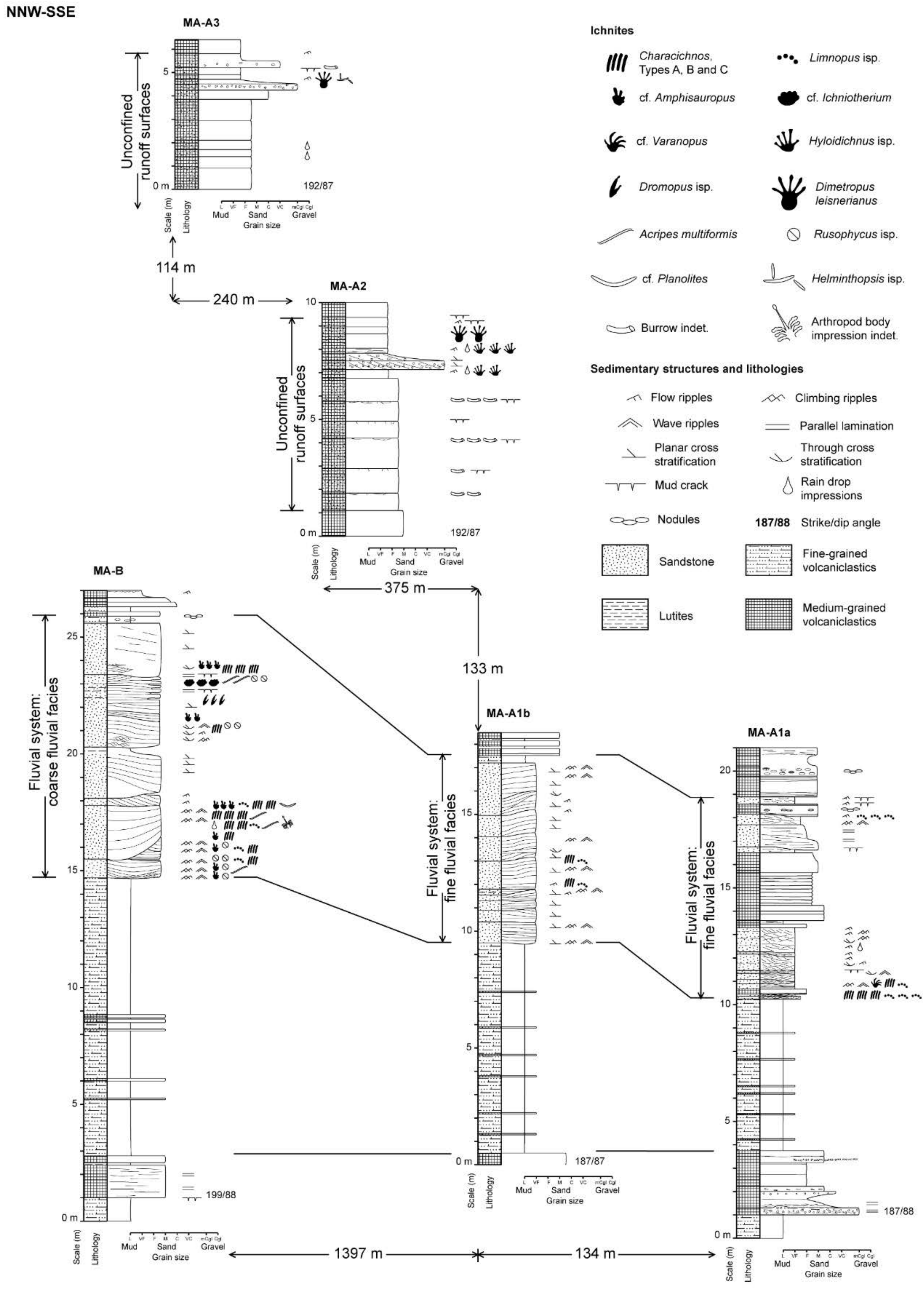

Figure S1. Correlated stratigraphic sections.

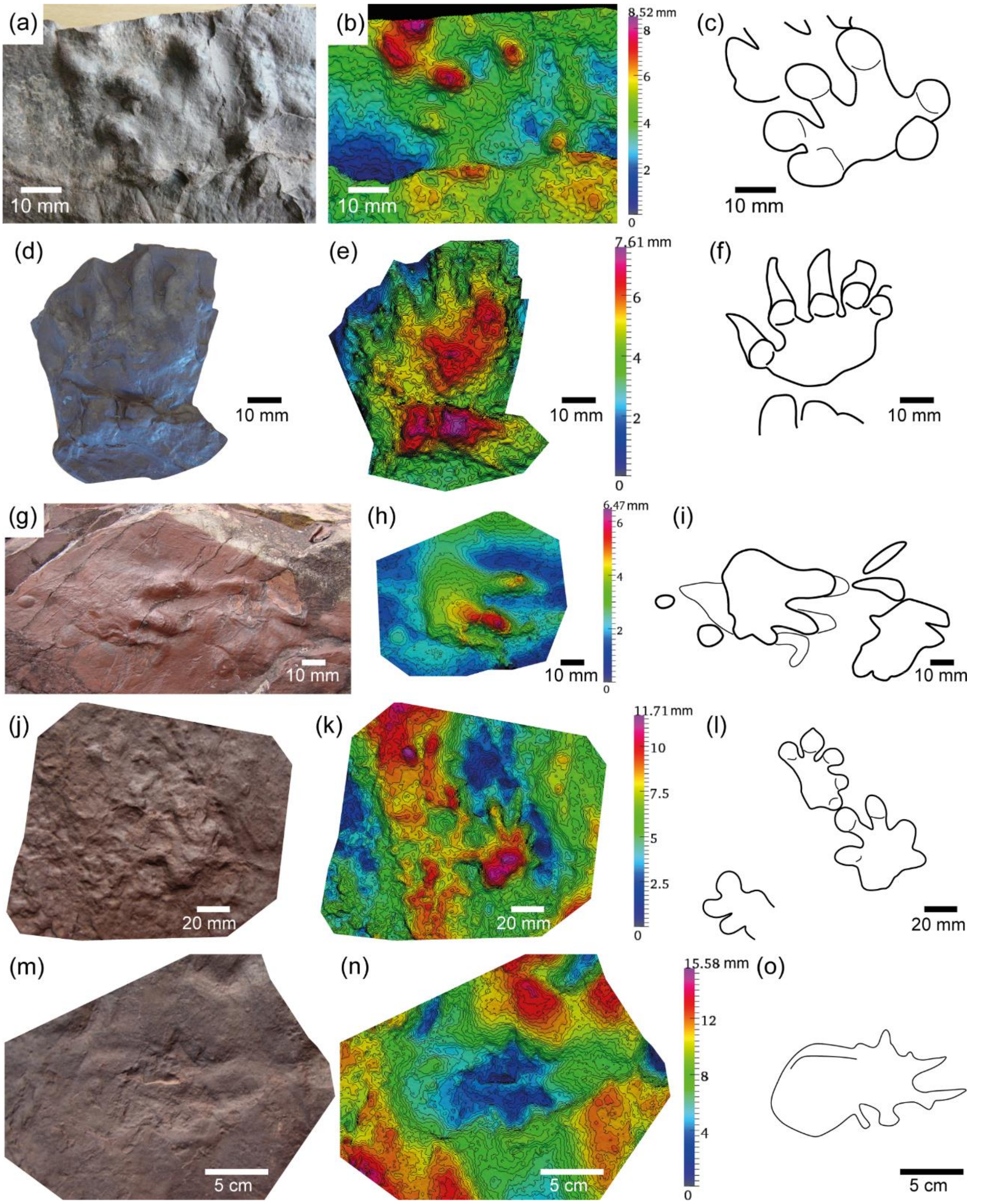

Figure S2. Additional tetrapod footprints specimens I. (a)-(c) *Limnopus* isp. manus and partial track (IPS-83730); (a) photo; (b) 3D model; (c) ichnites outline. (d)-(l) cf. *Amphisauropus* manus-pes sets from the section MA-B; (d) IPS-73723; (g) specimen at 15.20 m; (j) specimen at 21.50 m, corresponding 3D models (e, h, k) and ichnites outline (f, i, l). (m)-(o) *Dimetropus leisnerianus* from the section MA-A3 at 4.30 m; (m) photo; (n) 3D model; (o) ichnites outline.

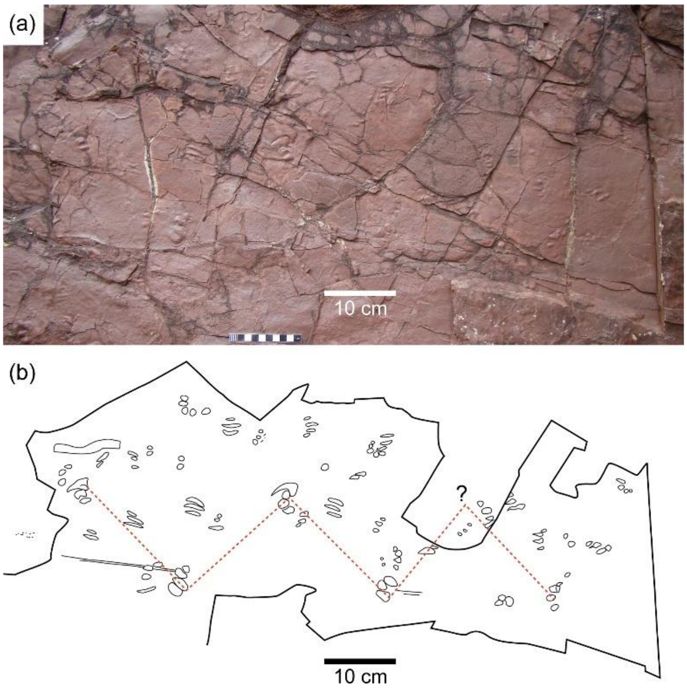

Figure S3. Additional tetrapod footprints specimens II. Surface at 17.75 m from the section MA-B. (a) *Characichnos* Type C, *Limnopus* isp. trackway (with paces outlined in (b)), and a burrow of cf. *Planolites* (top left); (b) ichnites outline.

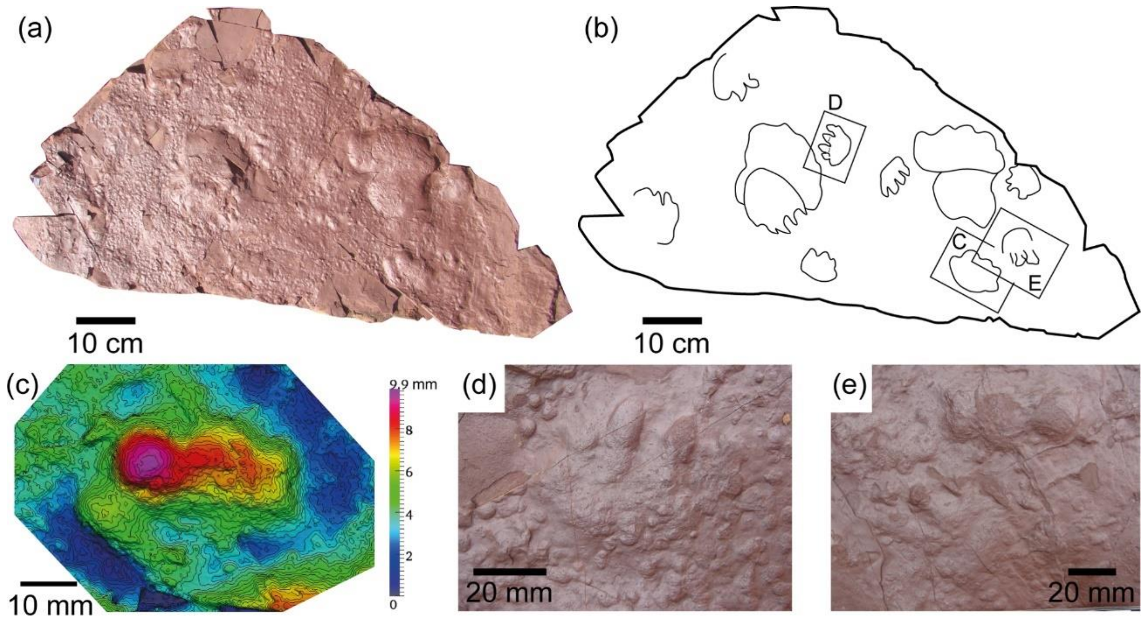

Figure S4. Additional tetrapod footprints specimens III. Unidentermined tetrapod footprints from site MA-B (block *ex situ* not recovered). (a) Entire block; (b) ichnites outline; (c) 3D model squared in (b); (d) and (e) ichnites squared in (b).

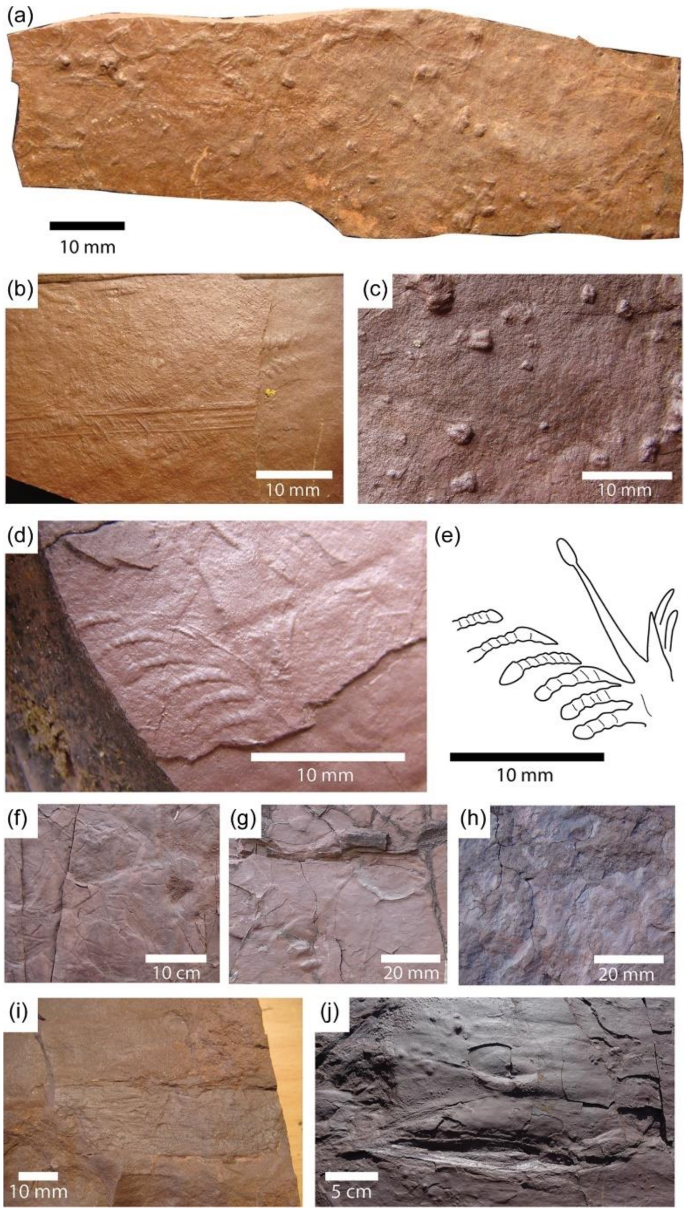

Figure S5. Invertebrate traces and plant remains. (a) *Acripes multiformis* and *Rusophycus* isp. (IPS-83712 at section MA-B 23.40 m); (b) *Acripes multiformis* (MA-B 16.80 m); (c) *Rusophycus* isp. (section MA-B 23.10 m); (d) and (e) undetermined arthropod body impression and ichnite outline, respectively (section MA-B 16.80 m); (f) several *Helminthopsis* isp. overprinting flow ripples (section MA-A3 4.70 m); (g) cf. *Planolites* and *Limnopus* isp. digit tip track (section MA-B 17.75 m); (h) Abundant vertical undetermined burrows (section MA-A2 4.20 m); (i) undetermined plant remain from site MA-B (block *ex situ*; IPS-83722); (j) undetermined plant remains from site MA-B (the block *ex situ* from Fig. 11b).

Appendix 2. Measurement tables of the tetrapod footprints

Table S1. *Batrachichnus salamandroides* (IPS-73741-5; site MA-A1a) track parameters in mm and degrees. Values preceded by asterisk (*) are estimated. N: element not found in tracks (i.e., tetradactyl manus). M: Manus tracks. P: Pes tracks.

Track Parameters	1st set		2nd set		3rd set		4th set		5th set		Mean	
	M	P	M	P	M	P	M	P	M	P	Manus	Pes
Lenght	6.94	-	4.87	-	7.29	7.76	-	9.07	-	7.41	6.27	8.05
Width	11.58	-	7.95	-	14.34	11.51	-	12.60	-	11.33	10.97	11.80
Length sole	*2.82	-	2.29	-	*3.11	4.29	-	4.70	-	3.21	2.72	4.02
Width sole	*3.55	-	2.32	-	*4.57	3.64	-	6.95	-	4.13	3.35	4.71
Length I	3.96	-	2.79	-	4.33	3.34	-	3.22	-	3.98	3.63	3.50
Length II	3.71	-	3.00	-	4.39	3.18	-	3.42	-	3.72	3.66	3.43
Length III	3.47	-	2.90	-	4.37	3.42	-	3.89	-	3.53	3.53	3.61
Length IV	3.54	-	3.22	-	4.64	3.67	-	3.75	-	3.42	3.75	3.61
Length V	N	N	N	N	N	4.54	N	3.64	N	3.12	N	3.72
Div. I-II	36.845	-	28.301	-	32.391	30.532	-	22.930	-	30.509	32.325	27.746
Div. II-III	51.154	-	37.828	-	29.801	24.447	-	31.040	-	39.756	38.634	31.130
Div. III-IV	51.963	-	39.325	-	54.687	35.955	-	31.948	-	32.585	48.167	33.451
Div. IV-V	N	N	N	N	N	46.422	N	23.840	N	46.789	N	37.273
Div. II-IV	109.112	-	75.710	-	88.081	62.088	-	65.365	-	77.978	89.943	68.146
Div. I-V or Div. I-IV	137.005	-	114.986	-	115.023	133.127	-	108.991	-	147.265	121.914	128.801
Length/Width	0.599	-	0.613	-	0.508	0.674	-	0.720	-	0.654	0.571	0.682

Table S2. *Batrachichnus salamandroides* (IPS-73741-5; site MA-A1a) trackway parameters in mm and degrees. Values preceded by asterisk (*) are estimated. Different columns correspond to the consecutive measured parameters, from the posterior (first) to the anterior (last) sets and tracks.

Trackway Parameters			Mean
Stride pes	39.34		39.34
Stride manus	39.56		39.56
Pace pes	41.84	41.85	41.84
Pace manus	36.20	50.11	42.59
Length pace pes	13.85	25.27	18.71
Length pace manus	9.89	29.67	17.13
Width pace pes	40.22	32.97	3.642
Width pace manus	35.16	40.44	37.71
Stride angulation pes	56.965		56.965
Stride angulation manus	51.067		51.067
Manus-pes distance	10.77		10.77
Interpedes distance	29.45	21.76	25.31
Intermanus distance	24.18	28.79	26.38
Width external	54.07		
Width internal	19.12		
Glenoacetabular distance	*34.51	30.55	32.47
Stride/Length pes	5.309		
Stride/Glenoacet. distance	1.140		

Table S3. *Limnopus* isp. track parameters in mm and degrees. Values preceded by asterisk (*) are estimated. N: element not found in tracks (i.e., tetradactyl manus), (continues on the next page).

Track Parameters	2nd set MA-A1a 18.15 m		3rd set MA-A1a 18.15 m		MA-A1a2	Set IPS - 73724		MA – Ala 10.20m	Mean	
	Manus	Pes	Manus	Pes	Pes	Manus	Pes	Pes (centre)	Manus	Pes
Length	38.27	48.75	38.11	-	32.07	34.28	45.91	36.89	36.84	40.34
Width	54.31	-	53.89	-	43.04	51.96	57.35	49.74	53.38	49.70
Length sole	20.48	28.85	21.48	-	13.61	16.59	19.69	19.11	19.40	19.61
Width sole	26.37	37.85	47.89	-	19.05	34.86	26.16	27.11	35.31	26.74
Length I	16.17	20.47	11.91	-	12.54	15.20	15.90	13.57	14.31	15.34
Length II	18.34	21.02	17.35	-	14.95	15.97	20.23	17.72	17.19	18.32
Length III	17.28	*22.63	21.67	-	17.34	17.33	26.16	1936	18.65	21.11
Length IV	15.06	*24.61	16.55	-	19.30	16.26	28.72	21.55	15.94	23.28
Length V	N	-	N	-	10.87	N	17.68	14.83	N	14.18
Div. I-II	29.198	32.398	18.614	-	25.724	28.313	21.994	24.691	24.873	25.937
Div. II-III	43.050	36.170	20.221	32.060	40.319	42.468	37.238	25.756	33.313	33.911
Div. III-IV	32.287	-	17.322	21.866	21.436	26.640	21.880	15.439	24.607	19.948
Div. IV-V	N	-	N	56.483	59.175	N	45.544	45.947	N	51.426
Div. II-IV	86.781	-	33.775	45.070	65.675	70.148	60.515	39.545	59.022	51.589
Div. I-V or Div. I-IV	113.682	-	57.953	-	139.012	93.341	113.998	121.061	85.038	124.256
Length/Width	0.705	-	0.707	-	0.745	0.660	0.801	0.742	0.690	0.762

Table S4. *Limnopus* isp. trackway parameters in mm and degrees. Values preceded by asterisk (*) are estimated. Values preceded by question mark (?) correspond to parameters of unidentified manus or pes tracks. Different columns for each trackway correspond to the consecutive measured parameters, from the posterior (first) to the anterior (last) sets and tracks, (continues on the next page).

Trackway Parameters	MA-A1a 18.15 m		MA-B 17.75 m			Mean
Stride pes	*312.44		?225.58	?277.91	?276.74	
Stride manus	-					
Pace pes	286.51		?194.15	?189.17	?196.55	
Pace manus	285.69					
Length pace pes	162.00		?141.86	?136.05	?141.86	
Length pace manus	16.100					
Width pace pes	237.00		?132.56	?131.40	?134.88	
Width pace manus	238.00					
Divarication manus	-25.388	-45.000	-	-		-33.800
Divarication pes	-		-	-		
Stride angulation pes	-		?92.946	?91.469		92.205
Stride angulation manus	68.919					68.919
Manus-pes distance	4.800	4.800		-		48.00
Interpes distance	-		?77.91	?73.26	?79.07	76.71
Intermanus distance	151.00					151.00
Width external	322.00		165.12			230.58
Width internal	138.00		72.09			99.74
Glenoacetabular distance	*231.00		-	-		231.00
Stride/Length pes	6.409		-	-		6.409
Stride/Glenoacet. distance	1.353		-	-		1.353

Table S5. cf. *Amphisauropus* track parameters in mm and degrees. Values preceded by asterisk (*) are estimated. Section MA-B.

Track Parameters	MA-B 21.50m		IPS - 73723	MA-B 15.2m	MA-B 17.75m												Mean	
	M	**P**	**M**	**P**	**M**	**M**	**M**	**M**	**P**	**P**	**P**	**P**	**P**	**P**	**P**	**P**	**M**	**P**
Length	32.14	57.74	27.82	40.90	18.81	39.37	33.60	23.14	45.80	41.14	44.11	32.28	57.13	45.15	49.17	56.96	28.31	46.35
Width	51.50	51.88	46.14	*36.06	30.81	47.22	39.59	35.33	*36.69	36.93	43.74	27.49	48.39	35.11	43.09	41.29	41.12	39.49
Length sole	16.26	33.87	17.58	18.41	7.96	19.17	21.73	11.20	27.98	-	25.65	21.35	34.04	25.25	30.03	-	14.82	26.55
Width sole	26.27	24.15	30.13	21.73	15.38	28.55	20.60	19.03	22.49	-	*20.52	14.95	25.77	20.67	21.64	-	22.68	21.26
Length I	11.02	13.68	8.20	08.15	8.97	12.49	10.31	7.20	10.32	-	*10.82	6.49	10.56	7.83	12.02	-	9.54	09.73
Length II	11.54	15.82	9.84	10.08	7.96	16.20	11.29	8.73	10.57	-	12.35	7.34	9.96	8.60	14.44	-	10.63	10.83
Length III	16.20	24.59	9.93	21.14	8.11	19.34	12.69	9.73	16.80	-	-	8.22	12.67	19.15	19.00	-	12.09	16.49
Length IV	19.64	26.55	10.56	22.08	6.90	22.22	13.33	10.88	-	-	17.95	12.70	23.64	21.82	17.84	-	12.90	19.89
Length V	14.18	17.84	9.05	-	6.75	11.39	10.26	8.01	-	-	13.07	9.80	13.33	07.25	13.86	-	9.66	12.05
Div. I-II	35.937	61.292	50.235	34.483	43.264	20.451	27.673	32.628	15.562	28.266	30.199	10.166	29.418	23.171	37.676	-	33.613	26.882
Div. II-III	29.212	34.153	12.856	38.926	20.720	11.855	45.247	17.766	40.456	36.395	*27.894	19.447	14.682	11.844	26.388	-	20.497	25.689
Div. III-IV	43.619	36.186	17.382	29.430	25.373	27.546	30.774	24.324	18.677	18.435	*8.500	24.995	37.917	21.808	11.672	-	27.106	20.872
Div. IV-V	38.533	33.696	16.325	-	31.732	35.305	34.695	30.375	-	-	49.459	38.012	71.790	72.284	18.503	-	30.093	42.725
Div. II-IV	71.839	76.929	21.539	63.714	60.910	41.262	69.114	52.397	69.369	50.865	45.991	55.818	50.968	47.261	34.880	-	49.142	115.751
Div. I-V	137.500	161.212	104.990	-	122.032	100.160	125.322	117.375	-	-	131.843	110.206	144.202	125.218	93.406	-	117.230	125.732
Length/Width	0.624	1.113	0.603	*1.134	0.611	0.834	0.849	0.655	1.248	1.114	1.008	1.174	1.181	1.286	1.141	1.380	0.688	1.174

Table S6. cf. *Ichniotherium* track parameters in mm and degrees. Values preceded by asterisk (*) are estimated. MA-B 23.2m.

Track Parameters	Track 1	Track 2	Track 3	Track 4	Track 5	Track 6	Track 7
Length	70.378	73.919	-	-	-	-	*86.612
Width	91.455	*80.088	-	-	-	-	*95.672
Length sole	43.661	31.275	36.336	37.165	41.552	42.793	43.481
Width sole	61.301	63.762	60.052	63.664	63.246	61.707	82.253
Length I	24.654	-	-	-	-	-	-
Length II	30.439	33.001	-	-	-	-	-
Length III	25.769	39.251	-	-	-	-	-
Length IV	24.812	42.297	-	-	-	-	-
Length V	30.259	-	-	-	-	-	-
Div. I-II	26.983	-	-	-	-	-	-
Div. II-III	29.286	27.099	-	-	-	-	-
Div. III-IV	36.537	29.489	-	-	-	-	-
Div. IV-V	15.338	-	-	-	-	-	-
Div. II-IV	66.411	57.107	-	-	-	-	-
Div. I-V	108.561	-	-	-	-	-	-
Length/Width	0.77	*0.923	-	-	-	-	*0.905

Table S7. *Dromopus* isp. track parameters in mm and degrees. Section MA-B 22.40 m.

Track Parameters	Track 1	Track 2	Track 3	Track 4	Track 5	Track 6	Mean
Length	22.715	-	-	-	-	-	22.715
Width	14.49	-	-	-	-	-	14.49
Length sole	5.718	-	-	-	-	-	5.718
Width sole	6.738	-	-	-	-	-	6.738
Length I	3.679	-	-	-	-	-	3.679
Length II	5.04	4.94	-	-	-	-	4.99
Length III	7.798	6.987	10.271	7.375	7.267	6.33	7.671
Length IV	16.706	14.211	16.742	12.368	11.661	12.125	13.969
Length V	4.102	-	-	-	-	-	4.102
Div. I-II	41.849	-	-	-	-	-	41.849
Div. II-III	54.775	33.651	-	-	-	-	44.213
Div. III-IV	18.025	17.561	38.087	24.039	24.184	26.844	24.79
Div. IV-V	47.787	-	-	-	-	-	47.787
Div. II-IV	81.262	49.521	-	-	-	-	65.392
Div. I-V	170.349	-	-	-	-	-	170.349
Length/Width	1.568	-	-	-	-	-	1.568

Table S8. cf. *Varanopus* track parameters in mm and degrees. Values preceded by asterisk (*) are estimated. Section MA-A1a 10.50 m.

Track Parameters	1st set		2nd set		3rd set		4th set		Mean	
	Manus	Pes	Manus	Pes	Manus	Pes	Manus	Pes	Manus	Pes
Length	37.80	22.89	38.59	42.44	41.79	26.62	35.57	38.72	38.37	31.63
Width	39.02	15.40	51.85	33.88	*40.54	19.07	28.38	*34.00	39.06	24.12
Length sole	19.68	*13.38	14.89	17.17	18.25	*15.47	10.79	19.92	15.50	16.31
Width sole	17.13	*10.92	17.34	22.81	*25.38	*13.14	7.29	*18.24	15.31	15.63
Length I	15.97	-	24.87	12.09	12.11	-	11.05	-	15.18	12.09
Length II	15.82	-	27.43	14.07	17.93	-	16.20	15.52	18.84	14.78
Length III	19.16	-	26.99	15.02	22.36	-	18.56	15.05	21.52	15.03
Length IV	19.54	-	27.70	24.48	25.68	-	24.34	19.40	24.12	21.79
Length V	12.37	-	19.82	*21.14	-	-	12.71	*15.15	14.61	17.90
Div. I-II	45.401	-	32.293	27.102	41.895	-	48.184	-	41.477	27.102
Div. II-III	47.366	-	25.208	16.599	23.755	-	24.146	53.728	28.767	29.864
Div. III-IV	18.958	-	28.428	24.715	11.001	-	59.924	27.302	24.414	25.976
Div. IV-V	28.655	-	72.540	36.201	-	-	30.972	17.463	40.079	25.143
Div. II-IV	71.907	-	60.791	24.652	47.187	-	89.171	76.247	65.488	43.355
Div. I-V	132.714	-	151.955	85.030	-	-	133.904	-	139.254	85.030
Length/Width	0.969	1.486	0.744	1.253	1.031	1.396	1.253	1.139	0.982	1.312

Table S9. cf. *Varanopus* trackway parameters in mm and degrees. Section MA-A1a 10.50 m. Different columns correspond to the consecutive measured parameters, from the posterior (first) to the anterior (last) sets and tracks.

Trackway Parameters					Mean
Stride pes	211.11	234.92			222.70
Stride manus	217.46	242.06			229.43
Pace pes	163.82	182.40	193.97		179.63
Pace manus	171.17	165.42	193.67		176.34
Length pace pes	106.35	104.76	129.37		112.96
Length pace manus	119.84	96.83	144.44		118.79
Width pace pes	125.40	147.62	146.03		139.30
Width pace manus	119.84	132.54	130.16		127.39
Divarication manus	-38.454	-49.399	-20.674	-27.255	-32.165
Divarication pes	-	31.866	-	33.341	32.595
Stride angulation pes	77.295	77.689			77.492
Stride angulation manus	82.704	85.522			84.101
Manus-pes distance	37.63	52.69	44.09	58.06	47.46
Interpes distance	100.79	118.25	122.22		113.36
Intermanus distance	76.19	88.10	84.13		82.66
Width external	176.98				
Width internal	72.22				
Glenoacetabular distance	159.47	174.08			166.61
Stride/Length pes	5.969				
Stride/Glenoacet. distance	1.337				

Table S10. *Hyloidichnus* isp. track parameters in mm and degrees. Values preceded by asterisk (*) are estimated. Mean parameters correspond to tracks of both surfaces. Section MA-A2.

Track Parameters	MA-A2 7.90 m (Tracks ordered from top to bottom and left to right in the corresponding figure)														Mean	
	Left manus track	Right set		Left set		Right manus	Left set		Right manus	Left track	Isolated left track	Right set		Isolated track		
		Pes	Manus	Pes	Manus		Pes	Manus				Manus	Pes		Manus	Pes
Length	63.36	74.51	68.91	69.60	67.28	*44.11	-	40.75	-	*52.85	-	*60.03	*58.93	-	56.26	67.36
Width	*69.17	-	-	69.67	68.97	-	-	-	-	-	-	-	-	-	69.07	69.67
Length sole	25.85	26.56	26.41	24.78	25.21	16.03	-	14.82	*21.87	15.56	-	-	-	-	21.15	25.65
Width sole	34.18	39.01	33.74	40.08	38.12	17.99	-	25.07	-	28.94	-	-	-	-	28.80	39.54
Length I	-	34.68	28.60	25.19	16.20	24.67	-	-	17.11	18.03	-	-	-	-	21.03	29.56
Length II	27.14	47.96	32.68	33.57	23.25	25.34	*32.15	18.68	21.27	29.92	-	-	-	-	24.33	37.27
Length III	33.43	-	39.04	45.28	41.51	26.40	*45.59	25.65	*23.99	34.46	-	-	-	-	30.96	45.43
Length IV	34.98	45.87	40.69	54.71	39.14	-	-	26.13	-	-	-	-	-	-	34.73	50.10
Length V	22.06	-	-	19.02	22.01	-	-	-	-	-	-	-	-	-	22.03	19.02
Div. I-II	*21.872	35.036	32.029	10.620	56.819	27.408	-	-	22.627	32.725	17.521	24.757	16.245	29.388	29.131	18.216
Div. II-III	25.043	*15.582	19.925	15.381	22.848	10.182	17.295	16.420	7.797	15.573	27.733	19.136	17.366	12.141	16.133	16.380
Div. III-IV	14.612	*13.071	9.818	11.469	7.465	-	-	21.748	-	-	29.444	13.394	12.694	12.779	12.555	12.392
Div. IV-V	59.807	-	-	60.171	12.966	-	-	-	-	-	32.139	-	-	-	27.847	60.171
Div. II-IV	*22.154	29.389	28.208	29.222	25.873	-	-	47.538	-	-	55.815	34.768	41.659	21.559	30.576	32.951
Div. I-V	114.656	-	-	93.985	95.203	-	-	-	-	*108.579	103.070	-	-	-	104.478	93.985
Length/Width	*0.916	-	-	0.999	0.975	-	-	-	-	-	-	-	-	-	0.945	0.999

Table S11. *Dimetropus leisnerianus* track parameters in mm and degrees. Values preceded by asterisk (*) are estimated.

Track Parameters	Left set		Right set		Mean	
	Manus	Pes	Manus	Pes	Manus	Pes
Length	120.36	135.30	101.84	119.69	110.71	127.26
Width	*151.89	132.28	95.91	12.2.30	120.70	127.19
Length sole	60.19	73.54	56.36	82.36	58.24	77.83
Width sole	75.85	112.59	46.08	93.02	59.12	102.34
Length I	-	-	33.47	32.67	33.47	32.67
Length II	57.17	53.53	35.44	38.45	45.01	45.37
Length III	*61.27	51.23	44.69	32.85	52.33	41.02
Length IV	67.10	59.86	45.05	44.23	54.98	51.45
Length V	66.79	61.48	35.66	58.04	48.80	59.74
Div. I-II	-	*8.320	25.283	15.422	25.283	11.327
Div. II-III	37.026	26.229	34.069	32.334	35.517	29.122
Div. III-IV	11.921	27.678	15.118	9.614	13.425	16.312
Div. IV-V	37.945	8.886	36.591	19.942	37.262	13.312
Div. II-IV	31.649	48.819	51.060	36.699	40.199	42.327
Div. I-V	-	*66.842	110.283	70.150	110.283	68.476
Length/Width	*0.792	1.023	1.062	0.979	0.917	1.001

Appendix 3. Invertebrate traces and plant remains

Systematic ichnology

Ichnogenus ***Acripes*** (Matthew, 1910)

Ichnospecies ***Acripes multiformis*** Gand *et al.* 2008

(Appendix 1: Fig. S5a, b)

Material and Stratigraphic position: In section MA-B, at 14.80-15.00 m, 16.80-17.50 m and 23.40 m (in small slab with numerous traces; IPS-83712), slab *ex situ* (with *Characichnos* Type A scratches on the lower surface in convex hyporelief) (IPS-73726).

Substrate: Fine to very fine laminated sandstone with covers of thin mudstone layers.

Description: Trace pattern and general morphology consist of sinuous and straight lines with one or two furrows. There are some shape and width variations: 1) traces of 1 mm width with *Rusophycus* isp. associated with or at the end of the trace (Appendix 1: Fig. S5a); and 2) traces of 5 mm formed by two rows of fine lines perpendicular to the midline, without associated *Rusophycus* isp. (Appendix 1: Fig. S5b). In surfaces at 16.80 m and 17.50 m there are groups of parallel long and straight or slightly curved traces, each trace presenting one or two furrows and numerous lateral fine lines in angles of 12-17º (Appendix 1: Fig. S5b).

Discussion: Rectilinear or sinuous trace course with wide variability, as well as the two symmetric rows with fine impressions perpendicular to the midline of the trace and in association with ichnites of *Rusophycus* isp., are both characteristic of *Acripes multiformis* defined by Gand *et al.* (2008). This ichnospecies presents wide variability of size and morphology. *A. multiformis*, regarded as walking traces (generally *Repichnia*), are abundant in levels with scratches associated to *B. salamandroides* and *Limnopus* isp. (i.e., *Characichnos* Types A and B). They are often overprinted by these tetrapod tracks. Gand *et al.* (2008) and references therein interpreted similar palaeoenvironmental conditions and assigned these traces to notostracan arthropods or triopsids.

Ichnogenus ***Rusophycus*** Hall, 1852

Ichnospecies ***Rusophycus* isp.**

(Fig. 11b; Appendix 1: Fig. S5a, c)

Material and Stratigraphic position: In section MA-B, at 14.80-16.00 m, 21.15 m, 23.00-23.40 m (in small slab with numerous traces; IPS-83712), slab *ex situ* (with scratches of *Characichnos* Type A on the lower surface; IPS-73726), slab *ex situ* (with plant remains; IPS-83722).

Substrate: Fine to very fine laminated sandstone with covers of thin lutitic layers.

Description: Traces are small (0.5-1 mm), rounded to elliptical, and usually bilobated, with symmetric two halves. Medial sides are parallel on the midline furrow or slightly diverging at one end. In the latter case, edges from the diverging parts are pointed (bilateral symmetry). Some specimens are associated to *Acripes multiformis* (Appendix 1: Fig. S5a).

Discussion: The bilobated oval smooth traces with bilateral symmetry are traits of *Rusophycus*. In the literature, this shape has been also attributed to *Isopodichnus*, with several ichnospecies (Gand, 1994; Gand *et al.* 2008 for a revision). Gand *et al.* (2008) redescribed this and other associated traces and adapted the nomenclature to 'distinguish the resting (*Cubichnia*) and the digging/feeding (*Pascichnia*) traces' (Gand *et al.* 2008). However, when associated, there are intermediate forms between *Cubichnia* and *Pascichnia*. Herein described *Rusophycus* represent stationary digging or resting traces, therefore corresponding to *Cubichnia*. Ichnospecies cannot be ensured because no diagnostic striations are preserved. Following Gand *et al.* (2008) and the clear association with *A. multiformis*, notostracans are the potential trackmakers. At 21.15 m there are wave ripples overprinted by traces of *Rusophycus* isp. At 23.00 m the traces attributed to *Rusophycus* isp. also overprint digit tip tracks of *Limnopus* isp. Both associations indicate that *Rusophycus* isp. were impressed after water flow (low energy) in a probably shallow water conditions, indicating drying environment, although substrate was still soft.

Indeterminate arthropod body impression

(Appendix 1: Fig. S5d, e)

Material and Stratigraphic position: In section MA-B, surface at 16.80 m.

Substrate: Fine to medium sandstone with a covering thin lutitic layer.

Description: The body impression consists of one straight mark (distal appendix) with six associated curved prints, transversal ridges and rounded ends (lateral appendixes or limbs) in one side; on the other side there are two prints probably corresponding to the other limbs.

Discussion: Arthropod body impressions are well known and have been taxonomically identified (e.g., Minter & Braddy, 2009; Lucas *et al.* 2013; Voigt *et al.* 2013). However, the present impression cannot be determined because only the posterior half of the body is preserved and no diagnostic traits are observable. It is tentatively attributed to a crustacean or a large insect. Further analyses are needed for an accurate taxonomic assignment.

Ichnogenus ***Helminthopsis*** Heer, 1877

Ichnospecies ***Helminthopsis* isp.**

(Appendix 1: Fig. S5f)

Material and Stratigraphic position: In section MA-A3 numerous traces in surface at 4.70 m.

Substrate: Fine to very fine grain size beds of volcanic origin (ignimbrites) with lutitic thin layers, traces overprint flow ripples.

Description: Slightly meandering smooth traces preserved in surface without ornamentation. Mean sizes are 50 mm long and 2-3 mm wide. No crossing through other traces or self-overcrossing is observed.

Discussion: Trace shapes are those from *Helminthopsis*, which has a wide age range (Buatois *et al.* 1998; Avanzini *et al.* 2011*b*). Buatois *et al.* (1998) interpreted *Helminthopsis* as grazing trails (*Pascichnia*) of deposit-feeding organisms. These authors assigned different potential trackmakers depending on the palaeoenvironmental conditions: polychaete annelids in brackish to fully marine settings, and arthropods and nematodes in freshwater ones. The abundance of notostracan traces in section MA-B, similar in lithology, denotes arthropod abundance, but trackmakers assignation remains open.

Ichnogenus **cf. *Planolites*** Nicholson, 1873

(Appendix 1: Fig. S5g)

Material and Stratigraphic position: In section MA-B one specimen at 17.75 m.

Substrate: Fine to medium sandstone.

Description: Horizontal trace slightly sinuous with rounded section of 10 mm of diameter. Trace length cannot be established, as it is incomplete. Infilling sediment is the same as host one, but it has a different appearance. There are no clear ornamentations on the external wall.

Discussion: The traits observed are similar to those of *Planolites*. However, the entire external form is lacking and ichnospecies cannot be identified. The fact that the infilling is different than the host sediment is a common trait of this ichnogenus, although not diagnostic (Minter *et al.* 2007; Avanzini *et al.* 2011*b*). In the specimen of section MA-B, the infilling sediment (sandstone) is of the same grain size as the host sediment. The lack of lining parallel to trace length distinguishes it from *Paleophycus*, as is discussed in Minter *et al.* (2007) and Avanzini *et al.* (2011*b*). Moreover, possible striations are present on the described specimen. Therefore, despite the shape similarities with *Planolites* specimens from Demathieu *et al.* (1992), Minter *et al.* (2007) and Avanzini *et al.* (2011*b*), only a tentative ichnotaxonomic assignment is provided because the specimen is affected by weathering. Minter *et al.* (2007) attributed *Planolites* to deposit-feeding annelid burrows.

Indeterminate burrows (?*Skolithos*)

(Appendix 1: Fig. S5h)

Material and Stratigraphic position: In section MA-A2, several surfaces between 1.85-5.80 m. In section MA-A3, surface at 5.20 m.

Substrate: Fine to medium grain size beds of volcanic origin (ignimbrites) covered by thin lutitic layers.

Description: Burrows of 3 to 5 mm of diameter, abundant where present. Infilling and host sediment are the same, traces are identified by the presence of lutitic layers. Some burrows appear vertical, oblique, subhorizontal or horizontal to surface.

Discussion: Ichnotaxonomic assignation is not possible because burrows are observed on surface, and their structure and external wall aspect cannot be evaluated, nevertheless, the possible morphology is that similar to *Skolithos* (e.g., Demathieu *et al.* 1992). Although traits like transversal section are similar to *Planolites*, further studies and specimens are needed for a proper assignation.

Plant remains

Plant remains are scarce and preserved as impressions on *ex situ* slabs nearby section MA-B (5 in Fig. 11b; Appendix 1: Fig. S5i, j). These remains consist of fragments with no recognizable morphology, and thus they cannot be identified. High energy water flow events probably transported plants from their original environment through the fluvial channel. Accordingly, plant remains are not abundant on the probably quiet system interpreted for the studied sections.

References

GAND, G. 1994. Ichnocoenoses à *Isopodichnus furcosus* nov. ichnosp. dans le Permien du Bassin de Lodève (Massif Central, France). *Géobios* **27 (1)**, 73-86.

GAND, G., GARRIC, J., SCHNEIDER, J., WALTER, H., LAPEYRIE, J., MARTIN, C., THIERY, A. 2008. Notostraca trackways in Permian playa environments of the Lodève basin (France). *Journal of Iberian Geology* **34 (1)**, 73-108.

MINTER, N. J., KRAINER, K., LUCAS, S. G., BRADDY, S. J. & HUNT, A. P. 2007. Palaeoecology of an Early Permian playa lake trace fossil assemblage from Castle Peak, Texas, USA. *Palaeogeography, Palaeoclimatology, Palaeoecology* **246**, 390-423.

VOIGT, S., LUCAS, S. G., KRAINER, K. 2013. Coastal-plain origin of trace-fossil bearing red beds in the Early Permian of Southern New Mexico, USA. *Palaeogeography, Palaeoclimatology, Palaeoecology* **369**, 323-334.

Annex 5. Material suplementari del capítol 5

Table 1. Track parameters of Morphotype A. Units are in mm and degrees. Values with asterisk (*) are estimated.

Morphotype A		Left manus	Left manus	Right manus	Right manus	Left manus	Right manus	Right manus-pes set	Right manus	Right manus	Right manus	Right manus	Left manus	Right manus	Mean
		Fig. 12 A–C	Fig. 12 D–F	Fig. 12 G – I	Fig. 13 B, C	Fig. 13 D, E	Fig. 13 F, G	Fig. 14 A, B	Fig. 14 C, D	Fig. 14 E, F	Fig. 14 G, H (left)	Fig. 14 G, H (right)	Fig. 14 I, J	Fig. 14 K, L	
Pes	**Length**	-	-	-	-	-	-	-	-	-	-	-	-	-	-
	Width	-	-	-	-	-	-	-	-	-	-	-	-	-	-
Manus	**Length**	40.322	26.715	39.154	*27.190	24.613	30.164	*38.254	25.303	37.471	37.844	41.380	26.246	18.990	30.164
	Width	37.480	23.041	39.583	31.672	29.568	34.931	55.240	*26.054	40.497	*32.847	34.859	28.071	*20.322	32.847
Pes	**Digit I**	-	-	-	-	-	-	-	-	-	-	-	-	-	-
	Digit II	-	-	-	-	-	-	13.317	-	-	-	-	-	-	13.317
	Digit III	-	-	-	-	-	-	20.048	-	-	-	-	-	-	20.048
	Digit IV	-	-	-	-	-	-	47.772	-	-	-	-	-	-	47.772
	Digit V	-	-	-	-	-	-	-	-	-	-	-	-	-	-
Manus	**Digit I**	6.708	4.341	5.465	*4.111	*5.401	7.788	8.718	4.430	6.456	7.234	8.210	6.840	-	6.582
	Digit II	16.492	10.533	17.767	*15.063	12.594	16.064	16.736	9.647	14.767	14.257	21.423	12.828	8.092	14.767
	Digit III	27.981	16.656	25.210	19.403	18.068	20.288	29.163	14.151	25.982	20.852	27.024	17.600	14.121	20.288
	Digit IV	27.720	16.746	23.648	17.723	15.626	19.604	26.690	13.156	25.202	19.244	*25.762	15.276	13.901	19.244
	Digit V	12.213	5.552	11.670	*6.964	*7.060	9.701	17.097	-	12.183	-	11.147	-	-	11.147

Morphotype A		Left manus	Left manus	Right manus	Right manus	Left manus	Right manus	Right manus-pes set	Right manus	Right manus	Right manus	Right manus	Left manus	Right manus	Mean
		Fig. 12 A–C	Fig. 12 D–F	Fig. 12 G – I	Fig. 13 B, C	Fig. 13 D, E	Fig. 13 F, G	Fig. 14 A, B	Fig. 14 C, D	Fig. 14 E, F	Fig. 14 G, H (left)	Fig. 14 G, H (right)	Fig. 14 I, J	Fig. 14 K, L	
Divari-cation pes	I-II	-	-	-	-	-	-	-	-	-	-	-	-	-	-
	II-III	-	-	-	-	-	-	9.381	-	-	-	-	-	-	9.381
	III-IV	-	-	-	-	-	-	5.736	-	-	-	-	-	-	5.736
	IV-V	-	-	-	-	-	-	-	-	-	-	-	-	-	-
	II-IV	-	-	-	-	-	-	12.147	-	-	-	-	-	-	12.147
Divari-cation manus	I-II	19.373	30.517	33.265	32.395	55.359		28.570	19.599	38.758	44.257	37.556	42.251	-	33.265
	II-III	23.697	24.760	32.411	19.688	22.433		35.087	30.060	29.494	30.548	13.775	17.632	37.073	27.127
	III-IV	22.351	8.942	15.173	18.957	9.724		24.806	14.512	21.870	30.816	21.172	12.987	18.312	18.635
	IV-V	54.404	57.102	32.885	*30.170	*53.012		50.881	-	50.748	-	60.745	-	-	51.947
	I-IV	70.017	65.159	77.252	75.713	82.135		80.704	65.257	75.821	92.454	64.111	73.770	-	75.713
	I-V	131.496	123.650	108.617	*99.096	*129.433		126.358	-	124.780	-	125.161	-	-	124.971
Length /Width	Pes	-	-	-	-	-	-	-	-	-	-	-	-	-	-
	Manus	1,076	1,159	0,989	*0.858	0,832	0,864	*0.693	*0.971	0,925	*1,152	1,187	0,935	*0.934	1

Table 1. *(continued)* Trackway parameters of Morphotype A. Units are in mm and degrees. Values with asterisk (*) are estimated.

Morphotype A	Trackway Fig. 13 A			Mean
Stride Manus	293.555			
Pace Manus	201.892	176.934		189.413
Pace angulation Manus	102.850			
Trackway width Manus	116.574			
Divarication III from midline Manus	13.466	17.031	17.590	17.031

Annex 6. Material suplementari del capítol 6

Text S1. Palaeomagnetic data

Methods

Hand-oriented samples were collected from 39 stratigraphic levels distributed along the 145 m studied Permian section at Coll de Terrers for magnetostratigraphic purposes. Samples were subsequently cut in standard palaeomagnetic cubes for laboratory analysis. Natural remanent magnetization (NRM) and remanence through demagnetization were measured on a 2G Enterprises DC SQUID high-resolution pass-through cryogenic magnetometer (manufacturer noise level of 10-12 Am^2) operated in a shielded room at the Istituto Nazionale di Geofisica e Vulcanologia in Rome, Italy. A Pyrox oven in the shielded room was used for thermal demagnetizations and alternating field (AF) demagnetization was performed with three orthogonal coils installed in line with the cryogenic magnetometer. Progressive stepwise AF demagnetization was routinely used and applied after a single heating step to 150°C. AF demagnetization included 14 steps (4, 8, 13, 17, 21, 25, 30, 35, 40, 45, 50, 60, 80, 100 mT). Thermal demagnetization included 13 demagnetization steps up to 680°C. Characteristic remanent magnetizations (ChRM) were computed by least-squares fitting (Kirschvink, 1980) on the orthogonal demagnetization plots (Zijderveld, 1967). Thermomagnetic curves on selected specimens were performed on a MFK1 apparatus (AGICO).

Results

The NRM intensity of the studied samples is in the range 2-12 $x10^{-3}$ A/m. Stepwise demagnetization of the samples shows a characteristic remanent magnetization (ChRM) component trending toward the origin of the demagnetization diagrams after the removal of a soft viscous component below 150-200°C. Alternating field (AF) demagnetization subsequent to a single heating step of 150°C usually only removes a small proportion of the ChRM (Fig. A1A-C) or does not substantially removes any component (Fig. A1D). The ChRM component unblocks successively up to temperatures of 650-680°C. Thermal demagnetization alone unblocks the ChRM component above 150-200°C up to the highest mentioned temperatures. This behaviour suggests hematite as the main carrier of the magnetization with a minor proportion of a magnetite like phase in some instances. Thermomagnetic runs on some specimens (Fig. A3) confirm the presence of hematite with Curie temperatures approaching 700°C (Fig. A3 phase 2) and a second magnetic phase which appears to unblock in the range 520-580°C (phase 1) that is more obvious in the cooling curve (Fig. A3B).

Computed ChRM directions both before and after bedding tilt correction are shown in Fig. A2. A stability fold test is not possible for the present dataset as the studied section displays a homogeneous bedding attitude. However, the general tilt of about 40º towards the S-SW permits comparison of the computed mean directions before and after tilt correction. The intermediate mean magnetic inclination of about 42° in tilt-corrected coordinates together with the shallow inclination in in-situ coordinates (before tilt correction) suggests a secondary origin for the magnetization (see discussion below). This results hamper any attempt to retrieve a magnetostratigraphy for this section.

Discussion

The first palaeomagnetic results on Permo-Triassic red-beds and andesites in the Western Pyrenees provided varied results. Schwarz (1963) reported directions from a collection of 8 samples from sediments and 14 samples from andesites in a locality from the upper Aragon Subordan valley indicating that sediments were remagnetized in post-Alpine times whereas andesites retained a primary palaeomagnetic direction. In contrast, Van der Lingen (1960) had previously reported primary Permo-Triassic direction from both redbed sediments and andesites from the Anayet area. All these primary directional data were classically used for the determination of the rotation of the Iberian Peninsula (e.g. Van der Voo, 1963). These data and directional data from Permian dykes and diorites from the Catalan Coastal Ranges (Parés, 1988) indicate a shallow S-SE directed reverse direction for these Permian rocks which is usually ascribed to the Kiaman superchron. Moreover, it has become clear that the Permo-Triassic red-bed sequences from Iberia in addition to portray the Mesozoic rotation of the Iberian Peninsula also indicate a sharp increase in latitude in the upper Triassic (Parés and Dinarès-Turell, 1994). Consequently, shallow inclinations are only expected for Permian and early Triassic primary palaeomagnetic directions. Van Dongen (1967) studied 41 andesitic samples of lower Permian radiometric age holding a Kiaman shallow reverse palaeomagnetic direction. However, palaeomagnetic results from pelitic sediments were more tentative.

A recent reappraisal of the Permo-Triassic red-bed sequences palaeomagnetism in the west-central Pyrenees (Oliva-Urcia et al., 2012) has evidenced a relatively complex scenario involving Cenozoic postfolding remagnetization in some structural domains (Bielsa area). In the Bielsa area the retrieved post-folding magnetization in the Permian red-beds displays always reverse polarity (N=20, Dec= 186, Inc= −39, α_{95}=5, k= 47) and is similar to the Cenozoic remagnetization (Dec: 198, Inc:−43; α_{95}= 4 k= 18) identified in Upper Cretaceous and Eocene sediments from the northern part of the South Pyrenean zone (Internal Sierras) (Oliva-Urcia et al., 2012 and references therein). In addition to this Cenozoic reverse remagnetization a primary Permian direction including both polarities was also identified in about 40% of the studied samples from 17 sites in the Bielsa area (Oliva-Urcia et al., 2012).

In the studied Coll de Terrers collection the ChRM component better conforms a pre-folding remagnetization. The shallow inclination of the mean direction in geographic coordinates (*in.situ*) (Dec: 358.1, Inc:2.8; α_{95}=8.4 k= 9.4) rules out the possibility of a post-folding remagnetization. Tilting to the South of the strata in the Serra del Cadí unit is associated to the growth of South Pyrenean orogenic wedge from Early Eocene to Late Oligocene times (Vergés et al., 1995; Meigs and Bourbank, 1997, Vergés et al., 2002 and references therein). In consequence, the acquisition time of the Coll de Terrers remagnetization predates the age of tilting of the strata. The possibility of a remagnetization of early Triassic age can be ruled out because the Buntsandstein facies (ascribed to the Early Triassic) conformably overly the Permian deposits at Coll de Terrers. Thus, no significant bedding angle differences exists to account for the required geometry at the eventual remagnetization time. A lower Cretaceous remagnetization event has been described further south in the Organyà basin which is part of the Bóixols thrust sheet in the hanging-wall of the Cadí Unit, (Dinarès-Turell and García-Senz, 2000). However, at this stage it is not clear that the remagnetization at Coll de Terrers may be related to the same event and further regional studies are required to shed light to this possibility.

References

Dinarès-Turell, J., Garcia-Senz, J., 2000. Remagnetization of Lower Cretaceous limestones from the southern Pyrenees and relation to the Iberian plate geodynamic evolution. Journal of Geophysical Research 105(B8), 19405-19418. https://doi.org/10.1029/2000JB900136

Kirschvink, J.L., 1980. The least-squares line and plane and the analysis of palaeomagnetic data. Geophys. J. R. Astronom. Soc. 62, 699-718.

Meigs, A.J., Burbank, D.W., 1997. Growth of the South Pyrenean orogenic wedge. Tectonics 16, 239-258.

Oliva-Urcia, B., Pueyo, E.L. Larrasoaña, J.C., Casas, A.M., Román-Berdiel, T., Van der Voo, R., Scholger, R., 2012. New and revisited paleomagnetic data from Permian–Triassic red beds: Two kinematic domains in the west-central Pyrenees. Tectonophysics 522-523, 158-175. http://dx.doi.org/10.1016/j.tecto.2011.11.023

Parés, J.M., 1988. Estudio paleomagnético de las rocas tardihercinianas de la Cadena Costero Catalana: primeros resultados. Cuadernos de Geología Ibérica 12, 171-179.

Parés, J.M., Dinarès-Turell, J., 1994. Iberian Triassic paleomagnetism revisited: Intraplate block rotations versus polar wandering. Geophysical Research Letters 21, 2155-2158. https://doi.org/10.1029/94GL01914

Schwarz, E.J., 1963. A paleomagnetic investigation of Permo-Triassic red-beds and andesites from the Spanish Pyrenees. Journal of Geophysical Research 68, 3265-3271.

Van Dongen, P.G., 1967. The rotation of Spain: paleomagnetic evidence from the eastern Pyrenees. Paleogeography, Palaeoclimatology, Palaeoecology 3(4), 417-432.

Van der Lingen, G.J., 1960. Geology of the Spanish Pyrenees, north of Canfranc, Huesca Province. Estud. Geol. Inst. Invest. Geol. "Lucas Mallada" 16, 205–242.

Van der Voo, R., 1969. Paleomagnetic evidence for the rotation of the Iberian Peninsula. Tectonophysics 7, 5-56.

Vergés, J., Millán, H., Roca, E., Muñoz, J.A., Marzo, M., Cirés, J., Den Bezemer, T., Zoetemeijer, R., Cloetingh, S., 1995. Eastern Pyrenees and Related Foreland Basins: Pre-, Syn- and Post-Collisional Crustal-Scale Cross-Sections. Marine and Petroleum Geology 12, 903-15. https://doi.org/10.1016/0264-8172(95)98854-X.

Vergés, J., Fernàndez, M., Martínez, A., 2002. The Pyrenean orogen: pre-, syn-, and post-collisional evolution. In: Rosenbaum, G. and Lister, G.S. (Eds.), Reconstruction of the evolution of the Alpine-Himalayan Orogen. Journal of the Virtual Explorer, 8, 55-74.

Zijderveld, J.D.A., 1967. AC demagnetisation of rock: analysis of results. In: D.W. Collinson and others (Eds.), Methods in palaeomagnetism. Elsevier, Amsterdam, 254-286.

Figures

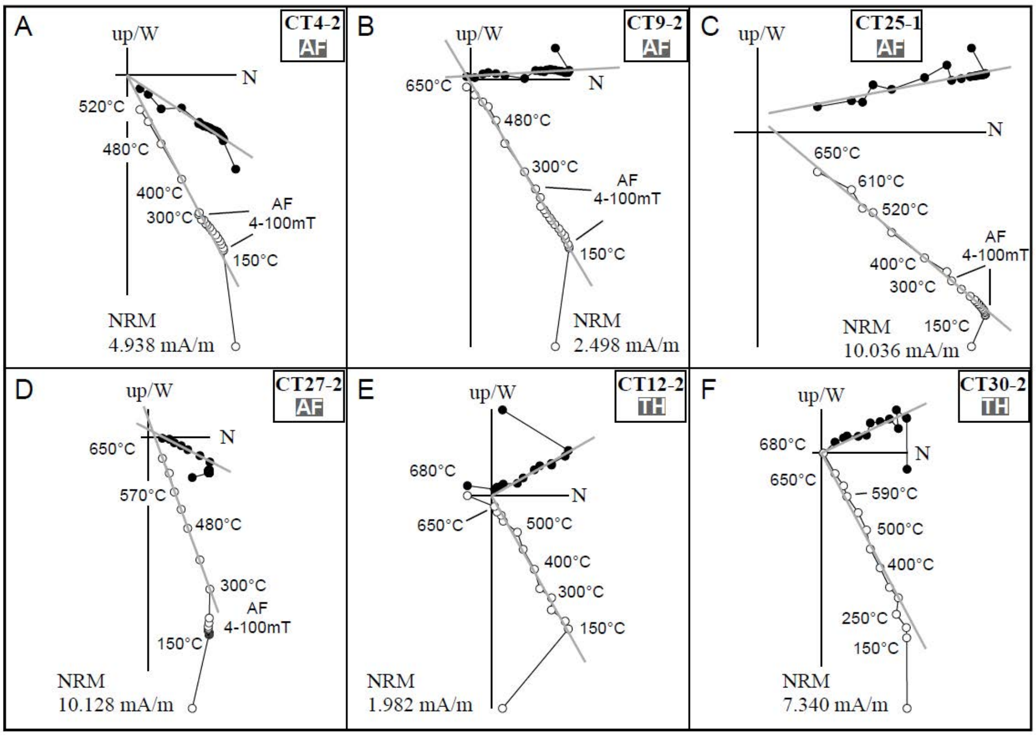

Figure A1. Representative in-situ orthogonal demagnetization diagrams from the studied Coll de Terrers section. (A-D) Samples following a stepwise alternating field (AF) demagnetization protocol after a single heating step to 150ºC; (E-F) samples demagnetized with a stepwise thermal protocol. The natural remanent magnetization (NRM) intensity and some demagnetization steps are indicated. Open and closed symbols indicate projections onto the upper and lower hemisphere respectively. The computed ChRM direction is shown by a solid grey thick line.

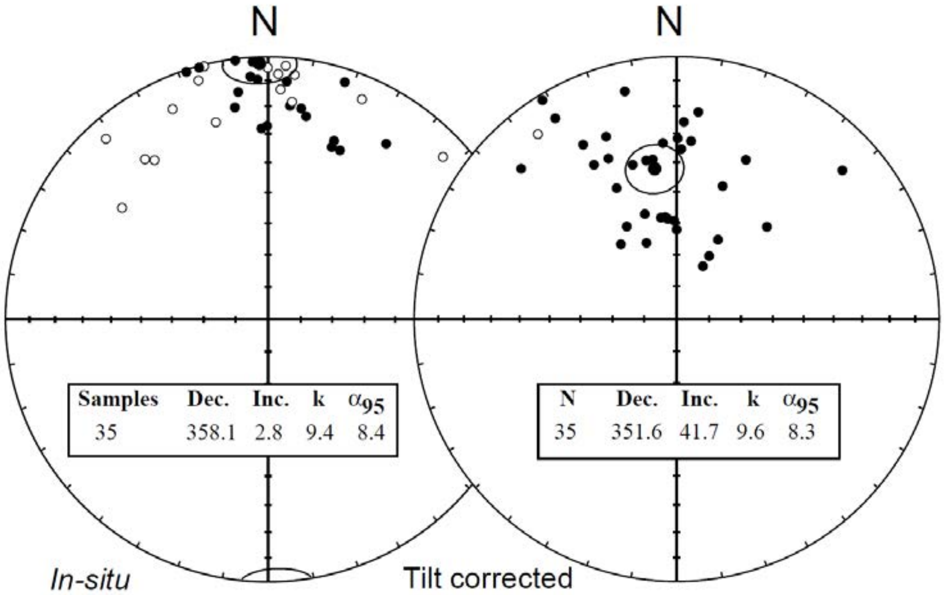

Figure A2. Stereographic projections of the ChRM computed components before (in situ) and after bedding correction (tilt corrected). Open and closed symbols indicate projections onto the upper and lower hemisphere respectively. Mean direction and statistics are given. N = number of samples; Dec = declination; Inc = inclination; k = fisher's statistical parameter; α_{95} = semiangle of the 95% cone of confidence.

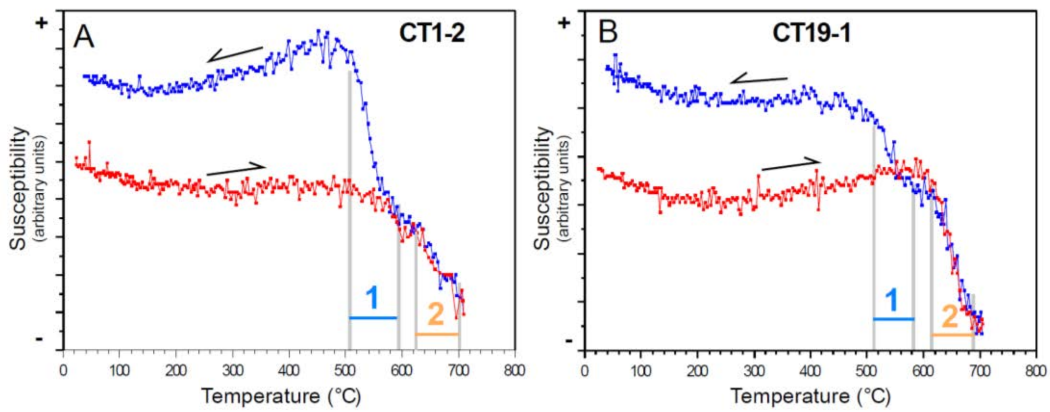

Figure A3. (A-B) Typical thermomagnetic curves for representative samples. Directions of arrows indicate heating and cooling curves. Two intervals of appreciable susceptibility drop corresponding to respective mineral phases are indicated (see text).

Supplementary Figures

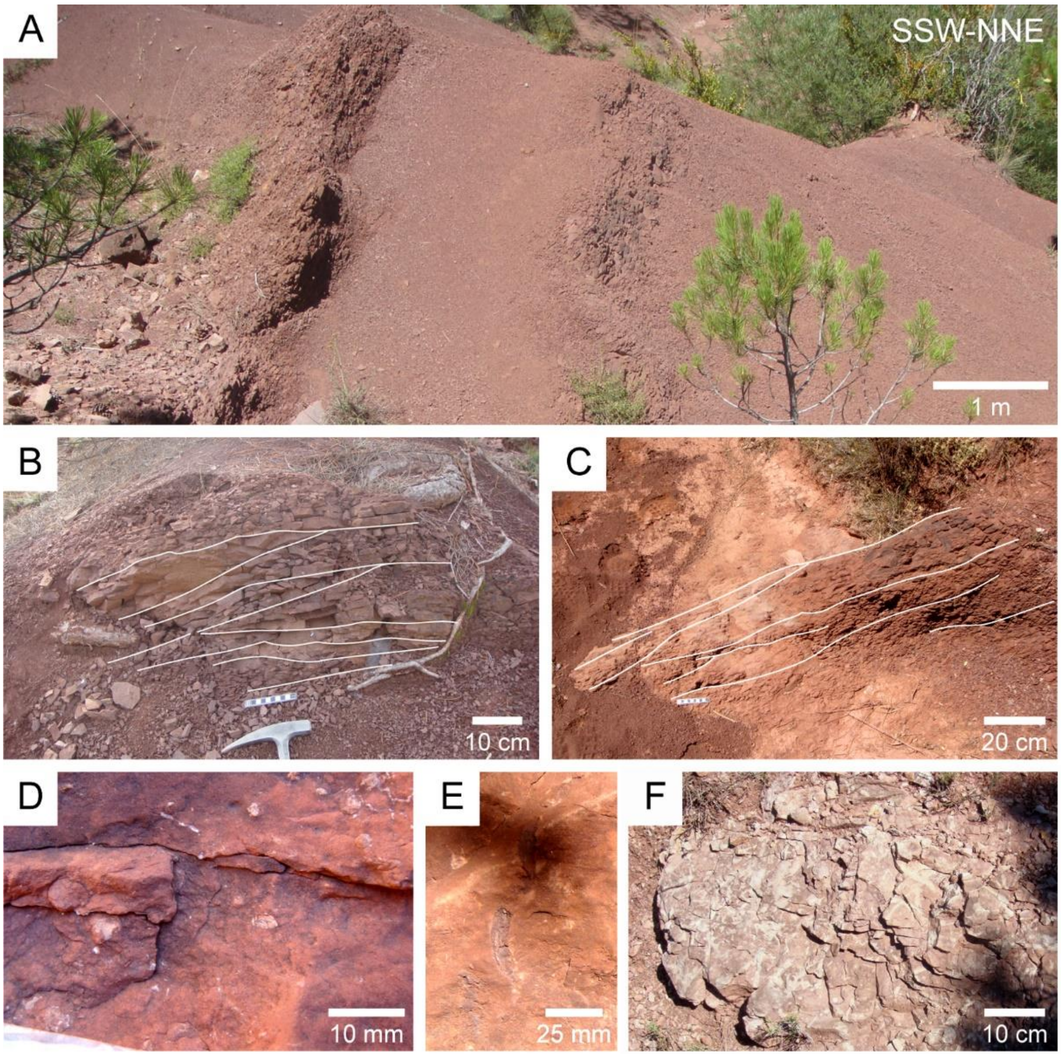

Figure S1. The lower URU. A. Overview of the mudstones with fine-grained sandstone channels. B, C. Lateral accretions within sandstone channels. D. Small carbonate edaphic nodules. E. Vertical invertebrate burrow. F. Root trace fossils (whitish) in a medium- to coarse-grained sandstone.

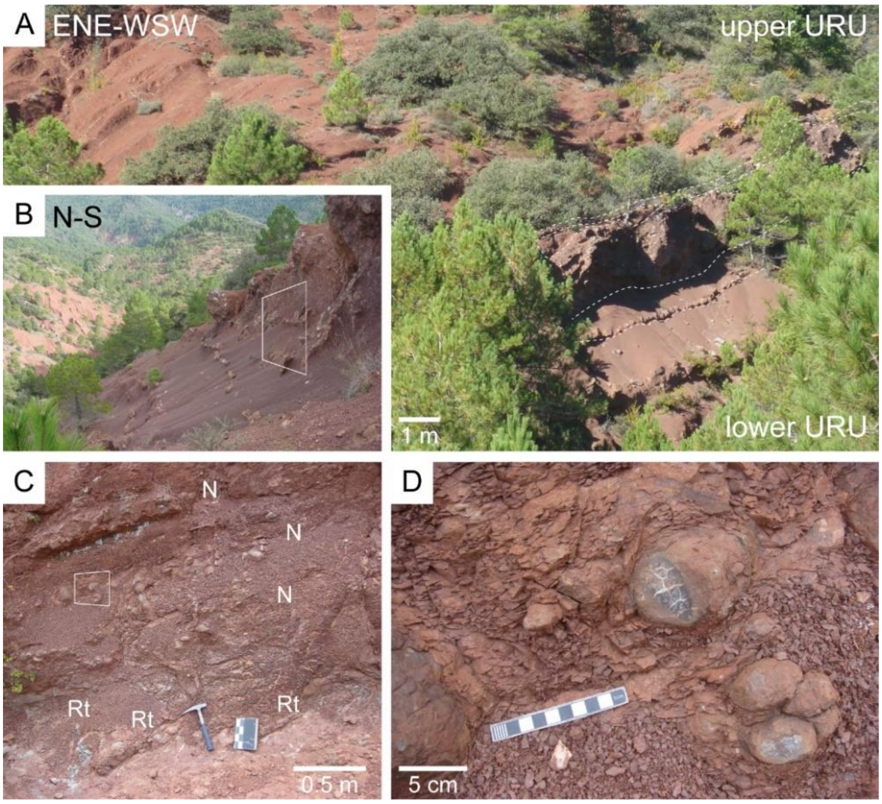

Figure S2. Lower/upper URU boundary. A. Overview of the transition with three levels of nodules (white dashed lines); note the colour change between the lower and upper URU mudstones. B, C. Close view of the nodular levels (C squared in B), including septarian nodules (N) and root traces (Rt). D. Example of septarian nodules squared in C.

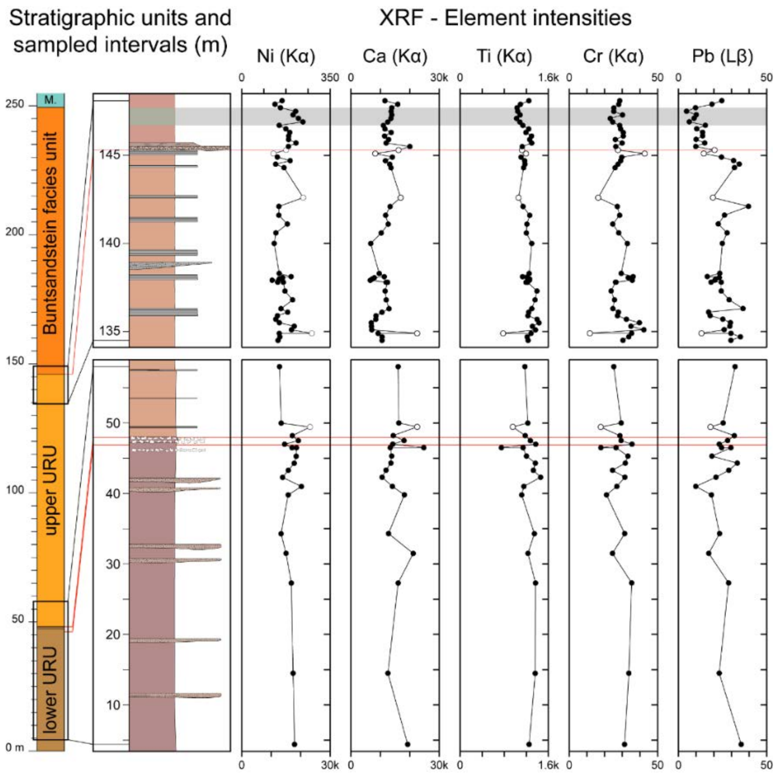

Figure S3. Element intensities obtained by XRF. Black and white circles correspond to mudstone and sandstone samples, respectively. Red lines and grey interval as in Fig. 4.

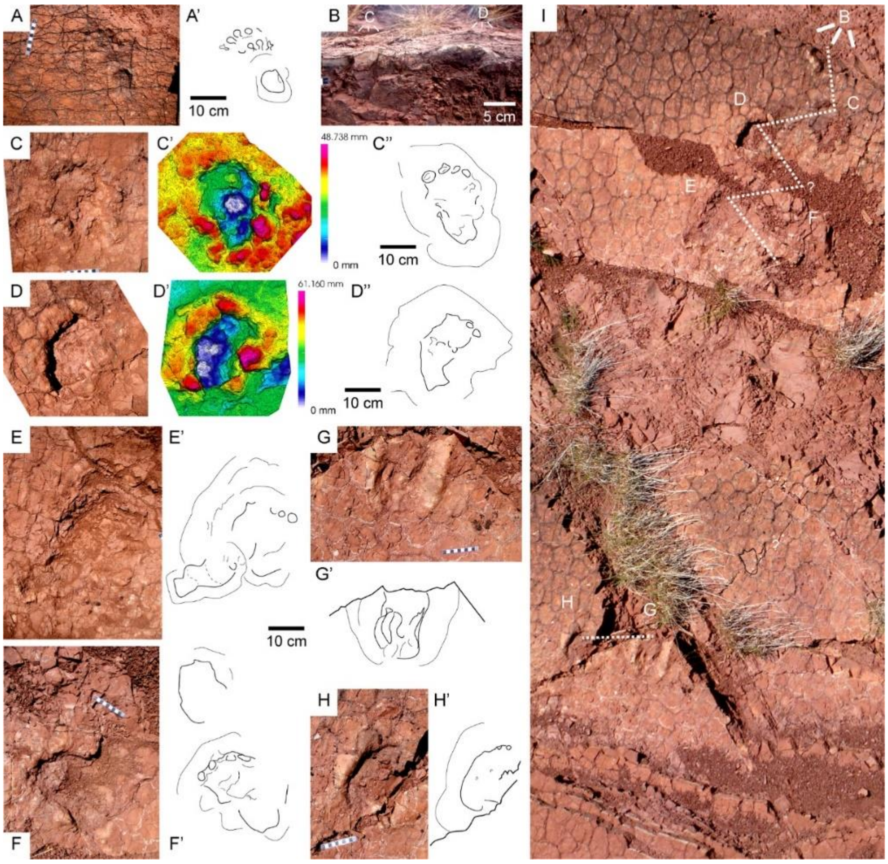

Figure S4. Tetrapod footprints of Morphotype I. A. Manus-pes set from cycle 9. B-I. Trackway from cycle 23, with track in cross section (B), the manus-pes sets with partial overstepping of pes to manus impressions (C-H) and general view of the trackway with manus paces in white dashed line (I).

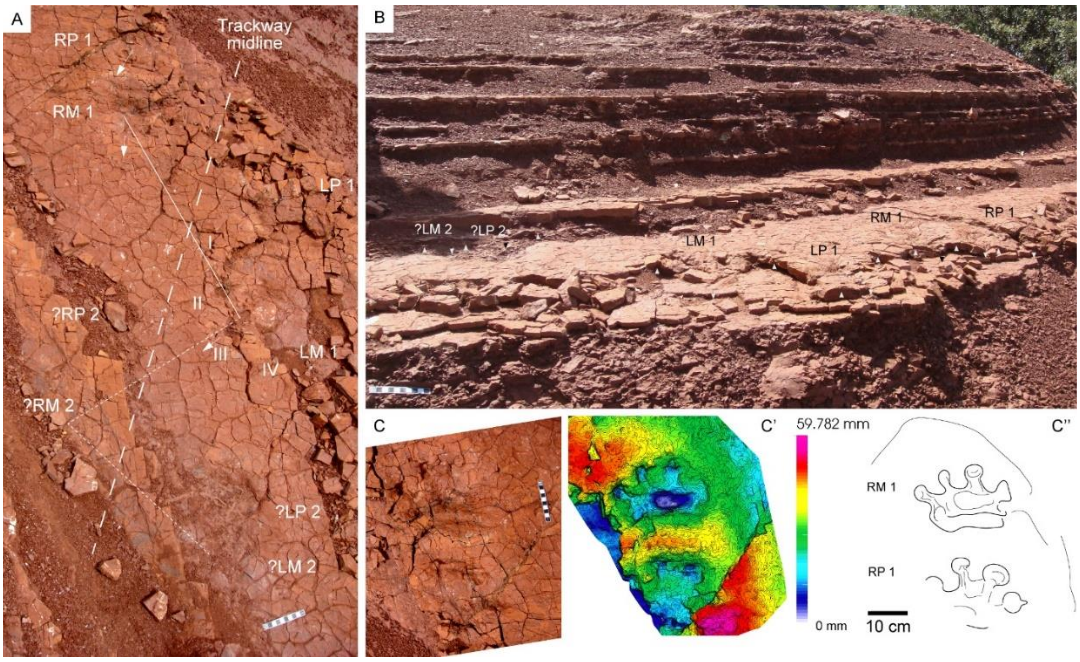

Figure S5. Tetrapod footprints of Morphotype I from cycle 38. A. General view of the trackway with the different manus-pes sets (RM-RP and LM-LP). B. Trackway in cross section. C. Well-preserved manus and partial pes, including 3D model and ichnites outline (as in Fig. 6B).

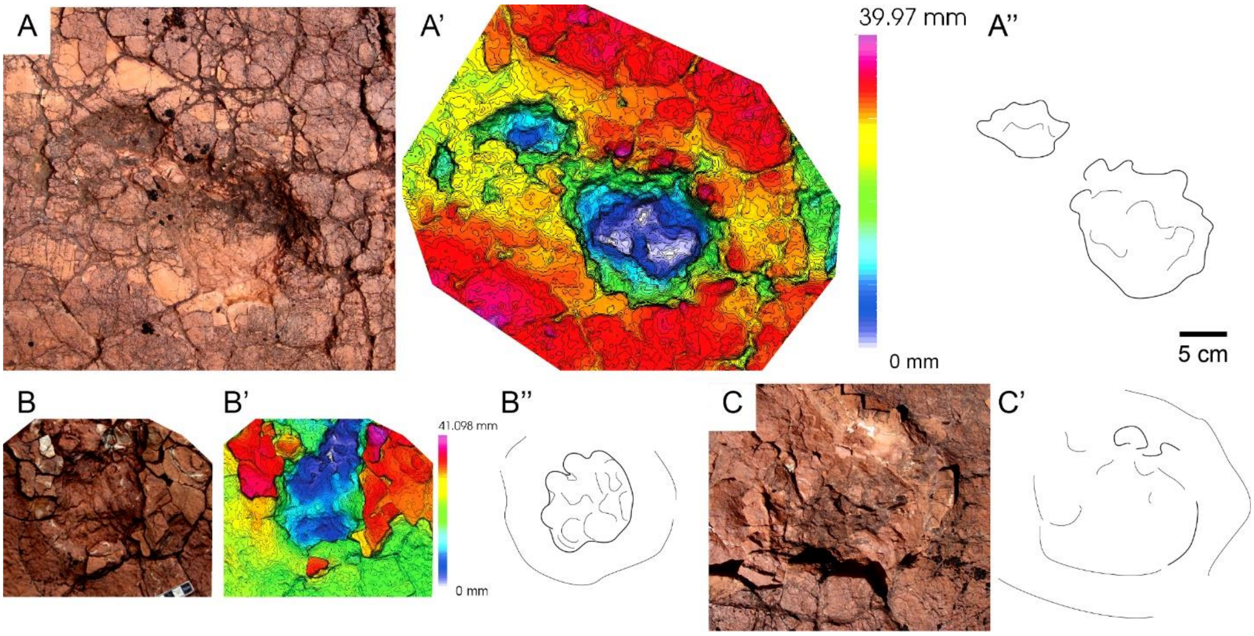

Figure S6. Tetrapod footprints of Morphotype II from cycle 39. A. Manus-pes set. B, C. Pes impressions.

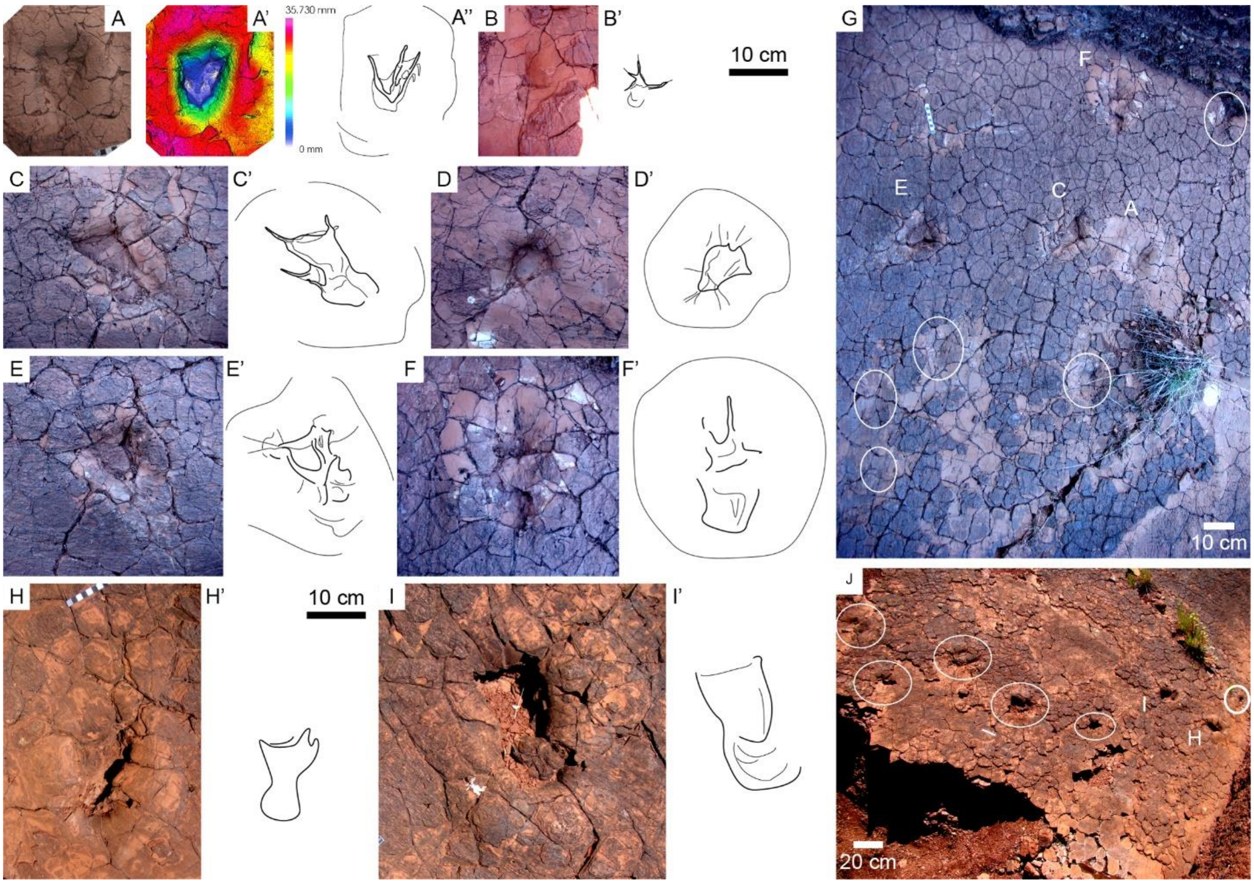

Figure S7. Tetrapod footprints of Morphotype III from cycle 27. A-F. Footprints in surface G. H, I. Footprints from surface J. Note the different shapes of the heel (A-F, H, I) and the rough alignments of the footprints, possibly from the same trackways (G, J).

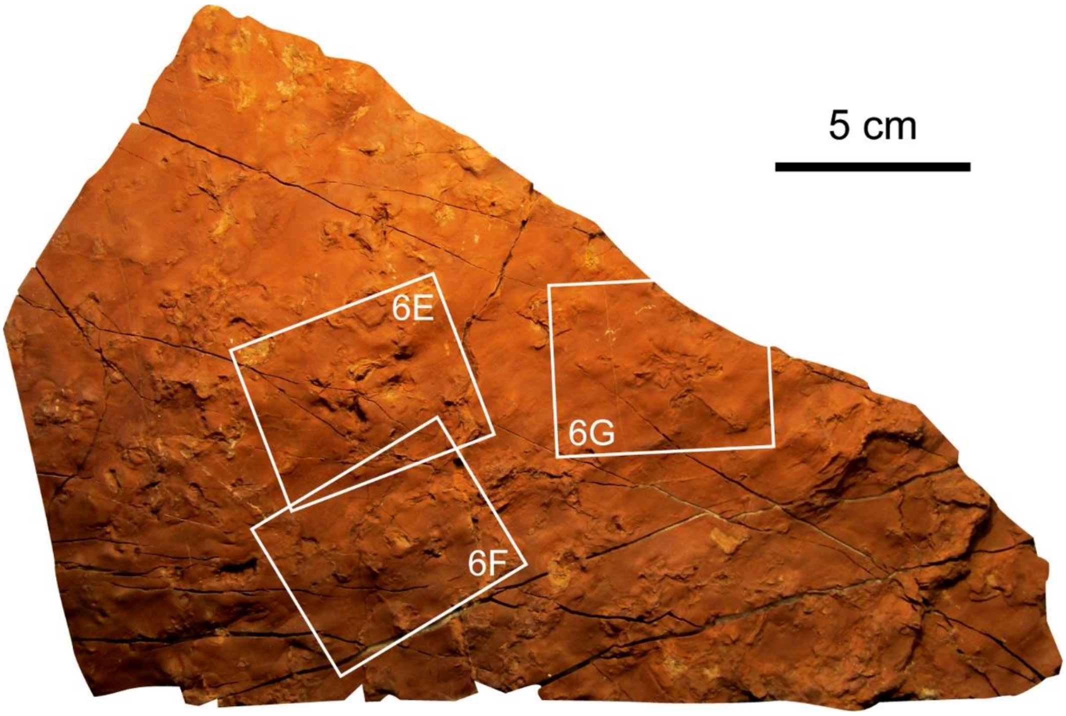

Figure S8. Slab with tetrapod footprints from Morphotype IV, close to cycle 49. Squares are those of Fig. 6.

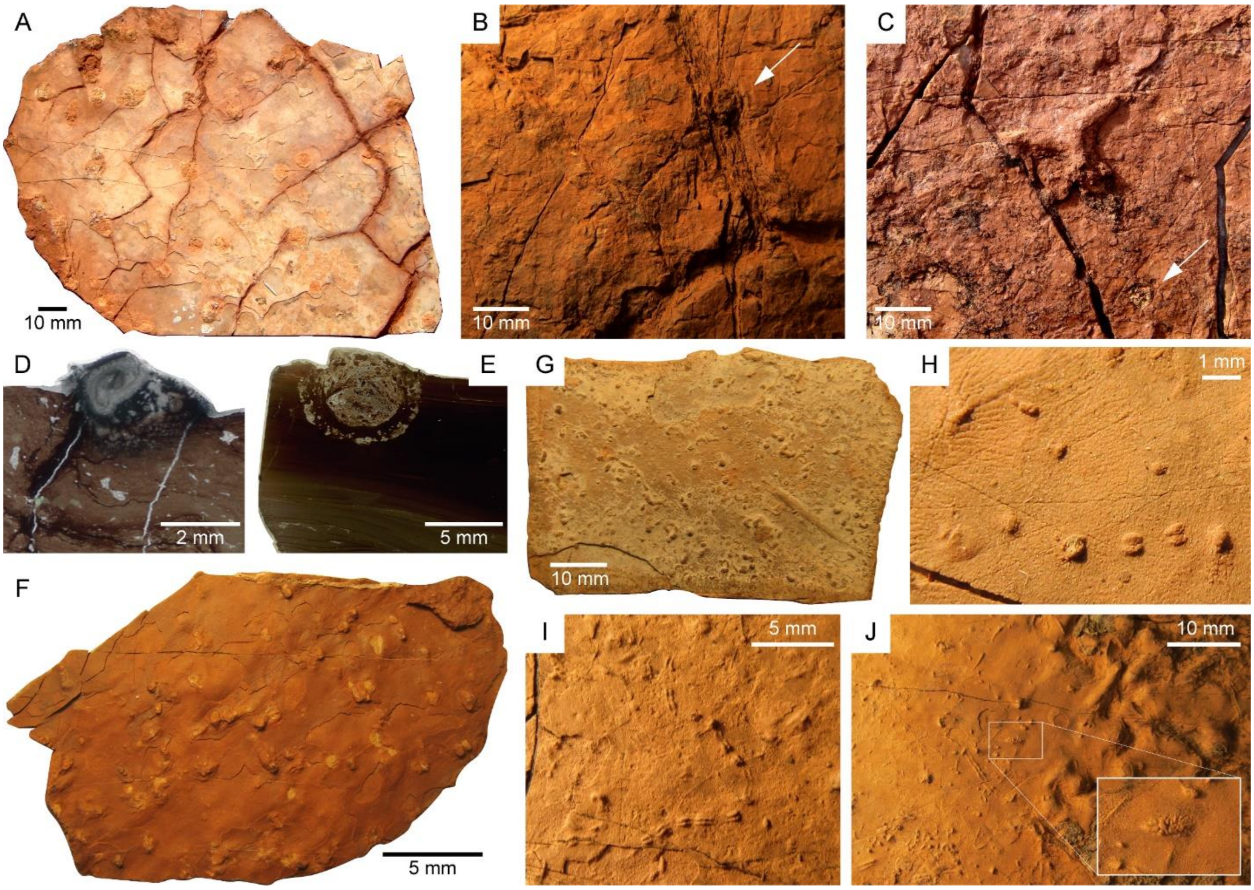

Figure S9. Invertebrate trace fossils from the upper URU. A. Abundant vertical burrows. B. Vertical burrows located in mud-cracks (arrow). C. Ramified horizontal burrow and vertical burrow (arrow). D, E. Horizontal burrows in cross section. G-J. Ichnites of notostracan arthropods (triopsids), including resting traces (*Rusophycus*, F-H) and locomotion traces (*Acripes*) associated to *Rusophycus* (I, J) and potential pellet (detail in J).

Annex 7. Material suplementari del capítol 7

S1 Text. Sedimentology.

Facies Description and Interpretation

Facies Gh: They are composed of clast-supported conglomerates, with subordinate matrix-supported levels, generally massive, with crude stratification. The matrix is composed of coarse to very coarse sandstone. Bedding is up to 50 cm thick and is often arranged as fining-upwards sequences and present erosive bases with flow structures such as flute casts. They are mainly located in the conglomerate unit (associated with facies *Gmpt*, *St* and *Sp*) and occasionally in the shale and sandstones unit (associated with *St*). These facies are interpreted as basal lag deposit or the frontal part of a channel bar.

Facies Gmpt: They are composed of clast- to matrix-supported conglomerates, with crude planar stratification, planar cross stratification, or trough cross stratification, and levels with imbricated pebbles. Sets thickness range from 50 to 90 cm, and cosets are up to 2 m. Matrix is composed of coarse to very coarse sandstone. These facies occasionally grade upwards to facies *St* and *Sp*. *Gmpt* is interpreted as longitudinal bars from high-flow braided streams, as minor channel fills, or as lag deposits when associated with sandstone facies.

Both facies *Gh* and *Gmpt* are oligomictic in composition (reworked dyke quartz mostly rounded to sub-rounded) with occasional black and greenish lydite and slate fragments. Clasts average size is of 10 cm (with pebbles up to 15 cm) in some beds, and of 2-4 cm (with pebbles up to 6-7 cm) in others. These facies are mostly the result of high-flow braided fluvial systems, and occasionally correspond to minor lag deposits of meandering fluvial systems.

Facies St: They are composed of fine- to medium-grained sandstones (rarely coarse to very coarse), with trough cross stratification. Beds present lenticular geometry, but in some cases are tabular. They build up fining-upwards sequences ranging from 10 to 90 cm thick (commonly of 20-30 cm), and often grade to facies *Sp*. Cosets are up to 1.5 m thick. Sets are bounded by facies *Fsc* or partially eroded by other *St* and *Sp* sets, the latter corresponding to low- to medium-angle dipping surfaces (reactivation surfaces). Soft (mudstone) pebbles are present in some levels. In some cases clasts as those from *Gmpt* are found as lag deposits. The facies *St* are interpreted as subaqueous dunes associated to channel fills, minor bars and sand flats of braided systems (conglomerate unit), and as point bars of meandering fluvial systems (shale and sandstones unit).

Facies Sp: They are composed of fine- to medium-grained sandstones (rarely coarse to very coarse), with planar cross stratification. Sets resemble those of facies *St*, but generally display a tabular geometry with subordinated lenticular bodies. In the shale and sandstones Unit often grades to facies *Sr*, *Sh* and *Fsc* (fining upwards sequences). The facies *Sp* are interpreted as linguoid bars and sand flats of braided systems (conglomerate unit) and transverse bars of meandering systems (shale and sandstones unit).

Facies Sr: They are composed of fine- to very fine-grained sandstones with abundant climbing ripples, and also flow and wave ripples. Beds are of 10 to 30 cm thick, in sets of tabular and channel geometry. Cosets are up to 1.5 m thick, and are commonly grading from *Sp* to *Sl* and *Fsc* (fining upwards sequences), and also present interbedded *Fl*. The upper part of some bodies are burrowed. The facies *Sr* are interpreted as the result of low regime flows, corresponding to the upper part of the scroll bar of meandering systems.

Facies Sh: They are composed of fine- to very fine-grained sandstones with parallel laminations. Bodies are of tabular geometry and grouped in sets up to 20 cm thick. Greenish reduction mottles are common. The facies *Sh* are interpreted as planar beds from upper flow regime.

Facies Sl: They are composed of fine- to very fine-grained sandstones with climbing and flow ripples. Sets (up to 30 cm thick) and cosets (up to 1 m thick) are bounded by low- to medium-angle inclined planes (reactivation surfaces, similar to those of *St* and *Sp*, but finer grained). These facies are often associated with facies *Fl*, forming both fining and coarsening upwards sequences. Isolated lenticular beds with erosive bases also occur. The facies *Fl* are interpreted as scour fill deposits or washed-out dunes.

Facies Se: They are composed of fine- to coarse-grained sandstones with crude trough cross stratification and soft pebbles. Bodies present strong erosive bases and are laterally discontinuous. The thickness varies from 15 to 35 cm. Mud-cracked and bioturbated surfaces occur, denoting occasional energetic episodes with long subaerial exposure. The facies *Se* are interpreted as scour fill deposits.

Facies Fl: They are composed of very fine-grained (occasionally fine-grained) sandstones and siltstones with fine lamination and flow ripples. They are found as deposits of 6-8 m thick, interbedded with facies *Sl* and *Fsc*. These facies often grade from facies *Sp* and *Sr*. The facies *Fl* are interpreted as overbank deposits associated to meandering channels.

Facies Fsc: They are composed of siltstones and claystones, and very fine-grained sandstones. They are massive or fine laminated. Thickness is up to 7 m. The facies *Fsc* are the most abundant in the shale unit, and are always present in transition to the Muschelkalk facies. The facies *Fsc* are interpreted as floodplain deposits.

Facies Fm: They are composed of siltstones and claystones with mud-cracked surfaces. Bodies are interbedded with facies *Fsc* and *Fl*, and are often eroded by deposits of facies *Sp* and *Sr*. Set thickness is about 0.5 m, but sequences up to 4 m also exist. Some levels present edaphic carbonate nodules (transition to facies *P*) and reduction mottles. The facies *Fm* are interpreted as overbank or drape deposits that underwent subaerial exposure.

Facies Fr: They are composed of massive siltstones and claystones with root traces, bioturbations and rain drops. Small greenish reduction mottles as those of facies *Sh* are common. The facies *Fr* are interpreted as muddy floodplain deposits.

Facies P: They are composed of massive siltstones and claystones. Two main types of intervals are distinguished: (1) levels with carbonate nodules, where nodules are generally small (0.5-1 cm of diameter), but occasionally (i.e., in the upper part of the Buntsandstein succession from Erillcastell locality) they are larger, reaching 4-5 cm of diameter, purple-yellowish colored and with little mudstone matrix; (2) hardened siltstone and claystone intervals (associated to facies *Fsc*) displaying large green reduction mottles that build up continuous levels parallel to stratification, these levels may preserve slickensides and root traces in the uppermost part. The facies *P* are interpreted as paleosols, resulting from pedogenic processes, developed in overbank deposits from floodplain systems.

Architectural Elements

Element CH1: It is composed of conglomerates and coarse-grained sandstone bodies, constituted by facies *Gh*, *Gmpt*, *St* and *Sp*. It is located at the basal conglomerate unit and interpreted as channels and longitudinal bars of braided river systems.

Element CH2: It is composed of medium-fine grained sandstone bodies, constituted by facies *St*, *Sp*, *Sr*, and occasionally *Gh*. It is located at the shale and sandstones unit and interpreted as channels of small river streams associated to occasional events.

Element GB: It is composed of conglomerate and very coarse deposits, constituted by facies *Gh* and *Gmpt*. It is located at the basal conglomerate unit and interpreted as gravel bars and bedforms, usually of tabular geometry.

Element SB: It is composed of coarse to very fine sandstones, constituted by facies *St*, *Sp*, *Sr*, *Sh*, *Sl* and *Se*, and sometimes grading to facies *Fsc*. It is located at the upper part of the conglomerate unit, where corresponds to channel fills or minor bars of braided systems. It is also located at the shale and sandstones unit as sandy bedforms associated to lateral accretions (facies association *St*-*Sp*), thus corresponding to upper part of the point bars from meandering systems, but also as crevasse splay, minor bars and channel fill deposits.

Element LA: It is composed of medium to fine-very fine sandstones, constituted by facies *St* and *Sp*. It is located at the shale and sandstones unit, corresponding to lateral accretions of meandering point bars.

Element LS: It is mostly composed of fine sandstones, constituted by facies *Sh* and *Sl*, and minor facies *Sp* and *Sr*. It is located at the shale and sandstones unit and the shale unit, corresponding to laminated sand sheet deposits.

Element OF: It is composed of claystones and siltstones and subordinated very fine-to fine-grained sandstones, constituted by facies *Sl*, *Fr*, *Fl*, *Fm* and *Fsc*. It is located at the shale and sandstones unit and the shale unit, corresponding to overbank fines deposits that may fill abandoned channels.

S1 Table. Track measurements of the *Prorotodactylus mesaxonichnus* isp. nov. trackways. Values resumed in Table 1.

Trackway holotype (IPS-93870)	Length	Width	Digit I	Digit II	Digit III	Digit IV	Digit V	Length I – IV	Width I – IV	Div. I – II	Div. II – III	Div. III – IV	Div. IV – V	Div. II – IV	Div. I – IV	Div. I – V
Manus #1	50.288	30.503	12.973	23.128	33.219	27.521	12.666	41.791	24.658	21.132	14.763	10.840	41.393	25.603	46.735	88.128
Pes #1	-	-	-	-	42.07	-	-	-	-	-	-	-	-	-	-	-
Manus #2	34.819	32.712	11.011	18.575	22.342	19.788	14.249	30.982	26.369	14.838	14.562	21.858	19.705	36.42	51.258	70.963
Pes #2	50.125	-	21.144	-	30.598	26.667	-	41.778	44.263	-	-	15.068	-	-	46.861	-
Manus #3	40.672	28.741	12.233	18.490	25.646	19.947	14.792	38.059	22.547	32.835	16.999	8.479	33.371	25.478	58.313	91.684
Pes #3	62.313	-	23.037	30.503	38.499	36.149	-	53.121	44.388	18.564	18.968	9.841	-	28.809	47.373	-
Manus #4	43.782	31.483	13.539	18.49	23.259	21.908	13.074	40.301	22.848	25.241	17.236	5.584	30.629	22.82	48.061	78.69
Pes #4	61.464	-	25.461	32.144	40.21	35.533	-	50.873	53.513	18.865	16.682	16.977	-	33.659	52.524	-
Manus #5	26.672	-	10.384	14.286	16.954	10.781	-	24.124	18.981	11.138	12.703	17.489	-	30.192	41.33	-
Pes #5	60.438	-	27.269	36.850	39.889	37.657	-	53.923	48.919	17.617	19.492	16.407	-	35.899	53.516	-
Manus #6	42.285	31.815	12.580	16.867	24.391	23.338	14.375	38.135	22.262	21.625	14.682	9.038	44.892	23.72	45.345	90.237
Pes #6	54.277	-	23.612	32.175	36.415	30.583	-	43.745	48.529	12.947	17.326	15.057	-	32.383	45.33	-
Manus #7	48.226	35.813	14.831	20.404	27.802	25.904	18.878	40.111	26.957	25.453	21.678	9.269	39.389	30.947	56.4	95.789
Pes #7	67.09	-	29.98	36.774	43.949	42.295	-	55.961	44.776	14.509	18.151	18.485	-	36.636	51.145	-
Manus #8	45.491	-	11.131	19.246	27.726	25.85	-	36.929	26.36	27.441	16.674	16.704	-	33.378	60.819	-
Pes #8	64.948	-	28.068	37.095	42.096	38.564	-	57.781	39.142	9.297	10.03	11.04	-	21.07	30.367	-
Mean Manus tracks	41.529	31.845	12.335	18.686	25.167	21.880	14.672	36.304	23.873	22.463	16.162	12.408	34.897	28.570	51.033	85.915
Mean Pes tracks	60.094	-	25.510	34.257	39.216	35.350	-	51.026	46.219	15.300	16.775	14.696	-	31.409	46.731	-

Units in mm and degrees. Highlighted values are estimated.

S1 Table. *(continued)*

Trackway Paratype (IPS-93867)	Length	Width	Digit I	Digit II	Digit III	Digit IV	Digit V	Length I-IV	Width I-IV	Div. I-II	Div. II-III	Div. III-IV	Div. IV-V	Div. II-IV	Div. I-IV	Div. I-V
Manus #1	27.632	19.582	8.480	10.573	16.179	15.587	10.506	24.224	14.629	36.870	23.420	8.228	7.585	31.648	68.518	76.103
Pes #1	47.282	31.481	22.052	24.206	33.511	29.499	13.609	42.541	22.627	15.018	9.421	6.919	25.488	16.340	31.358	56.846
Manus #2	28.860	18.449	-	12.032	14.295	13.559	11.806	-	13.298	-	13.626	14.826	37.679		-	-
Pes #2	-	-	19.237	22.052	24.641	-	-	-	-	14.364	12.274	-	-	-	-	-
Manus #3	-	-	-	-	15.360	15.799	13.052	-	-	-	-	12.130	15.489	-	-	-
Pes #3	42.394	24.367	19.593	25.327	29.032	28.284	16.731	38.861	17.200	11.591	9.783	8.151	15.905	17.934	29.525	45.430
Manus #4	21.368	19.58	7.639	10.483	13.167	12.739	8.336	16.101	13.782	21.498	23.523	11.206	45.772	34.729	56.227	101.999
Manus #5	23.165	18.325	7.498	8.895	12.507	12.794	8.958	18.24	13.746	21.267	7.243	11.958	31.75	19.201	40.468	72.218
Pes #5	36.542	-	14.265	15.540	18.977	18.104	-	31.515	17.706	15.299	14.774	10.78	-	25.554	40.853	-
Manus #6	23.439	15.649	6.041	8.889	15.289	11.635	6.942	20.122	12.739	40.409	15.377	10.107	47.491	25.484	65.893	113.384
Pes #6	32.507	26.111	12.087	14.327	20.008	18.325	-	25.649	20.576	14.087	13.666	15.748	44.105	29.414	43.501	87.606
Manus #7	24.425	17.349	6.704	8.891	15.063	14.489	8.143	22.602	13.378	16.905	11.937	7.655	20.716	19.592	36.497	57.213
Pes #7	46.521	29.446	12.775	18.663	24.942	24.01	-	33.772	23.692	11.868	13.302	10.789	38.006	24.091	35.959	73.965
Manus #9	23.168	23.105	10.275	10.026	12.348	9.300	8.480	16.167	19.582	15.183	9.802	11.763	19.896	21.565	36.748	56.644
Pes #9	40.281	-	19.201	20.243	23.487	21.526	-	32.824	31.803	9.868	10.564	10.099	-	20.663	30.531	-
Mean Manus tracks	24.580	18.863	7.773	9.970	14.276	13.238	9.528	19.576	14.451	25.355	14.990	10.984	28.297	25.370	50.725	79.594
Mean Pes tracks	40.921	27.851	17.030	20.051	24.943	23.291	15.170	34.194	22.267	13.156	11.969	10.414	30.876	22.333	35.288	65.962

S1 Table. *(continued)*

Trackway S1A Fig	Length	Width	Digit I	Digit II	Digit III	Digit IV	Digit V	Length I – IV	Width I – IV	Div. I – II	Div. II – III	Div. III – IV	Div. IV – V	Div. II – IV	Div. I – IV	Div. I – V
Manus #1	25.284	-	9.112	15.010	17.786	15.617	-	22.502	16.398	36.777	5.603	6.341	-	11.944	48.721	-
Pes #1	54.793	-	20.952	25.119	30.562	29.284	-	46.212	32.872	9.271	12.218	12.319	-	24.537	33.808	-
Manus #2	40.339	27.977	12.485	19.157	22.099	19.769	14.487	28.922	21.454	16.274	14.481	14.717	38.246	29.198	45.472	83.718
Pes #2	-	-	-	-	-	-	-	-	-	17.745	-	-	-	-	-	-
Manus #3	32.473	24.321	9.672	17.090	21.259	19.504	13.437	32.802	20.048	26.630	12.757	12.010	29.281	24.767	51.397	80.678
Pes #3	-	-	-	-	-	-	-	-	-	-	-	-	-	-	-	-
Manus #4	29.827	-	11.801	15.300	19.295	15.918	-	26.565	19.054	17.494	14.273	15.555	-	29.828	47.322	-
Pes #4	45.138	-	21.973	26.750	31.353	27.126	-	39.527	38.254	10.876	12.370	20.045	-	32.415	43.291	-
Manus #5	34.052	24.752	9.044	13.620	20.983	20.077	11.338	28.167	18.940	23.867	15.129	11.443	33.331	26.572	50.439	83.77
Pes #5	-	-	18.663	-	-	-	-	-	-	-	-	-	-	-	-	-
Manus #6	36.693	29.389	10.787	16.257	20.563	18.932	14.34	27.55	22.543	18.915	16.198	11.997	41.389	28.195	47.11	88.499
Pes #6	56.013	-	21.128	33.566	35.591	35.042	-	47.553	40.293	17.309	19.888	20.917	-	40.805	58.114	-
Mean Manus tracks	33.111	26.610	10.484	16.072	20.331	18.303	13.401	27.751	19.740	23.326	13.074	12.011	35.562	25.084	48.410	84.166
Mean Pes tracks	51.981	-	20.679	28.478	32.502	30.484	-	44.431	37.140	13.800	14.825	17.760	-	32.586	45.071	-

S1 Table. *(continued)*

Trackway S1B Fig	Length	Width	Digit I	Digit II	Digit III	Digit IV	Digit V	Length I-IV	Width I-IV	Div. I-II	Div. II-III	Div. III-IV	Div. IV-V	Div. II-IV	Div. I-IV	Div. I-V
Manus #1	43.338	-	-	-	-	24.479	17.453	-	-	-	-	-	25.816	-	-	-
Pes #1	55.418	-	26.530	34.682	39.937	36.532	-	56.702	32.970	12.698	10.445	13.444	-	23.889	36.587	-
Manus #2	35.368	25.269	12.434	13.766	18.246	16.956	-	24.997	21.099	12.760	10.764	11.835	-	22.599	35.359	-
Pes #2	-	-	-	-	-	-	-	-	-	11.635	-	-	-	-	-	-
Manus #3	32.015	23.835	11.748	15.071	20.368	18.103	9.975	22.901	19.168	13.370	21.842	12.273	24.332	34.115	47.485	71.817
Pes #3	51.493	46.895	26.014	28.295	34.344	31.890	-	48.412	33.495	13.076	9.165	7.988	57.596	17.153	30.229	87.825
Manus #4	32.235	24.214	11.376	18.538	23.673	21.496	12.163	25.754	23.086	20.783	16.406	14.799	15.723	31.205	51.988	67.711
Pes #4	42.428	-	21.805	26.647	30.858	30.505	-	40.738	39.075	18.119	21.135	16.878	-	38.013	56.132	-
Manus #5	30.502	22.360	9.111	14.123	20.970	19.520	11.579	27.550	16.507	25.275	15.571	10.622	35.530	26.193	51.468	86.998
Pes #5	49.098	-	24.379	31.122	33.406	28.377	-	46.393	35.119	19.818	3.701	12.402	-	16.103	35.921	-
Mean Manus tracks	34.692	23.920	11.167	15.375	20.814	20.111	12.793	25.301	19.965	18.047	16.146	12.382	25.350	28.528	46.575	75.509
Mean Pes tracks	49.609	46.895	24.682	30.187	34.636	31.826	-	48.061	35.165	15.069	11.112	12.678	57.596	23.790	39.717	87.825

S1 Table. *(continued)*

Trackway S1C Fig	Length	Width	Digit I	Digit II	Digit III	Digit IV	Digit V	Length I-IV	Width I-IV	Div. I-II	Div. II-III	Div. III-IV	Div. IV-V	Div. II-IV	Div. I-IV	Div. I-V
Manus #1	27.027	22.984	9.68	12.341	17.082	14.576	10.476	23.095	15.161	21.263	14.489	11.354	40.577	25.843	47.106	87.683
Manus #2	31.219	24.77	9.318	10.712	16.034	14.046	11.916	21.408	18.353	14.129	11.774	15.038	49.821	26.812	40.941	90.762
Pes #2	50.372	-	19.606	22.462	25.851	24.595	-	41.775	33.136	7.715	13.38	10.651	-	24.031	31.746	-
Manus #3	38.848	23.300	8.988	13.560	21.312	20.754	12.995	32.555	16.609	19.569	15.436	12.508	59.403	27.944	47.513	106.916
Manus #1bis	30.626	20.494	8.903	11.865	16.855	15.883	12.149	22.475	14.568	19.339	17.449	12.174	23.527	29.623	48.962	72.489
Mean Manus tracks	31.930	22.887	9.222	12.120	17.821	16.315	11.884	24.883	16.173	18.575	14.787	12.769	43.332	27.556	46.131	89.463
Mean Pes tracks	50.372	-	19.606	22.462	25.851	24.595	-	41.775	33.136	7.715	13.38	10.651	-	24.031	31.746	-

S1 Table. *(continued)*

Trackway S1D Fig	Length	Width	Digit I	Digit II	Digit III	Digit IV	Digit V	Length I-IV	Width I-IV	Div. I-II	Div. II-III	Div. III-IV	Div. IV-V	Div. II-IV	Div. I-IV	Div. I-V
Manus #1	13.724	13.032	3.653	4.885	-	7.979	4.891	12.09	8.321	18.077	-	-	83.372	40.771	58.848	142.22
Manus #3	13.975	12.153	3.845	4.33	6.199	5.347	4.481	9.579	9.459	25.903	12.461	21.537	68.199	33.998	59.901	128.1
Mean Manus tracks	13.850	12.593	3.749	4.608	6.199	6.663	4.686	10.835	8.890	21.990	12.461	21.537	75.786	37.385	59.375	135.160

S1 Table. *(continued)*

Tracks	Length	Width	Digit I	Digit II	Digit III	Digit IV	Digit V	Length I – IV	Width I – IV	Div. I – II	Div. II – III	Div. III – IV	Div. IV – V	Div. II – IV	Div. I – IV	Div. I-V
Total Mean Manus tracks	37.167	24.088	13.190	17.425	22.953	21.014	12.447	31.248	22.867	20.748	15.731	11.883	33.477	27.494	48.606	84.424
Total Mean Pes tracks	45.453	29.989	18.147	22.988	27.475	25.215	15.170*	38.602	29.657	14.348	13.240	12.744	33.768	25.941	40.177	71.865

** The mean length of the pedal digit V is not representative, as it is observed in few tracks and usually only preserved by the tip impression*

S2 Table. Trackway measurements of *Prorotodactylus mesaxonichnus* isp. nov. Values resumed in Table 2

Trackway holotype (IPS-93870) Fig 5A								
Stride manus	256.043	314.023	323.778	308.696	325.867	-	240.899	
Stride pes	260.468	291.34	320.193	309.45	296.639	-	242.538	
Pace manus	166.452	152.423	214.443	174.315	207.938	180.049		
Pace pes	269.712	254.260	271.193	260.609	253.776	232.863		
Pace angulation manus	106.781	117.29	112.257	108.446	112.653	-		
Pace angulation pes	59.265	66.441	74.224	74.078	74.333	-		
Width pace manus	95.123	93.69	106.054	112.726	106.041			
Width pace pes	228.362	218.396	212.079	204.439	192.592			
Manus-Pes distance	53.977	84.709	50.052	76.328	40.045	67.693	64.608	65.002
Div. manus midline	14.831	9.155	17.521	12.268	-3.859	-7.475	-	-
Div. pes midline	46.572	47.397	52.535	52.902	44.094	62.94	-	-
Div. manus-pes digits III	31.741	38.242	35.014	40.634	47.953	70.415	24.417	18.468
Glenoacetabular distance	156.543	154.809	200.522	182.864	196.067			
Glenoacetabular Standard deviation	21.537							

Units in mm and degrees.

S2 Table. *(continued)*

Trackway paratype (IPS-93867) Fig 6A									
Stride manus	136.043	117.197	111.625	153.426	148.331	-	149.612		
Stride pes	102.905	141.093	121.171	146.669	153.612	169.545	136.078		
Pace manus	78.110	107.508	61.358	105.130	74.244	112.630	-	-	
Pace pes	155.670	158.794	134.939	144.739	133.887	163.316	176.635	187.661	
Pace angulation manus	94.485	81.448	77.857	116.101	105.201	-	-		
Pace angulation pes	37.616	56.479	51.592	63.459	60.994	60.640	43.279		
Width pace manus	63.435	65.720	66.249	49.407	59.459	-	-		
Width pace pes	147.819	130.345	125.928	118.442	127.795	147.545	169.416		
Manus-Pes distance	42.101	60.363	55.637	37.661	53.517	36.200	50.199	-	62.543
Div. manus midline	-3.270	6.567	-18.464	0.000	-1.121	-1.162	-0.181	-	-11.180
Div. pes midline	47.070	53.555	38.547	-	62.814	45.220	37.601	-	44.075
Div. manus-pes digits III	43.800	60.122	20.083	-	61.693	44.058	37.420	-	32.895
Glenoacetabular distance	94.787	94.054	89.679	99.378	104.303				
Glenoacetabular Standard deviation	5.581								

S2 Table. *(continued)*

Trackway S1A Fig						
Stride manus	277.587	276.801	274.572	280.653		
Stride pes	259.488	256.344	277.843	276.149		
Pace manus	148.569	182.773	139.242	172.691	140.794	
Pace pes	197.711	236.796	198.773	226.557	161.092	
Pace angulation manus	114.470	116.945	121.398	127.171		
Pace angulation pes	73.122	70.986	80.858	89.832		
Width pace manus	88.442	82.680	74.326	70.109		
Width pace pes	172.876	173.996	160.244	133.029		
Manus-Pes distance	48.511	39.413	54.635	50.470	-	39.956
Div. manus midline	-6.683	0.000	11.927	2.131	3.455	7.676
Div. pes midline	20.729	-	-	33.257	-	37.838
Div. manus-pes digits III	27.412	-	-	31.126	-	30.162
Glenoacetabular distance	138.942	159.272	147.733	137.517		
Glenoacetabular Standard deviation	10.014					

S2 Table. *(continued)*

Trackway S1B Fig					
Stride manus	244.694	255.025	250.344		
Stride pes	242.712	254.466	253.828		
Pace manus	119.644	165.706	129.415	162.386	
Pace pes	210.140	243.842	214.303	247.625	
Pace angulation manus	118.144	118.952	117.760		
Pace angulation pes	64.519	67.445	66.775		
Width pace manus	71.813	73.088	74.321		
Width pace pes	189.522	189.033	190.774		
Manus-Pes distance	61.841	64.132	52.523	70.071	50.362
Div. manus midline	0.000	0.000	0.000	-6.084	9.227
Div. pes midline	56.867	-	52.536	46.399	41.330
Div. manus-pes digits III	56.867	-	52.536	52.483	32.103
Glenoacetabular distance	136.469	139.476	147.250		
Glenoacetabular Standard deviation	5.563				

S2 Table. (continued)

Trackway S1C Fig			
Stride manus	374.792		
Stride pes	-		
Pace manus	232.552	172.288	
Pace pes	-	-	
Pace angulation manus	135.020		
Pace angulation pes	-		
Width pace manus	75.688		
Width pace pes	-		
Manus-Pes distance	-	49.782	-
Div. manus midline	0.000	-19.887	0.000
Div. pes midline	-	72.552	-
Div. manus-pes digits III	-	92.439	-

S2 Table. (continued)

Trackway S1D Fig			
Stride manus	106.110		
Stride pes	108.859		
Pace manus	76.279	68.180	
Pace pes	99.972	65.257	
Pace angulation manus	94.477		
Pace angulation pes	79.311		
Width pace manus	48.511		
Width pace pes	58.585		
Manus-Pes distance	39.641	20.269	36.307
Div. manus midline	0.000	-	0.000
Div. pes midline	-	-	-
Div. manus-pes digits III	-	-	-

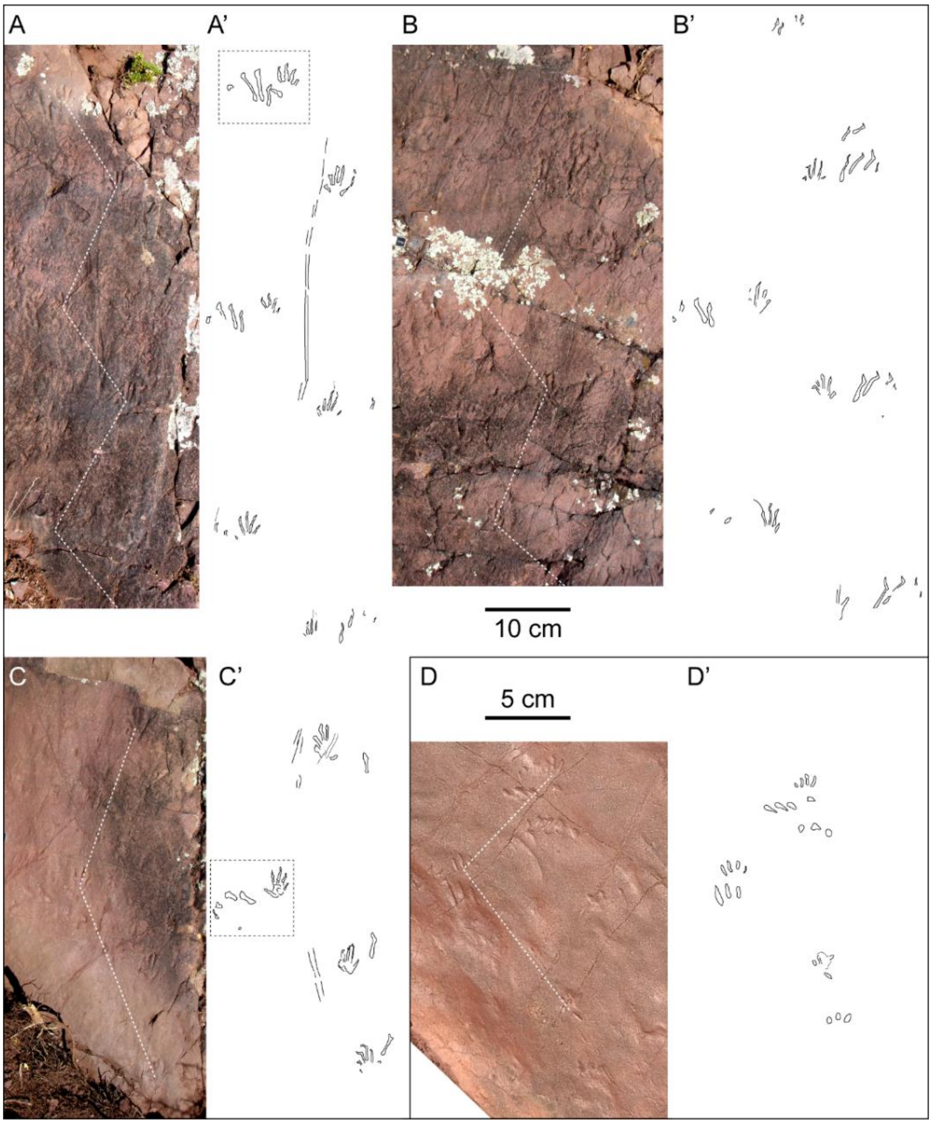

S1 Fig. Trackways of *Prorotodactylus mesaxonichnus* isp. nov. (A-C) Specimens from Erillcastell; dashed squares from A and C are correspond to manus-pes sets from Fig 7A and 7B, respectively. (D) Specimen from Buira.

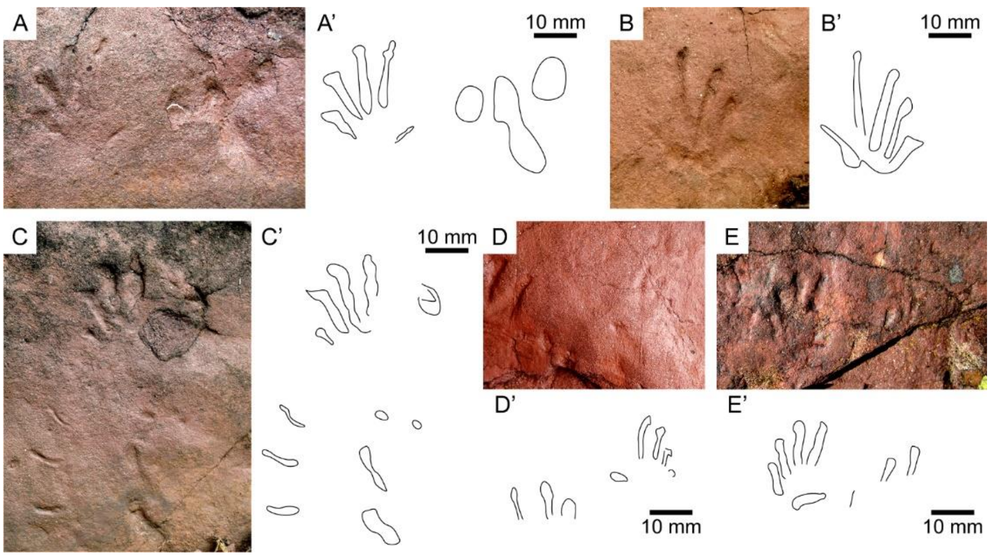

S2 Fig. Tracks of *Prorotodactylus mesaxonichnus* isp. nov. from Buira.

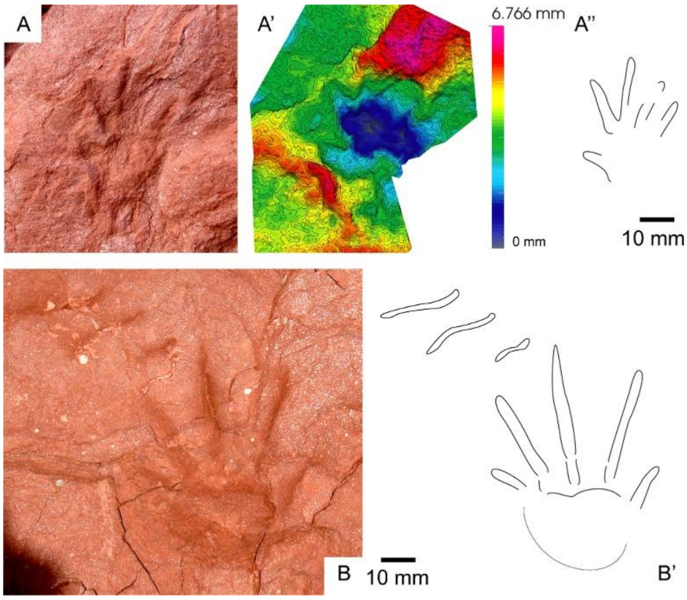

S3 Fig. Tracks of *Prorotodactylus mesaxonichnus* isp. nov. from Port del Cantó. Ichnites from sections IV (A) and VII (B).

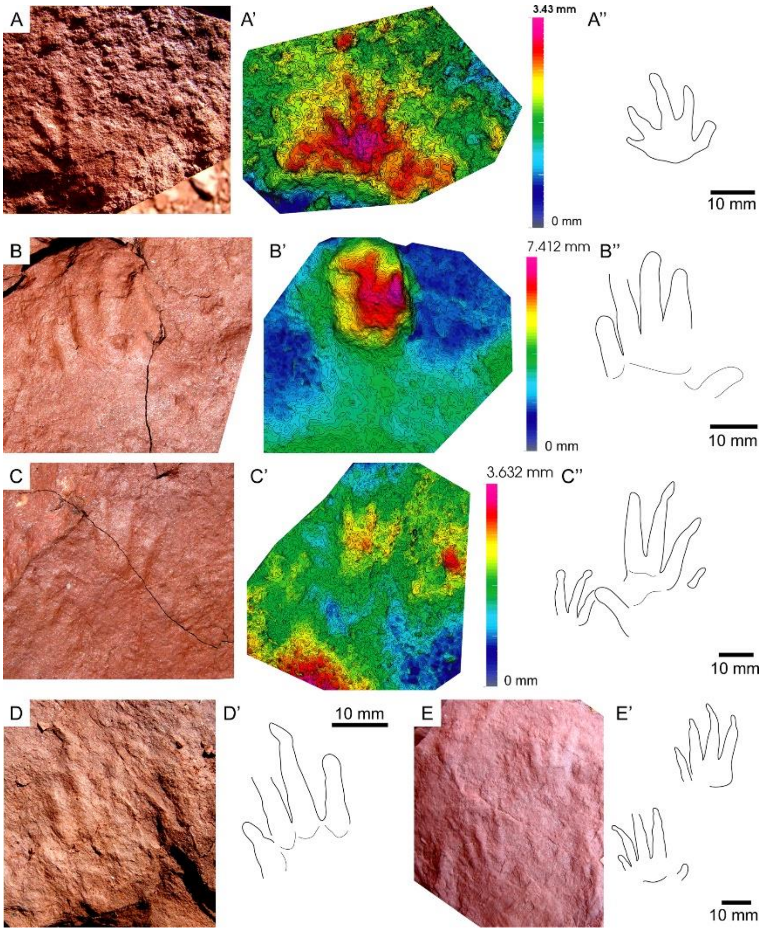

S4 Fig. Tracks of *Prorotodactylusmesaxonichnus* isp. nov. from Port del Cantó. (A) IPS-83740 from Argestues tracksite. (B-E) Isolated ichnites from RubioÂ tracksite. Note the relatively bad preservation of the ichnites, all in convex hyporelief, preserved in the bases of small meandering channels (facies *St*).

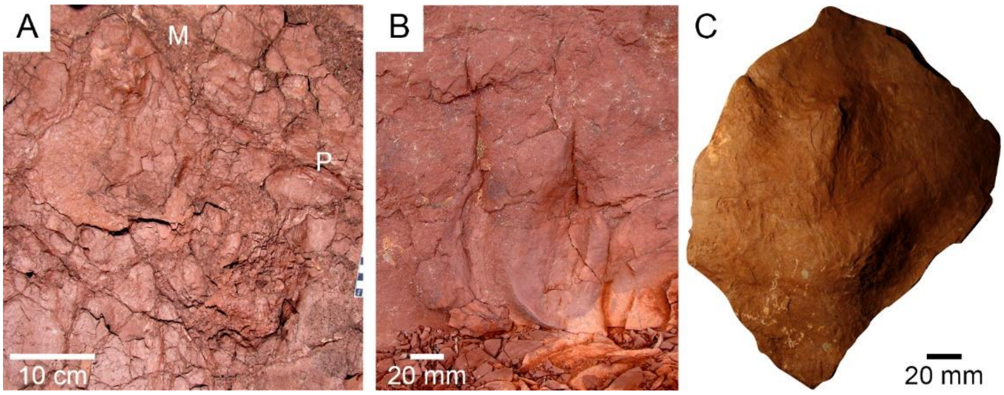

S5 Fig. Tracks of chirotheriid morphotype indet. from Port del Cantó. (A) Manus-pes set (M-P). (B) Scratch-like track. (C) Partial track of IPS-83750.

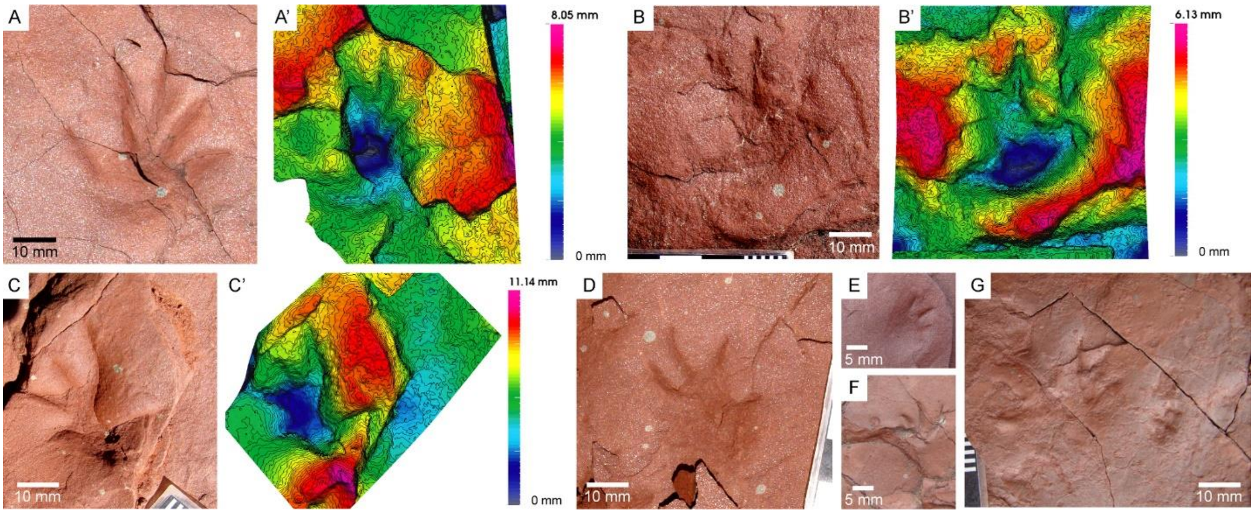

S6 Fig. Tracks of *Rhynchosauroides* morphotypes from Port del Cantó. (A-C) *Rhynchosauroides* cf. *schochardti*. (D) *Rhynchosauroides* isp. indet. 1. (E-G) *Rhynchosauroides* isp. indet.

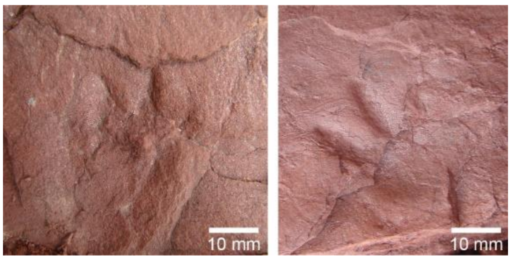

S7 Fig. Isolated and partially preserved tracks of the undetermined Morphotype A from Port del Cantó (section IV).

Detailed stratigraphic sections from Fig. 2 of chapter 7

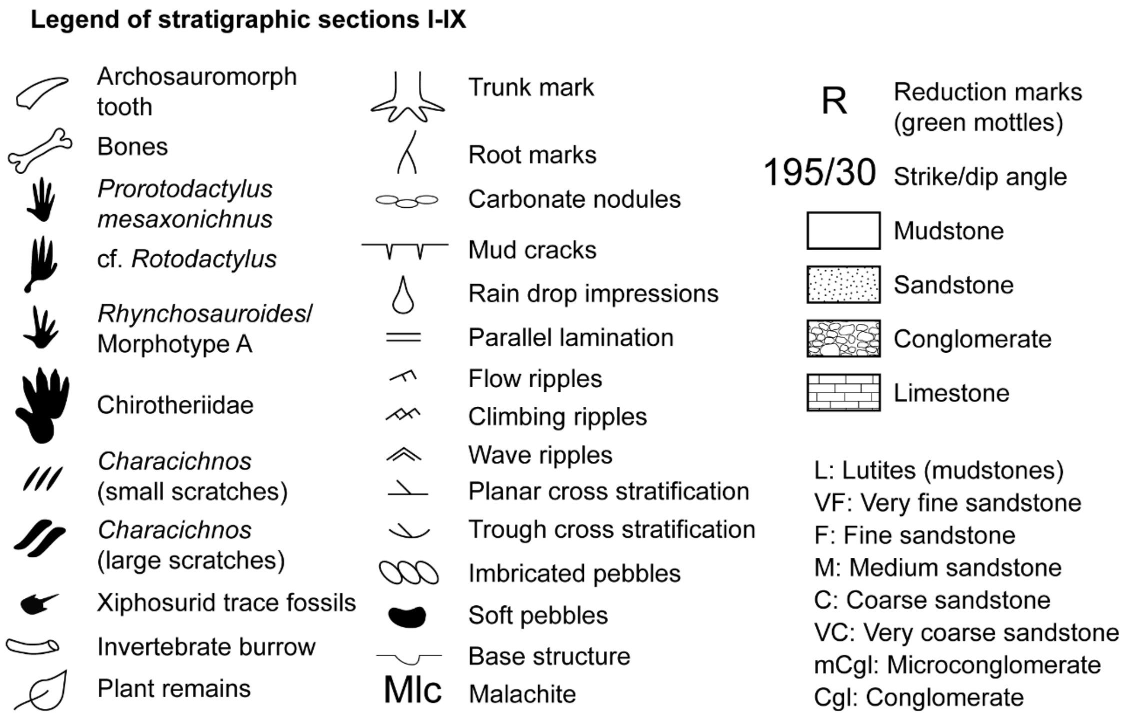

Stratigraphic seciton I – Erillcastell

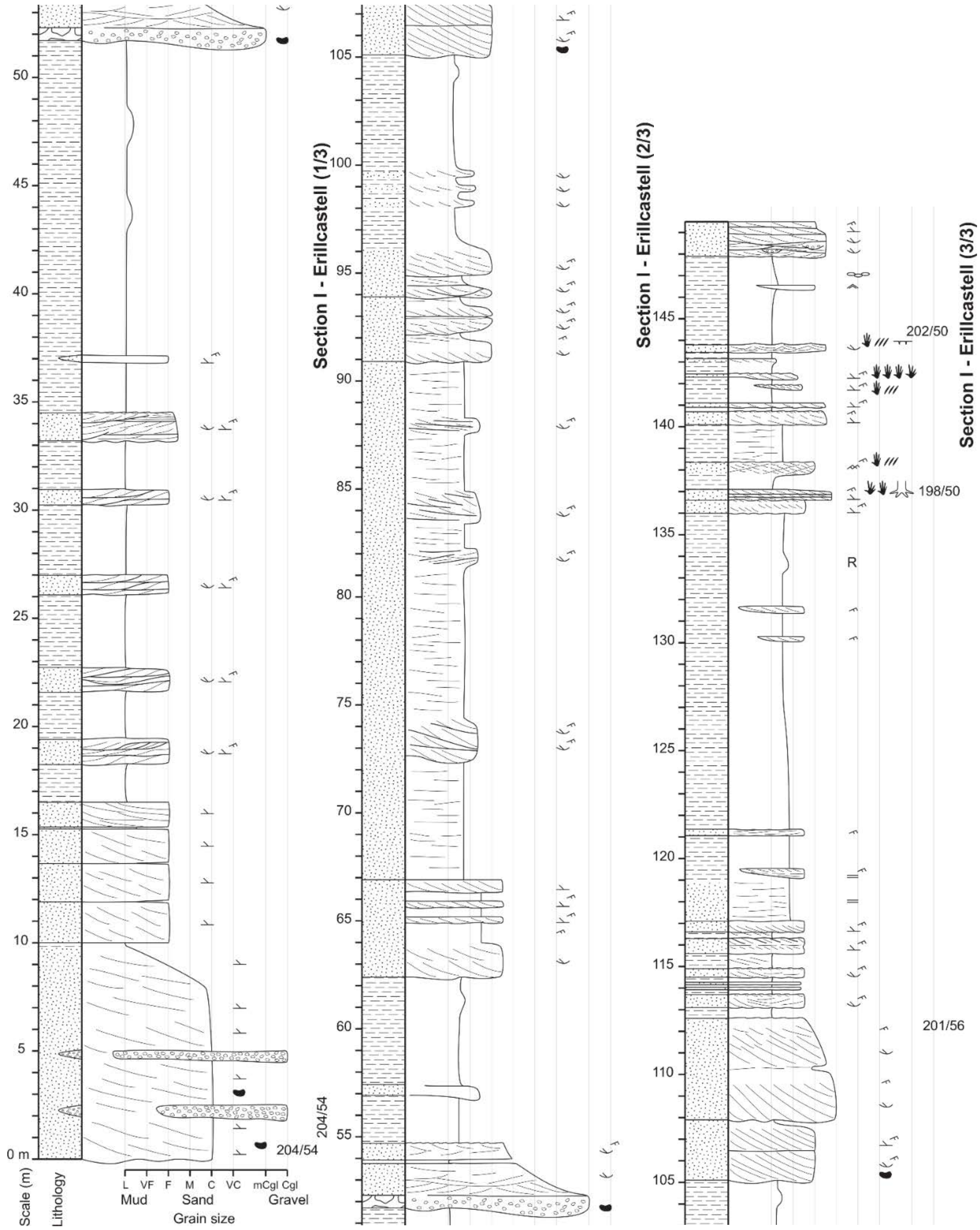

Stratigraphic section II – Buira

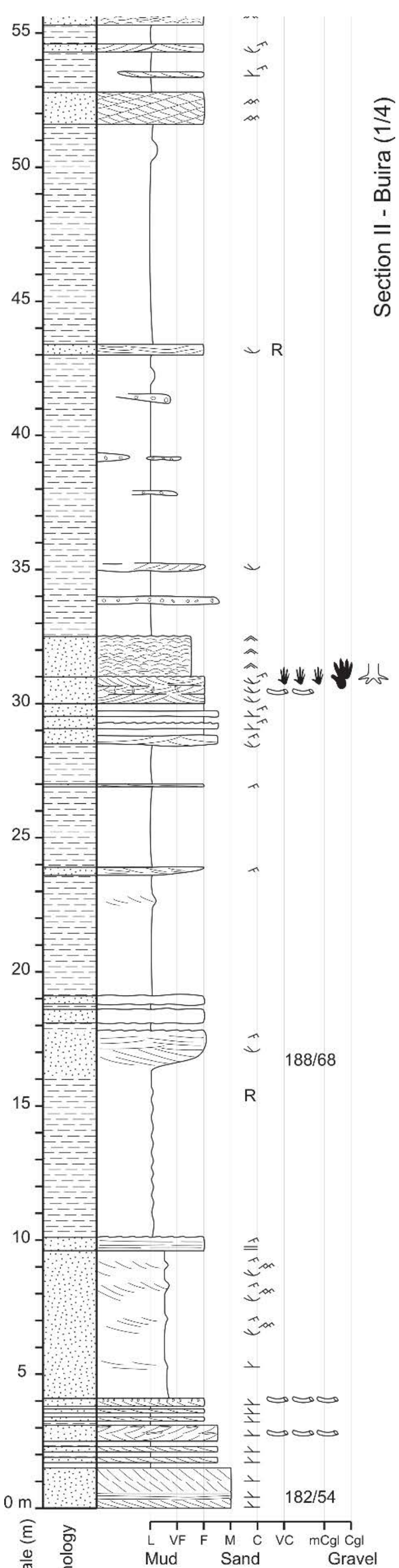

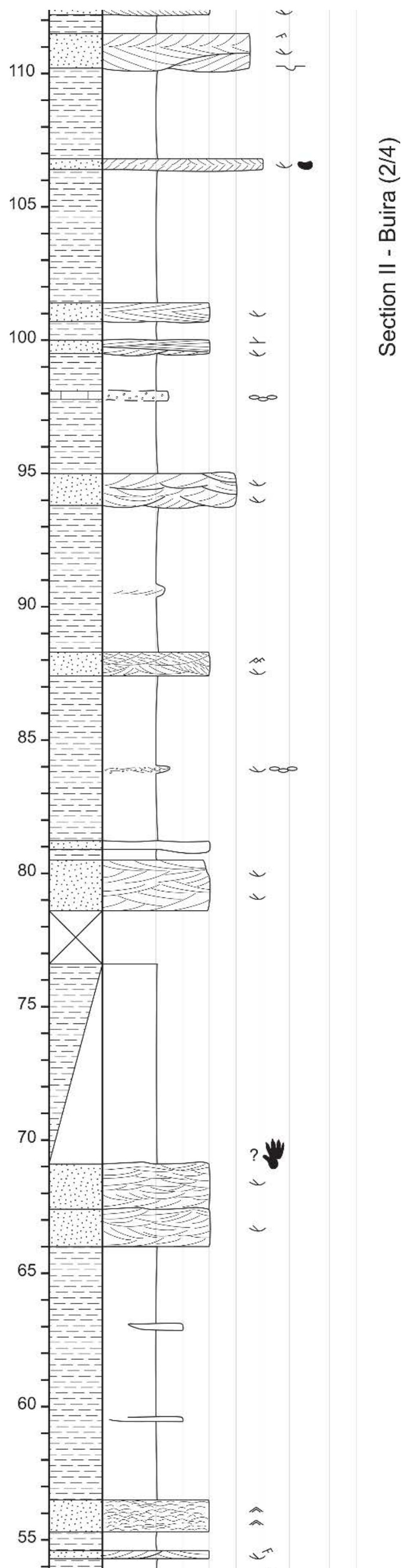

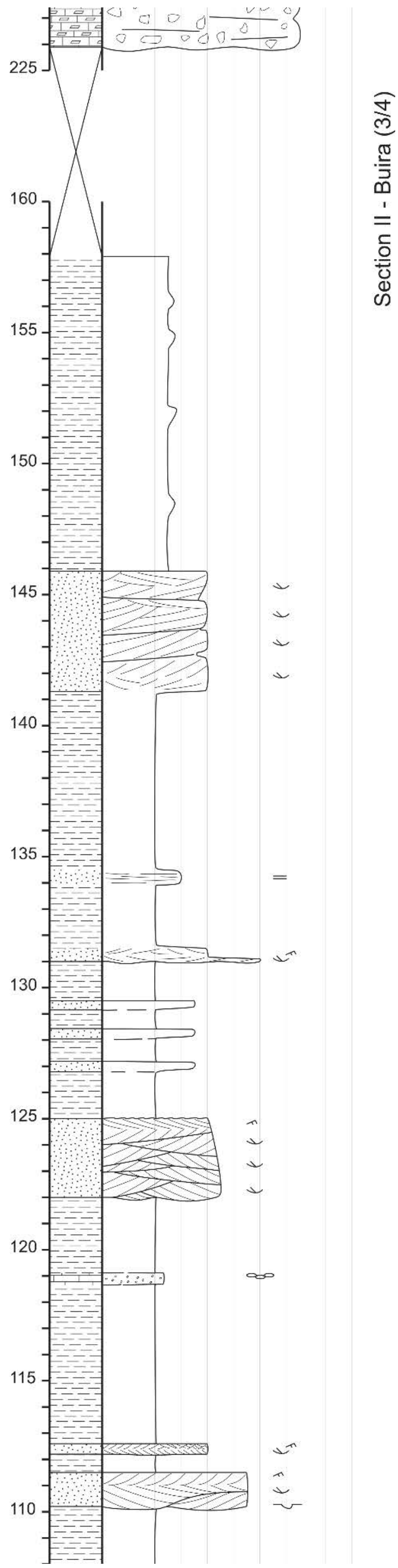
Section II - Buira (3/4)
225
160
155
150
145
140
135
130
125
120
115
110

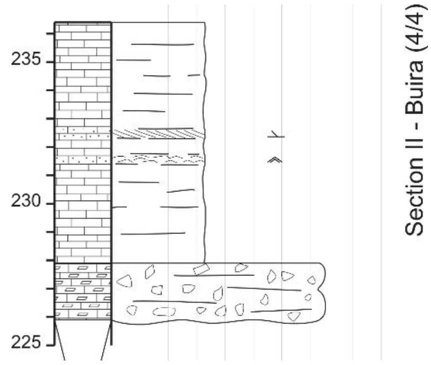
Section II - Buira (4/4)
235
230
225

Stratigraphic section III – Port del Cantó (1)

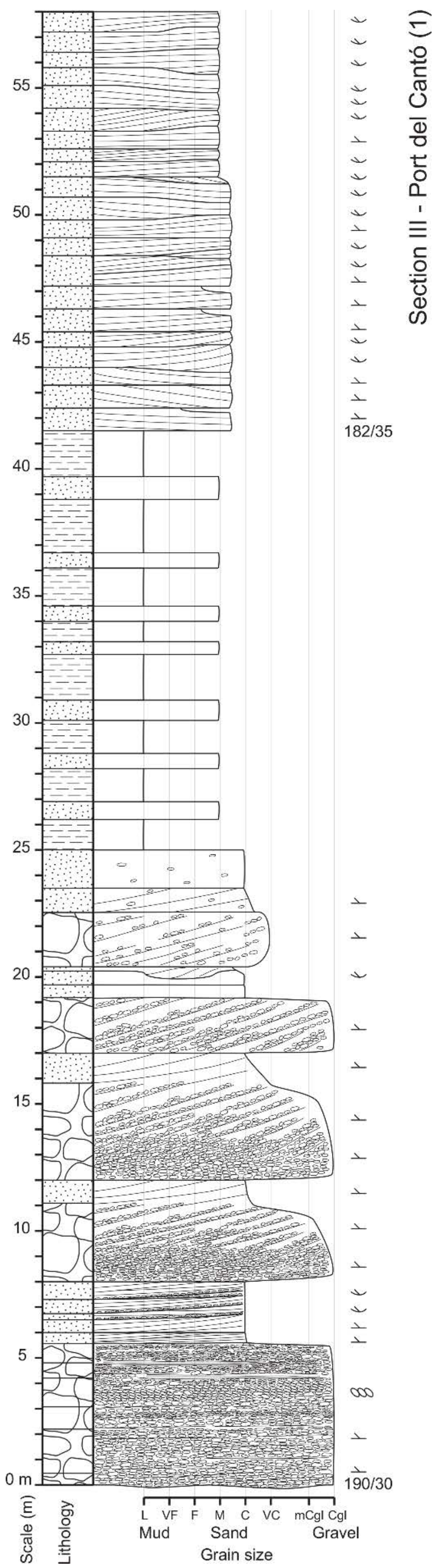

Stratigraphic section IV – Port del Cantó (2)

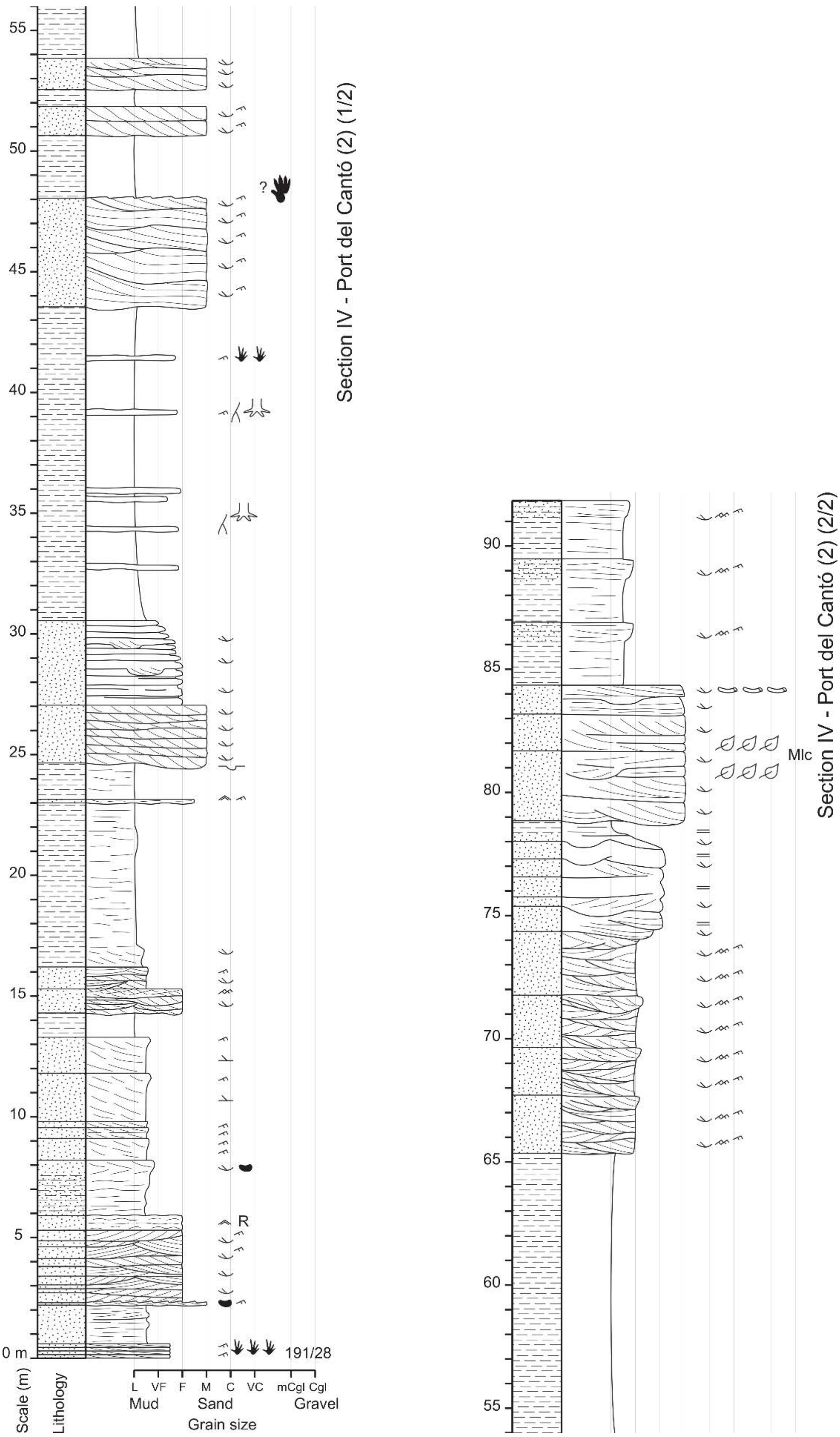

Stratigraphic section V – Port del Cantó (3)

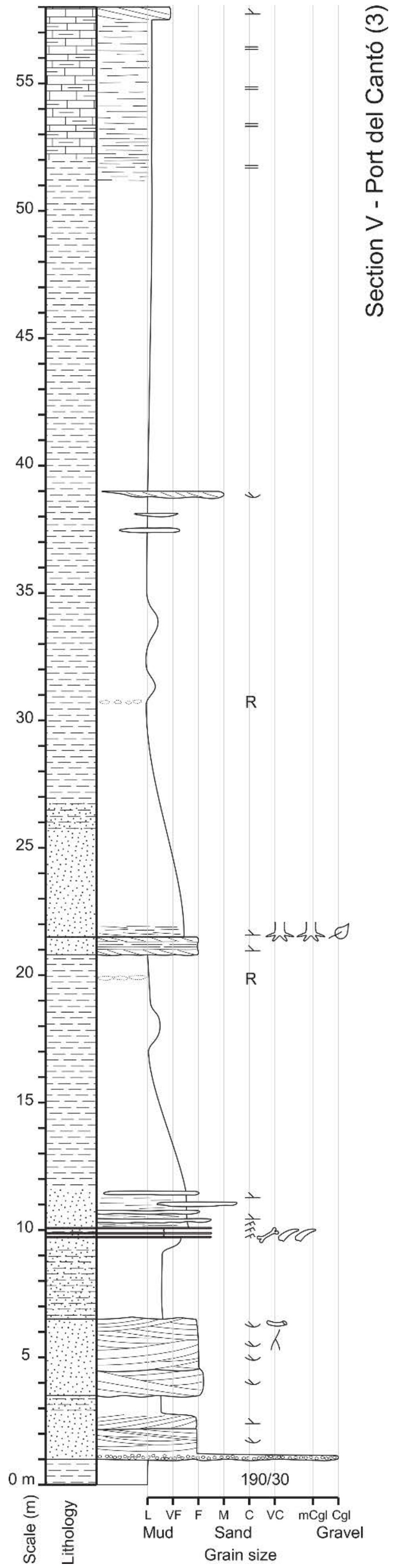

Stratigraphic sections VI and VII – Port del Cantó (4) and (5)

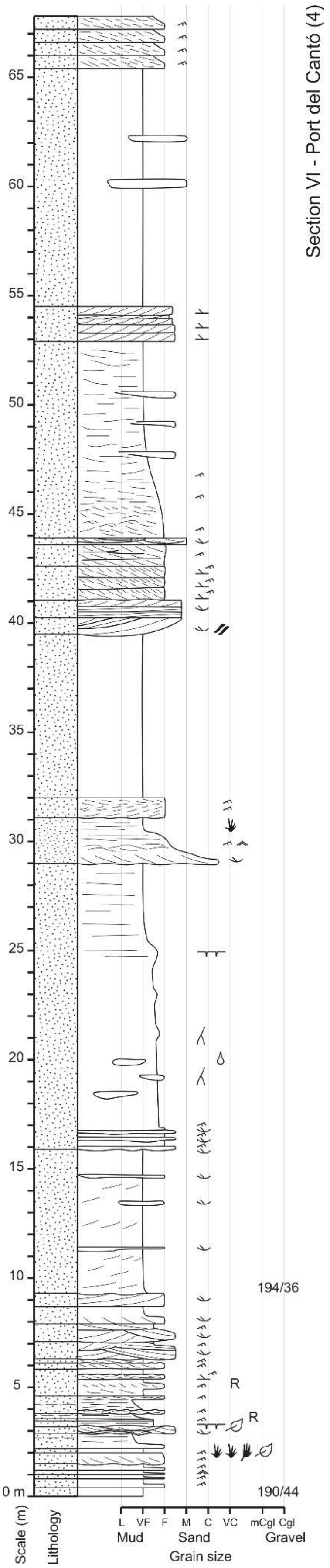

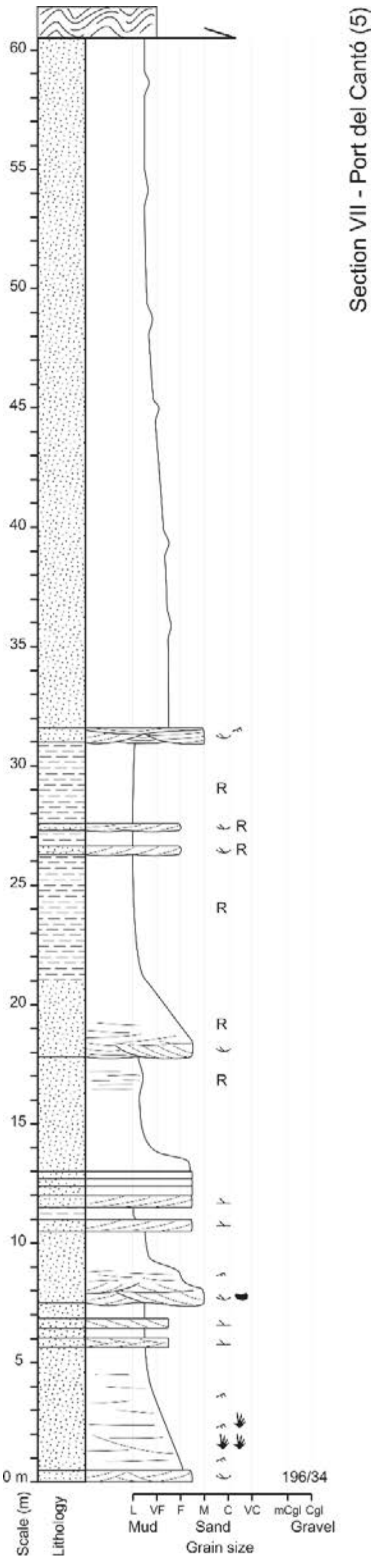

Stratigraphic section VIII – Port del Cantó (6)

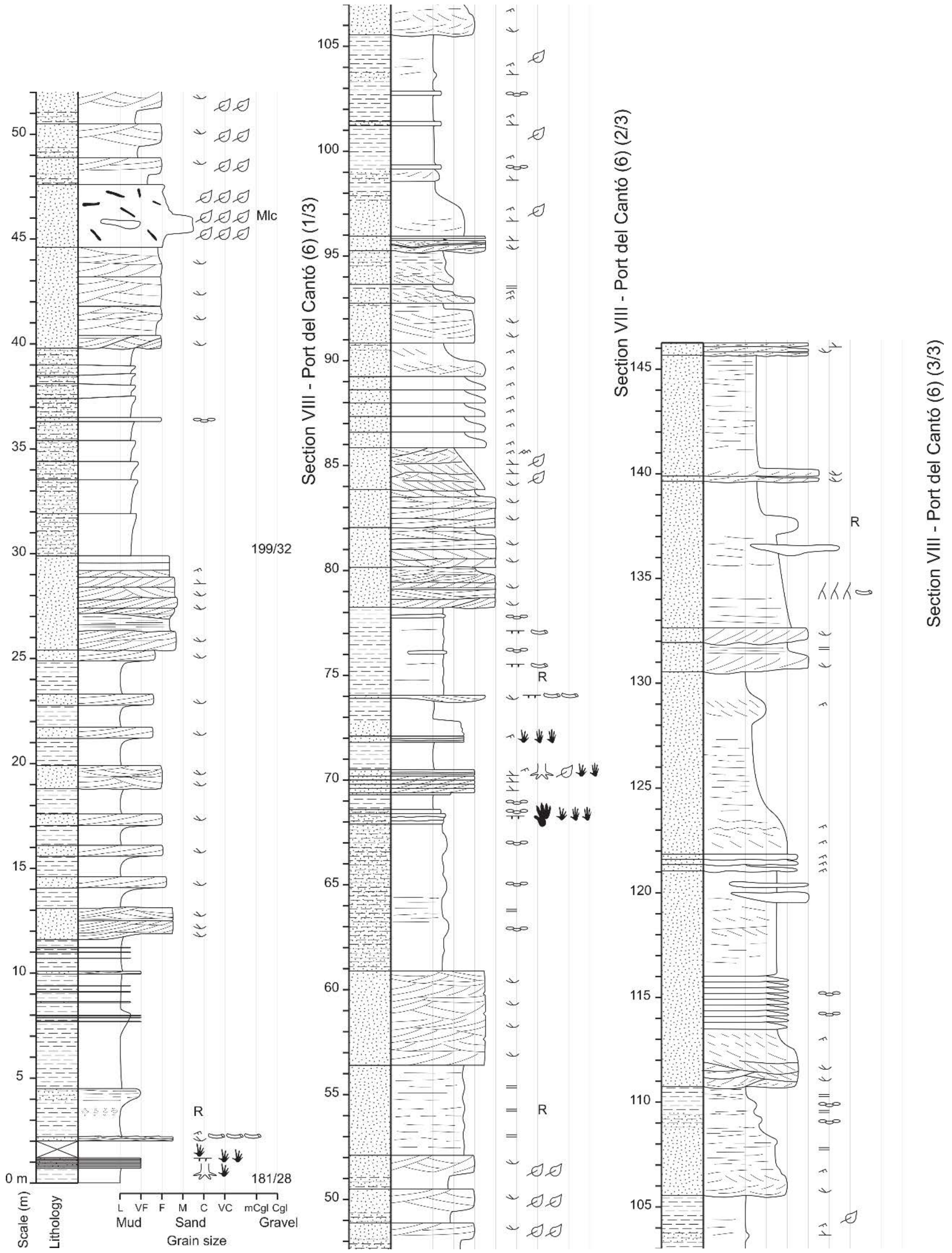

Stratigraphic section IX – Port del Cantó (7)